Aus dem Deutschen Krebsforschungszentrum Heidelberg
Abteilung Pathogenese infektionsbedingter Tumoren
Leiter: Prof. Dr. Dr. Henri-Jacques Delecluse

Cellular control of spontaneous replication in B cells infected by the Epstein-Barr virus

Inauguraldissertation
zur Erlangung des Doctor scientiarum humanarum
(Dr. sc. hum.)
an der
Medizinischen Fakultät Heidelberg
der
Ruprecht-Karls-Universität

vorgelegt von
Xianliang Cheng
aus
Heilongjiang, China
2023

Dekan: Prof. Dr. med. Dr. h.c. Hans-Georg Kräusslich

Doktorvater: Prof. Dr. Dr. Henri-Jacques Delecluse

Contents

Abbreviations

Δ	Knockout or deletion
Ab	Antibody
Amp	Ampicillin
BAC	Bacterial artificial chromosome
BL	Burkitt's lymphoma
cHL	classical Hodgkin's lymphoma
DNA	Deoxyribonucleic acid
E.coli	*Escherichia coli*
EDTA	Ethylenediaminetetraacetic acid
FBS	Fetal bovine serum
DLBCL	Diffuse large B cell lymphoma
ds	double-stranded
eBL	endemic Burkitt's lymphoma
EBV	Epstein-Barr Virus
EBNA	Epstein Barr Nuclear Antigen
FBS	fetal bovine serum
fwd	forward
GC	Gastric carcinoma
GFP	Green fluorescence protein
gp	Glycoprotein
HEK	Human Embryonic Kidney
HL	Hodgkin's lymphoma
HRP	Horseradish peroxidase
IF	Immunofluorescence
IM	Infectious mononucleosis
IE	Immediate Early lytic gene
Kb	Kilobase pair
kDa	Kilodalton

LB	Luria-Bertani
LCL	Lymphoblastoid cell line
LMP	latent membrane protein
moi	Multiplicity of infection
nt	nucleotide
NPC	Nasopharyngeal carcinoma
OriLyt	Lytic Origin of replication
OriP	Latent Origin of replication
ORF	open reading frame
PAGE	Polyacrylamide gel
PBS	Phosphate buffered saline
PCR	Polymerase chain reaction
PTLD	Post-transplant lymphoproliferative disorder
PBMC	peripheral blood mononuclear cells
qPCR	Quantitative polymerase chain reaction
rEBV	Recombinant EBV
rM81	Recombinant M81 EBV strain
RNA	Ribonucleic acid
rpm	Round per minute
RPMI	Roswell Park Memorial Institute
SDS	Sodium dodecyl sulfate
sBL	sporadic Burkitt lymphoma
Tet	Tetracycline
TPA	12-O-tetradecanoylphorbol-13-acetate
TR	Terminal repeat
Tris	Tris-Hydroxymethyl-Aminomethane
UV	Ultraviolet
WT	Wild type
WB	Western Blot

1 Introduction

1.1 The Epstein-Barr virus (EBV)

In 1964, the virologists Michael A. Epstein and Yvonne M. Barr successfully identified herpesvirus-like particles from African Burkitt's lymphoma tissues by using electron microscopy (Fig.1). EBV was the first human tumour virus to be discovered, and since then, the list of human cancers this virus causes has been steadily increasing (Epstein 2015; Henle et al. 1967).

The herpesvirus family consists of three subfamilies, alpha-, beta-, and gamma-Herpesviridae. Members of the gamma herpesvirus subfamily are widespread in nature and infect a variety of mammalian species, including humans. EBV, or Herpes Virus 4 (HHV4) belongs to this subfamily. It is a double-stranded DNA γ-herpesvirus of about 170-175 kilobases (kb) in size. EBV is recognized by the World Health Organization as a Class I oncogenic virus, and it accounts for over 200,000 cases of cancers (de Martel et al. 2012; Farrell 2019; Khan and Hashim 2014).

In humans, EBV spreads mainly through saliva, can infect B cells, and then establishes a lifelong latent infection pattern cells through a series of viral latent transcription programs. EBV can infect epithelial cells but does not trigger the full growth-transforming program of the virus and infrequently achieves full lytic replication in these cells. In contrast, the ability of EBV to transform resting B cells in lymphoblastoid cell lines (LCLs) has provided a versatile model of the virus infection and transformation (Young and Rickinson 2004).

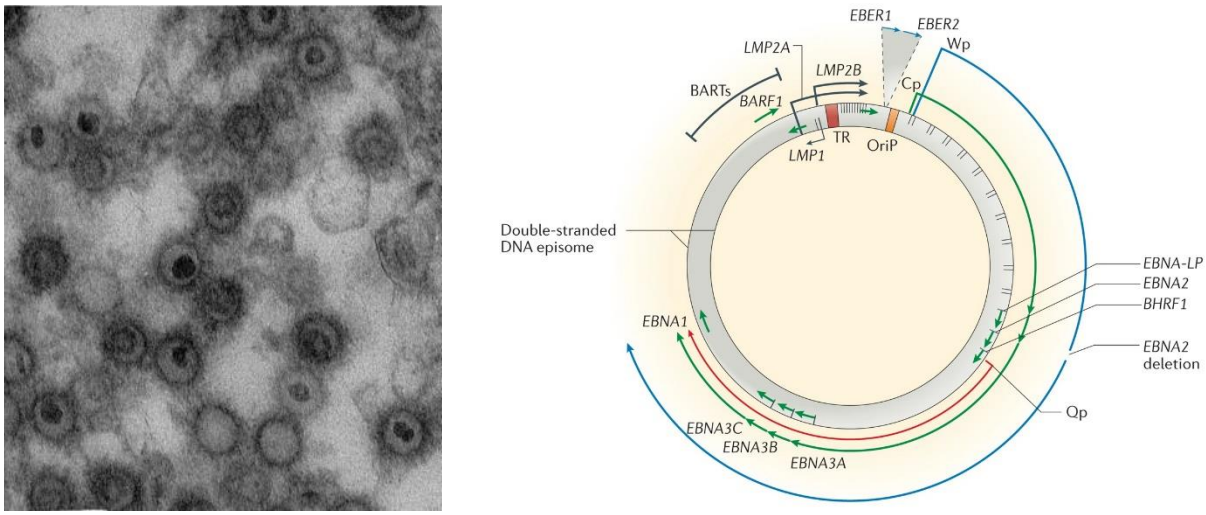

Fig.1 (A) The first electron micrograph of EBV. The figure was taken from Epstein A (2015) (Epstein 2015). (B) A diagram of location and transcription of EBV latent genes on the dsDNA episome from (Young and Murray 2003).

1.2 EBV genome

The EBV genome was the first herpesvirus genome to be sequenced (Baer et al. 1984). The introduction of EBV B95.8 genome into a Bacterial Artificial Chromosome (BAC) made it possible to create recombinant EBV (rEBV) mutant and to study single EBV gene functions (Delecluse et al. 1998). In fact, many EBV strains from patients have been now been isolated, sequenced and cloned into BAC, for example, the M81 strain from a Chinese patient with nasopharyngeal carcinoma (Tsai et al. 2013), as well as the SNU719 and YCCEL1 strains that were cloned from two gastric cancer cell lines (Kanda et al. 2016).

EBV possesses a large double stranded DNA genome, that persists in the nucleus of infected cells. The open reading frames (ORFs) of EBV are generally classified as lytic or latent. The EBV genome encodes more than 80 viral proteins as well as multiple noncoding RNAs (Baer et al. 1984; Notarte et al. 2021). The tandemly arranged terminal repeats (TRs) which are approximately 500 bp in size flank the EBV genome at both ends, allowing its circularization after infection of host cells (Zimmermann and Hammerschmidt 1995). In latent LCLs, the EBV genome exists in multiple circular forms known as episomes. The number of episomes can vary from 1 to more than 50 copies (Kripalani-Joshi and Law 1994).

The episomes are tethered to host cellular mitotic chromosomes via the virus protein EBNA1 that binds repetitive sequences in the latent origin of replication OriP to retain viral genomes in the nuclear and chromosomal domains during host cell division. There are RGG-like motifs in the EBNA1 N-terminal domain that can interact with the host cell protein EBP2 (Kapoor et al. 2005), with AT-rich DNA (Sears et al. 2004) and with G-quadruplex RNA (Norseen et al. 2009). Recent research has revealed that EBNA1 forms a DNA crosslink with the EBV origin of plasmid replication oriP, which is crucial for episome maintenance and the generation of EBV-transformed lymphoblastoid cell lines. This crosslinking is cell cycle-dependent, and EBNA1 tyrosine 518 (Y518) is essential for crosslinking to oriP and for replication fork termination at oriP in vivo. The study has also identified that EBNA1 forms tyrosine-dependent DNA-protein crosslinks and single-strand cleavage at oriP, which are required for replication termination and viral episome maintenance (Dheekollu et al. 2021).

1.3 The structure of EBV

The mature EBV virion is about 122-180nm in size (Aguayo et al. 2021). Starting from the inside, a herpesvirus particle comprises four layers: DNA core, capsid, tegument, and envelope. The innermost part of the EBV virion contains a copy of linearized viral DNA

surrounded by the nucleocapsid. The outer layer of an EBV viral particle is composed of a complex of viral glycoprotein spikes. The space between envelope proteins and viral nucleocapsid is filled with the so-called tegument proteins, which are crucial for the assembly infection and maturation of virus (Hutt-Fletcher 2015). The viral glycoproteins determine the tropism for host cells by interacting with different cellular surface molecules and mediate attachment, fusion, and entry into the host cells (Fig.2). B-lymphocytes and epithelial cells are the major sites for EBV infection and EBV uses different glycoprotein combinations to infect B cells and epithelial cells. CR2, also known as CD21, is expressed on B-lymphocytes and is the receptor for the attachment to the EBV viral envelope glycoproteins gp350/220 to its target cell (Young et al. 2007). Compared to B-lymphocytes entry, gp350/220 is not required for EBV infection for epithelial cells but may be replaced functionally by the EBV BMRF2 protein (Connolly et al. 2011; Xiao et al. 2008).

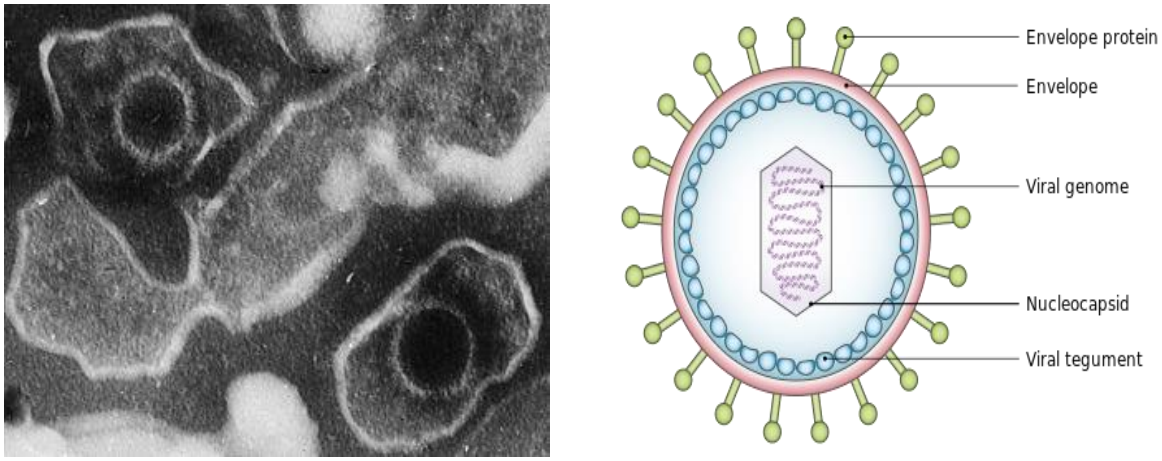

Fig.2: The EBV structure. An electron micrograph (left) and a simplified diagram of the structure of EBV (right) virions are shown. The electron micrograph of two Epstein Barr Virus virions (virial particles) shows round capsids-protein-encased genetic material loosely surrounded by the membrane envelope. The annotated representation of an EBV virion portrays the classic structural features of herpesviruses. The linear dsDNA genome is packaged by a protein nucleocapsid which is surrounded by an envelope containing both lipids and surface glycoproteins. The two pictures were taken from Wikipedia.

1.4 Entry into target cells

EBV can target either the B cells or epithelial cells via interactions with a wide range of glycoproteins (Mohl et al. 2019). The fusion of EBV with B cell or epithelial cells requires three glycoproteins, the gH, gL and gB which are partly conserved in the herpesvirus family (Spear and Longnecker 2003). Under some conditions, EBV may infect T cells, natural killer cells, smooth muscle cells, and monocytes (Hutt-Fletcher 2007). The function of each glycoprotein and glycoprotein subgroups greatly differs in attachment, binding, and membrane fusion entry processes, and targeting infection cells (Fig.3).

The mechanisms underlying the attachment of EBV to B cells and epithelial cells are different. The entry of EBV into B cells is through endocytosis (Tanner et al. 1987). Here, the interaction of gp350/220 with the host CR2 is responsible for EBV attachment to B cells with high affinity (Moore et al. 1989). EBV lacking gp350/220 have a greatly reduced binding and transforming ability in B cells (Janz et al. 2000). Both antibodies to gp350/220 or to soluble forms of CR2 block virus binding, thereby neutralizing B-cell infection (Moore et al. 1991; Tanner et al. 1988). EBV gp350/220 first attach with CR2, and then tethers EBV to B-cell membranes (Birkenbach et al. 1992). In a second step, gH/gL-gp42 binds to receptor HLA class II. This process of binding enables gH/gL-gp42 to interact with the prefusion form of gB.

In contrast to B-cells, the role of CR2 in epithelial cell infection, if any, remains unclear. Low levels of CR2 may be expressed by malignant epithelial nasopharyngeal cells (Billaud et al. 1989). Moreover, CR2/CD21 was detected on both apical and basolateral surfaces of polarized MDCK cells, with predominant expression basolaterally (Chodosh et al. 2000). However, CR2 expression on normal tissues is restricted to tonsil and adenoid epithelium (Jiang et al. 2012).

The current view is that epithelial cells generally do not express CR2 at significant levels (Fingeroth et al. 1999; Java et al. 2015; Miller and Hutt-Fletcher 1992). The entry of EBV into epithelial cells occurs through direct fusion with the cell membranes (Molesworth et al. 2000; Oda et al. 2000). This contrasts with B cells in which EBV entry relies on endocytosis after CR2 binding. BMRF2, a multi-span EBV membrane protein has been reported to play a significant role in epithelial entry. BMRF2 contains an extracellular RGD motif that acts as a ligand for α1, α5, α3, and αv integrins (Chesnokova and Hutt-Fletcher 2011). This interaction is particularly crucial for infecting polarized epithelial cells. Notably, antibodies targeting BMRF2 or alpha5β1 integrin effectively block EBV infection of polarized epithelial cells through the basolateral cell surface.

Two other glycoproteins, gH and gL, serve as ligands for epithelial cells. gH/gL can bind to the Ephrin receptor A2 (EphA2) and to the nonmuscle myosin heavy chain IIA (NMHC-IIA). EBV gB can also interact with NRP1. These interactions trigger a membrane fusion signal, facilitating the fusion of the viral envelope with the host cell membrane (Wang et al. 2015; Xiong et al. 2015; Zhang et al. 2018).

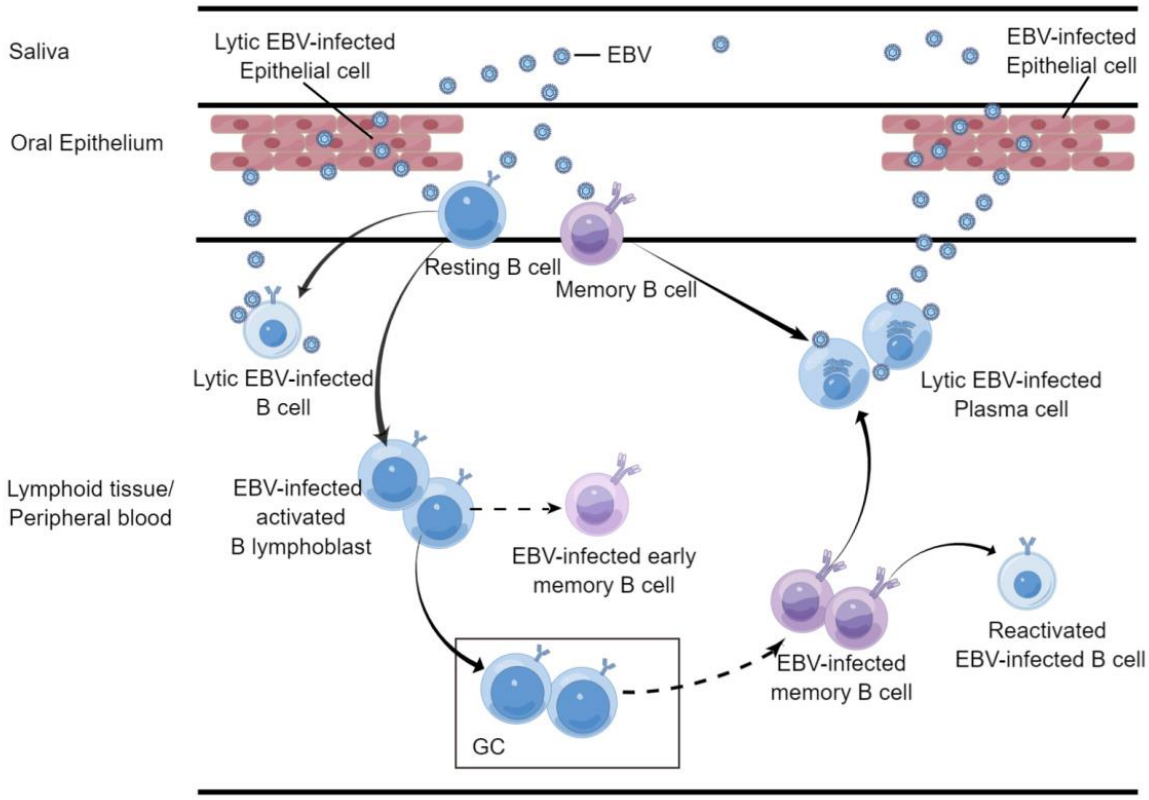

Fig.3: Model illustrating EBV infection in humans. EBV is transmitted through saliva usually and first comes in contact with oropharynx and tonsils, where it primarily infects naïve B cells, memory B cells and possibly epithelial cells. EBV then establishes latent infection in naïve B cells, while a small fraction of them enters lytic infection. The latently infected naïve B cells undergo a phase of rapid expansion under the influence of EBV latent genes, then enter the germinal centre (GC), transiting to a more restricted form of viral latency. The infected B cells differentiate into resting memory B cells, where EBV maintains its lifelong persistence. The EBV-infected resting memory B cells recirculate to the peripheral blood. Under certain stimulations, these resting memory B cells can differentiate into plasma cells. Then they re-enter a lytic infection state, producing infectious virions, which starts a new round of transmission. This image was adapted from Guo-Long Bu *et al*., 2022 (Bu et al. 2022).

1.5 The EBV lifecycle

EBV can induce in its target cells a latent or a lytic infection. EBV generally establishes latent infection in B cells and lytic infection in epithelial cells to generate progeny virions

(Kenney and Mertz 2014). Both latent and lytic infections of EBV are associated with viral persistence and lifelong infection in humans (Hatton et al. 2014).

1.6 Latent phase

When EBV accomplishes primary infection of B-lymphocytes, the EBV genomic DNA exists as a circular plasmid and behaves like a miniature host chromosomal DNA (Jochum et al. 2012). Latency results in the transformation of B-cells into proliferating lymphoblastoid cell lines (LCLs). During latency, no infectious viral particles are synthesized (Thorley-Lawson 2015), and only a few viral proteins and transcripts are produced (Babcock et al. 1998; Hochberg et al. 2004; Miyashita et al. 1997). These latent viral proteins activate the proliferation of host B-cells and contribute to lymphoproliferative disease in immunosuppressed patients.

In the early phases of EBV infection in B cells, six EBV nuclear antigens (EBNAs) are transcribed from an early latent promoter (Wp). Subsequently, promoter usage shifts to an upstream promoter, Cp, which is autoregulated by both EBNA1 and EBNA2 (Schlager et al. 1996; Woisetschlaeger et al. 1990). The transcription factor EBNA2 has the ability to activate viral LMP genes and around 300 cellular genes, such as MYC and RUNX3 (Spender et al. 2006; Zhao et al. 2006). These genes, along with their downstream targets, play a crucial role in promoting the proliferation and survival of EBV LCLs. EBNA-LP (EBNA leader protein), along with its role in co-activating certain genes with EBNA2, also facilitates the recruitment of multiple transcription factors to the viral genome, which enables the transcription of genes associated with EBV latency (Szymula et al. 2018). EBNA3 family proteins, including EBNA3A, EBNA3B, and EBNA3C, have distinct functions. While EBNA3A and -3C collaborate to facilitate transformation, EBNA3B is not required for this process (Allday et al. 2015). These proteins also function as gene expression regulators, either repressing or activating genes.

In addition to the EBNA and LMP proteins, EBV also produces several functional RNAs, including EBER RNAs and multiple miRNAs, after B cell infection. The BART miRNAs have been shown to target a range of potentially cancer-relevant genes, including tumor suppressors such as DICE1 (Lei et al. 2013), PUMA (Choy et al. 2008), PTEN (Cai et al. 2015), and BCL2L11 (BIM).

Deletions of specific viral genes in EBV mutants have demonstrated the indispensability of EBNA1, EBNA2, EBNA3C, and LMP1 in the conversion of primary human B cells to LCLs. In addition, at least one of the two viral anti-apoptosis genes, BHRF1 or BALF1, is necessary

for the process (Altmann and Hammerschmidt 2005).

1.7 Latency expression programs

During latency, LCLs express viral latent proteins that consist of six EBV nuclear antigens (EBNAs 1, 2, 3A, 3B, 3C, and EBNA-LP) and three latent membrane proteins (LMPs 1, 2A, and 2B). They also express viral noncoding EBER RNAs (EBER1 and EBER2) and EBV-encoded microRNAs (miR-BHRF1 and miR-BART) (Price and Luftig 2014). The viral products expressed in infected cells and in diseases caused by the virus are grouped in distinct programs during EBV latent infection. Three different latency programs are recognized depending on the lymphoproliferative disorders, each of which is associated with a different stage of B-cell infection. In Latency III, EBER1, EBER2, EBNA1–3, LMP1, LPM2A, and LMP2B are expressed. This viral expression pattern is associated with EBV post-transplant diffuse large B-cell lymphoma (PT-DLBCL). In Latency II, it is more restricted in its protein expression (EBER1, EBER2, EBNA1, LMP1, LMP2A) and is associated both with PT-DLBCL and Hodgkin lymphoma. The most restrictive latency program is Latency I with the expression of only EBER1, EBER2, EBNA1, that is associated with BL (Elgui de Oliveira et al. 2016; Kempkes and Robertson 2015; Morscio and Tousseyn 2016). Latency 0 is the predominantly silent state where only EBERs are expressed in peripheral memory B cells (Murata et al. 2014). The expression pattern of EBV proteins and RNAs under different latency programs is presented in Table. 1 for reference and comparison.

Table.1 EBV latency programs: expression of proteins and RNAs.

Type of latency	EBER	EBNA1	BART	LMP1/2	EBNA2, 3A/B/C, LP
Latency III	×	×	×	×	×
Latency II	×	×	×	×	
Latency I	×	×	×		
Latency 0	×				

After infection, EBV can express its genes in four different patterns referred to as type 0, type I, type II, and type III latency. Type 0 latency does not express any proteins, while type I expresses only EBNA1. Type II expresses EBNA1, LMP1, and LMP2, and type III expresses all of the EBV-associated latency proteins, including EBNA1, EBNA2, EBNA3, EBNA-LP, LMP1, and LMP2. However, in all types of latency, EBERs are expressed. BART, on the

other hand, is expressed in all forms of latency, except for latency 0.

1.8 Lytic phase

The lytic cycle is initiated by the viral immediate-early genes, BZFL1 (also known as ZEBRA, Zta, EB1, or Z) and BRLF1 (also known as Rta or R) (Binne et al. 2002; Miller et al. 2007). BZLF1 binds and activates promoters containing Z-response elements (ZREs) (Niller et al. 2009; Sinclair 2013), and seems to preferentially bind ZREs that are highly methylated (Kalla et al. 2010; Woellmer et al. 2012). BRLF1 can enhance transcription directly by binding DNA at GC-rich promoter sequences to activate transcription (Gruffat and Sergeant 1994) BZLF1 and BRLF1 are transcription factors, activating each other's promoters (Flemington and Speck 1990; Ragoczy et al. 1998; Zalani et al. 1996). The activation will then subsequently initiate the expression of a panel of EBV early genes, including BMRF1, a viral DNA polymerase processivity factor (also called early-antigen diffuse (EAD)) and BGLF4, a virus-encoded protein kinase (Kenney and Mertz 2014). Once the viral DNA has been replicated, the late lytic genes are expressed, many of which encode structural or packaging elements of the virus.

1.9 Reactivation from latent phase to lytic phase

Although EBV is usually found to be latent in infected cells both *in vivo* and *in vitro*, the virus regularly reenters the lytic cycle to produce progeny viruses and infect new cells within the host, thereby guaranteeing persistence and dissemination into new hosts. Thus, EBV occasionally reactivates out of latently infected B cells. While latent infection permits persistence of the virus for the life of the host, lytic replication enables production of infectious virions necessary for transmission from cell to cell and host to host. As it is known that EBV persists in a latent form in B cells, it can switch to a lytic infection which is called reactivation. The synthesis of BZLF1 is sufficient to induce reactivation in most-positive cell lines (Countryman et al. 1987), while BRLF1 induces reactivation in some cell lines (Wille et al. 2013; Zalani et al. 1996). EBV reactivation has been shown to occur in a subset of individuals with a variety of cancers, autoimmune diseases, the autoimmune-like diseases etc, (Kerr 2019). Chronic EBV reactivation plays an important role in the pathogenesis of many such diseases.

In 1970, HKLY-18, a B cell lymphoblastoid cell line (LCL), was established from the tissue

of a Hong Kong Chinese patient with nasopharyngeal carcinoma (De-The et al. 1970). Then virus from this line was passaged to B cells, and two LCLs (M81 and M82) were generated (Desgranges et al. 1976). M81 EBV virions were then used to generate LCLs from human cord blood and adult lymphocytes. The properties of LCLs infected by M81 were compared to those LCLs made from the prototype EBV strain B95-8 (Desgranges et al. 1979).

EBV lytic reactivation and viral particle production occur exclusively in plasma cells in healthy carriers (Heldwein 2016). M81 LCLs spontaneously expressed early lytic antigens at a significantly higher rate than B95-8-derived LCLs. M81 LCLs spontaneously expressed viral capsid antigens (VCAs) and produced infectious virions from cord blood LCLs, which were never observed with the B95-8-derived cord blood LCLs. M81 strain of EBV demonstrated lytic replication and high-titre virus production when compared to the prototype B95-8 EBV strain. In addition, M81 was demonstrated to possess enhanced epithelial cell tropism compared to B95-8. The enhanced lytic properties of M81 were shown to be partly attributable to the functional properties of the M81 BZLF1 trans activator protein (Kraus et al. 2017).

In vivo, the lytic cycle is thought to occur in terminally differentiated plasma cells and epithelial cells (Thorley-Lawson 2015). In vitro, replication occurs sporadically in a small population of cells in latent LCLs and tumour cell lines. Although the frequency and rate of lytic cycle activation can vary between cell lines and types, usually around 1-5% of cells are found to express the lytic cycle marker gene, BZLF1, in LCL cultures at any given time (Vrzalikova et al. 2011).

Reactivation of EBV can be induced in cultured cells by treatment with chemicals, such as phorbol esters, calcium ionophores butyrate (Gorres et al. 2014; Imai et al. 2012), histone deacetylase (HDAC) inhibitors, hypoxia, reactive oxygen species (Kenney and Mertz 2014; McKenzie and El-Guindy 2015) or lgG-receptor crosslinking, B-cell antigen receptor (BCR) activation (Thorley-Lawson 2015), and transforming growth factor β (TGF-β) (Fahmi et al. 2000; Iempridee et al. 2011), etc. Although the exact trigger remains elusive, EBV reactivation can occur in response to a variety of stimuli. However, these approaches are weakly effective.

1.10 EBV-associated malignancies

EBV is associated with multiple types of cancers, including Burkitt's lymphoma (BL), nasopharyngeal carcinoma (NPC), Hodgkin lymphoma (HL), gastric cancers (GC), diffuse

large B-cell lymphomas (DLBCL), and post-transplant lymphoproliferative diseases (PTLD) (Kutok and Wang 2006; Rickinson 2014) etc.

1.11 Burkitt lymphoma

Burkitt's lymphoma (BL) obtained its name from the Irish surgeon Denis Burkitt. Later it was identified as a rare, aggressive subtype of non-Hodgkin lymphoma. Among human neoplasms, it has the shortest doubling time, and the first malignancy to be linked to EBV.

The World Health Organization now recognizes the existence of three clinical subtypes of BL: endemic BL (eBL), sporadic BL (sBL), and immunodeficiency-related BL including HIV and organ transplantation (Satou et al. 2015). These types are similar in morphology, immunophenotype, and genetic features, but have different epidemiologic and clinical features (Sabattini et al. 2010). The eBL tumors are commonly associated with EBV infection. A key clinical observation is that the cases are confined to specific geographic regions. It remains the most prevalent pediatric cancer in sub-Saharan Africa, typically occuring in children between 5 and 9 years of age, with a male: female ratio of 2:1. The tumor involves the bones of the jaw and other facial bones, as well as kidneys, gastrointestinal tract, ovaries, breast, and other extranodal sites. However, contemporary studies show that abdominal involvement is now more common (Gopal and Gross 2018). It is thought that the oncogenic potential of EBV and malaria coinfection contributes to the oncogenesis (Crombie and LaCasce 2019) as the epidemiological maps of malaria and Burkitt's lymphoma overlap (Kafuko and Burkitt 1970). The sporadic type occurs throughout the rest of the world (predominantly North America and Europe), with no special climatic or geographical links, and is rarely associated with EBV infection. The immunodeficiency-related type is seen most often in immunosuppressed patients in non-endemic areas, especially when associated with HIV infection.

Of note, the disease is one of the first tumors shown to have a chromosomal translocation that activates the oncogene (c-MYC) (Adams et al. 1985). All the variants are associated with MYC oncogene deregulation and ectopic expression by chromosomal translocations which is the key molecular driver and hallmark of BL (Schmitz et al. 2014). The molecular consequence of the three translocations, t (8;14) (q24; q32), t (2;8) (p12; q24) and t (8;22) (q24; q11), is a deregulated expression of the MYC oncogene and uncontrolled tumor proliferation (Bernheim et al. 1981; Bertrand et al. 1981; Kaiser-McCaw et al. 1977).

While the overexpression of C-MYC can promote cell proliferation, it can also lead to

apoptosis, indicating that MYC translocation by itself is insufficient for cancer development (Lopez et al. 2019; McMahon 2014). Early genetic studies show that the presence of mutations in p53, along with mutations in the phosphatidylinositol 3-kinase (PI3K) signaling pathway that contributes to oncogenesis (Grande et al. 2019; Schmitz et al. 2012).

Although children and adolescents can be cured with a short course of chemotherapy, progress in the advancement of therapeutics has been difficult and almost all cases of recurrent or refractory disease are fatal (Ngoma et al. 2012). BL has the shortest doubling time among human neoplasms, and its unequalled proliferation rate can create challenges for its diagnosis and treatment. Adults are more susceptible to the toxic effects of treatment, but 75 to 85% of patients have a long-term remission (Evens et al. 2021).

By gaining a deeper comprehension of the biological mechanisms underlying resistance of these tumors to current treatments, the development of novel pathway inhibitors and immunotherapy will be facilitated, thereby advancing the field of global oncology and improving the survival rates of patients with BL tumors (Kaymaz et al. 2017; Oduor et al. 2017; Panea et al. 2019).

1.12 Nasopharyngeal Carcinoma

Nasopharyngeal carcinoma (NPC) originates from the epithelial cells of the nasopharynx. It is a unique type of metastatic head-and-neck neoplasm that is particularly prevalent in Southern China and some other areas in East and Southeast Asia but is rare in western countries.

NPC has various histological subtypes and can be classified into three main subtypes: keratinizing squamous cell carcinoma (WHO type 1), differentiated non-keratinizing carcinoma (WHO type 2), and undifferentiated non-keratinizing carcinoma (WHO type 3) (Badoual 2022). Type 1 NPC is typically found in the older adult population, and type 3 NPC is frequent in adolescents or young adults along with few type 2 cases (Young and Miller 1975).

NPC is the endemic disease most closely related to EBV as nearly all patients diagnosed with undifferentiated NPC are EBV-positive, and partially differentiated cases are also detected as EBV-positive (Young and Dawson 2014). Elevated IgG and IgA antibody titers directed against EBV viral capsid antigens (VCA) and early antigen diffuse (EAd/BMRF1) are characteristic of NPC patients, and historically established a link between EBV infection amd the tumor (Gunven et al. 1970; Sinha and Gajra 2022).

EBV infection is predominantly latent in NPC and most viral genes are transcriptionally silent. However, some latent viral proteins and a number of untranslated latent viral transcripts are consistently active inside NPC, including latent membrane proteins 1 and 2 (LMP1/2), EBV-encoded RNAs (EBERs) and EBV-encoded BamH I-A rightward transcripts (BART) microRNAs (miR-BARTs). The contributions of these genes to NPC pathogenesis have been increasingly recognized (Iwakiri et al. 2009; Tsao et al. 2017; Zhang et al. 2017; Zhu et al. 2016; Zhu et al. 2022).

Although EBV is present in nearly all malignant NPC cells, viral gene expression can vary. While it's typically categorized as EBV latency II, LMP1 expression can be undetectable in many cells. Mutations in the NF-κB pathway may complement the role of LMP1 and allow for its loss (Li et al. 2017). Both LMP1 and LMP2A have been found to promote epithelial cell growth or prevent differentiation in vitro, with LMP2A often present in NPC cells. However, all EBV-infected cells have detectable levels of EBNA1, EBER RNAs, and BART miRNAs, with the latter being highly expressed in NPC and potentially contributing to its tumorigenicity through the inhibition of epithelial cell apoptosis (Kang et al. 2015).

During tumorigenesis, the EBV infection may cause epigenetic alterations (Kaneda et al. 2012). CpG hypermethylation, a mechanism that inactivates tumor suppressor genes, has been observed in NPC (Li et al. 2014). Methylome profiling of NPC cell lines and primary tumors has revealed extensive and genome-wide methylation of cellular genes involved in Wnt, MAPK, TGF-β, and hedgehog signaling. Although it is not yet known whether latent EBV infection is directly responsible for the methylation profile observed in NPC, EBV infection has been shown to drive DNA methylation in other types of cancer cells, such as the gastric cancer cell line, AGS (Kaneda et al. 2012). The expression of latent EBV genes could be directly involved in methylation of the host genome and inactivation of tumor suppressor genes to support the growth of EBV-infected cells.

The detection of EBV episomes that carry the same number of terminal repeats in NPC suggests that the viral infection occurs before the clonal expansion of cancerous cells (Raab-Traub and Flynn 1986). High-grade and carcinoma *in situ* lesions in nasopharyngeal carcinoma carry monoclonal EBV genomes. Additionally, genetic changes such as deletions on chromosomes 3p, 9p, 11q, 13q, and 14q, and promoter hypermethylation of specific genes on chromosomes 3p and 9p have been observed. Interestingly, 3p and 9p deletions have also been identified in low-grade dysplastic lesions and normal nasopharyngeal epithelium of individuals at high risk of developing NPC, even in the absence of EBV infection (Lo et al. 2012; Lung et al. 2012). This suggests that these genetic events occur early in NPC

development and may predispose to subsequent EBV infection (Chan et al. 2002; Chan et al. 2000). In vitro data support the idea that stable EBV infection of epithelial cells requires an altered cellular environment. Some other etiological factors for NPC include genetic susceptibility, consumption of food containing carcinogenic volatile nitrosamines as well as phorbol esters (Huang et al. 2010; Jia and Qin 2012; Shao et al. 1988).

EBV can cause genomic instability in infected cells through the expression of both lytic and latent genes. NPC cells often exhibit the presence of lytic EBV genes in small clusters (Martel-Renoir et al. 1995; Sengupta et al. 2006).The recurrence of lytic infection in epithelial cells infected with EBV increased their tendency to form tumors, indicating the involvement of lytic reactivation of EBV in the progression of NPC (Fang et al. 2009). Moreover, the gene products of lytic EBV may cause DNA damage and aid in the development of NPC. The expression of the lytic EBV gene BGLF5 resulted in higher levels of micronuclei and brought about genomic instability (Wu et al. 2010). The lytic EBV gene BALF3 was found to cause DNA strand breaks and the formation of micronuclei (Chiu et al. 2014). Recent research indicated that in EBV-infected B-lymphocytes, expression of BNRF1 increased chromosomal instability and centrosome amplification, suggesting a potential role for BNRF1 in promoting genomic instability during EBV-associated tumorigenesis (Shumilov et al. 2017). Despite the challenging anatomical location of the nasopharynx, chemotherapy and radiotherapy have been shown to be effective treatments for NPC. Early-stage and locally advanced NPC generally carry a good prognosis, but for the patients with recurrent/metastatic disease, alternatives are limited. Many patients who are cured still suffer undesirable effects, which strongly undermines their quality of life. Therefore, there is still an urgent need for more effective and more selective treatments.

1.13 Hodgkin lymphoma

Hodgkin lymphoma (HL) was first reported in 1832 and was initially called “Hodgkin’s disease”. HL is an uncommon neoplasm, and its overall incidence of HL is low, with about 3 new cases per 100,000 individuals per year. It is, however, one of the most common cancers diagnosed in adolescents and young adults. Albeit less frequently diagnosed, HL can also affect elderly individuals. HL is associated with peripheral lymph nodes and can also affect organs such as liver, lung, and bone marrow. HL has a few typical characteristics such as large multinucleated cells derived from B lymphocytes (also known as Hodgkin and Reed-Sternberg (HRS) cells). HLs are defined based on histological and immunohistochemical

analyses and is mainly divided in two forms, classical HL (cHL) and nodular lymphocyte predominant HL (NLPHL). HRS cells in cHL and lymphocyte predominant (LP) cells in NLPHL differ in morphology and immunophenotype, microenvironment, and their clinical behavior (Swerdlow et al. 2016).

The majority of cases, around 90% of all patients with HL, are cHL. The tissue morphology and antigen expression profile enable classification of cHL into four subtypes: nodular sclerosis HL (NSHL), mixed cellularity HL (MCHL), lymphocyte-rich HL (LRHL) and lymphocyte-depleted HL (LDHL), each having a distinct epidemiology, biology, and prognosis. It has been postulated that EBV plays an important role in the pathogenesis of cHLs as the tumor cells are infected by EBV in about 40% of cases, which is of pathogenetic relevance (Kapatai and Murray 2007).

The screening and prevention of HL is not feasible at present due to the scarcity of the tumor cells in the affected lymph nodes and no methods with sufficient sensitivity and specificity. Fortunately, HL is among the best treatable lymphomas and the preferred treatment for cHL is chemotherapy followed by radiation therapy, showing about 80-90% cure rates (Aurer et al. 2020; Borchmann et al. 2012).

New treatment approaches to reduce toxicity of treatment in particular the development of less toxic, targeted drugs have been evaluated. The CD30 antigen has been a focus of interest due to HRS cells expressing tumor necrosis factor (TNF) receptor superfamily member 8, also known as the cell surface CD30 antigen. When the relevant drugs were conjugated with anti-CD30 antibodies, it showed promising results toward cure and reduced side effects from long-term toxicity (Boll et al. 2005; Younes and Ansell 2016).

1.14 Gastric Carcinoma

Gastric cancer is a major contributor to cancer-related deaths, causing around 780,000 deaths worldwide every year, ranking as the third-highest in terms of cancer mortality globally (Anonymous 2020; Yang et al. 2020). Studies have shown that EBV is present in up to 10% of all gastric cancer cases worldwide, with the prevalence varying depending on geographic location and tumor subtype. EBV genomes were first detected in gastric carcinomas in 1990 using polymerase chain reaction and in situ hybridization for EBV-encoded small ribonucleic acid 1 (EBER1) (Burke et al. 1990). Among the various types of gastric cancer, Epstein–Barr virus-associated gastric cancer (EBVaGC) defines a separate distinct entity. The percentage of EBVaGC varies depending on geographic distribution (Camargo et al. 2011; Cristescu et al.

2015; Murphy et al. 2009; Naseem et al. 2018) and ranges from 1.3% to 30.9% of all gastric cancers (Young and Rickinson 2004). EBVaGC is considered a type of neoplasm that exhibits latency I, which is characterized by the expression of EBNA1, EBER, BART, and sometimes (in 40% of cases) latent membrane protein 2A (LMP2A) (Imai et al. 1994). Currently, EBV-negative GC (EBVnGC) and EBVaGC are typically differentiated using EBV-encoded small RNA 1/2 in situ hybridizations (EBER1/2-ISH) in histopathological specimens (Sugiura et al. 1996; Yang et al. 2020). Furthermore, the droplet digital PCR (ddPCR) technique offers a novel approach for diagnosing EBVaGC in tissue samples, as it allows for the quantification of EBV-DNA copy numbers (Shuto et al. 2019). Research has demonstrated that EBVaGC has a higher prevalence in males. While this predominance decreases with age, EBVaGC is more prevalent than EBVnGC in younger patients. Additionally, EBVaGC is often found in the middle and upper stomach, particularly in the remnant stomach after partial gastrectomy (Murphy et al. 2009; van Beek et al. 2004; Yanagi et al. 2019). After gastrectomy and chemotherapy, the plasma EBV-DNA load in patients with EBVaGC drops, whereas it increases during disease progression, indicating the potential involvement of EBV in gastric oncogenesis (Qiu et al. 2020).

Compared to other gastric cancers, EBV-associated adenocarcinomas exhibit unique features in their mutation profile, including a lack of p53 mutations, relatively frequent PI3K mutations, and a high degree of CpG methylation in the cell genome (Anonymous 2014). Methylation of host genes has been observed in several contexts upon EBV infection, and this may lead to the inactivation of tumor suppressor genes such as p73 in gastric carcinoma (Ushiku et al. 2007). The expression of p53 protein in EBV-associated gastric cancers suggests that EBV may bypass the need for p53 mutation, but further research is needed to confirm this speculation (Ribeiro et al. 2017). EBVaGC has a higher frequency (40%-80%) of PIK3CA mutations compared to other GC subtypes (3%-42%). These mutations are also more dispersed in EBVaGC than in EBVnGC (Bass et al. 2014; Cristescu et al. 2015; Gulley 2015).

Currently, there are no specific treatment options for EBVaGC, and standard treatment protocols for gastric cancer are typically employed. However, recent studies have shown that immune checkpoint inhibitors, which target the PD-L1/PD-1 axis, may be effective in treating EBVaGC. High levels of PD-L1 expression in EBVaGC cell lines suppress T-cell activation, and clinical trials of PD-L1 monoclonal antibody in patients with advanced PD-L1-positive GC are ongoing (Panda et al. 2018).

EBVaGC is a distinct subtype of gastric carcinoma associated with EBV infection,

characterized by unique clinicopathological and molecular features. The exact mechanisms by which EBV contributes to the development of gastric cancer are not fully understood, but several studies have suggested that the virus may promote carcinogenesis through various pathways. For example, EBV can infect and transform gastric epithelial cells, leading to the activation of oncogenic signaling pathways and the inhibition of tumor suppressors. Further exploration is needed to understand the specific mechanism of EBV infection in gastric carcinogenesis and the genomic profile of cancer cells. Understanding these relationships can improve diagnosis and targeted treatment strategies for patients with EBVaGC.

1.15 Diffuse large B-cell lymphoma

Lymphoma is a type of cancer that originates from lymphocytes, which can be B cells, T cells, or natural killer (NK) cells, during their maturation process in the lymphoid system. Hodgkin's and Non-Hodgkin's lymphoma (NHL) are the two main categories. NHL comprises approximately 80% of all lymphomas. More than 30 subtypes of NHL have been identified, with diffuse large B-cell lymphoma (DLBCL) and follicular lymphoma (FL) being the most common ones (Morton et al. 2006; van Leeuwen et al. 2014). DLBCL, which accounts for 25-35% of all reported cases of non-Hodgkin lymphoma, is the most common type of malignant lymphoma, and has a higher incidence in elderly individuals (Alaggio et al. 2022; Chabay 2021; Soltani et al. 2021). There is a higher occurrence of the disease in white individuals, followed by African Americans and Asians, with a higher incidence in males and a median age of 64 years, with the overall incidence increasing exponentially with age. In Asia, about 10% of DLBCL cases have EBV in the cancer cells, whereas in Western countries, that percentage falls to only about 5%, and EBV-associated cases are considered to have a worse prognosis (Lu et al. 2015).

DLBCL cases are differentiated into two categories based on their cell gene expression: germinal center B cell-like (GCB) and activated B cell-like (ABC). Although there are EBV-positive cases in both groups, the majority of them are found in the ABC group (Montes-Moreno et al. 2012).

B cell lymphomas are treated based on staging, type of disease (indolent or aggressive), and molecular subtype. Treatment for indolent lymphomas depends on the extent of the disease and on wheter the disease is symptomatic. Aggressive low-grade disease is treated with allogeneic transplantation, while mantle cell lymphomas are treated with immuno-chemotherapy and autologous stem cell transplants (Coiffier et al. 2002; Liu and Barta 2019;

Sehn et al. 2005).

Although standard immunochemotherapy is successful in treating diffuse large B-cell lymphoma (DLBCL), about 30% of patients still experience short survival (Wang et al. 2023). Additionally, the exact cause of EBV+ DLBCL is unclear and understanding the relationship between different factors and EBV infection in causing transformation will provide valuable insights into the pathogenesis of DLBCL and lead to the development of new treatments for this aggressive cancer.

1.16 Post-transplant lymphoproliferative disorders

Post-transplant lymphoproliferative disorders (PTLDs) refer to the uncontrolled proliferation of lymphoid cells resulting from extrinsic immunosuppression following solid organ transplantation (SOT) and hematopoietic stem-cell transplant (HSCT) (Aghsaeifard and Alizadeh 2022; Dharnidharka 2018).

The occurrence of PTLD differs across transplant centers and is influenced by factors such as the type of organ transplanted, the degree of HLA mismatch in allogeneic HSCT, the use of specific immunosuppressive regimens, the presence of other risk factors, and individual patient characteristics (Bustami et al. 2004; Dharnidharka 2005; Dierickx and Habermann 2018; Dierickx et al. 2015; Funch et al. 2005; Kirk et al. 2007; Reshef et al. 2011; Savani et al. 2009; Vincenti et al. 2007).

EBV is known to have a significant influence on the development of early-onset PTLD through various mechanisms. In particular, the majority of early-onset PTLD cases are associated with EBV in both SOT and HSCT patients. The incidence of PTLD follows a bimodal distribution, with a rise in incidence of SOT PTLD after 5 years of transplantation (late-onset PTLD). However, it should be noted that late-onset PTLD cases may often be EBV-negative (Curtis et al. 1999; Dharnidharka 2018; Dierickx et al. 2015; Landgren et al. 2009; Luskin et al. 2015).

The manifestation of symptoms and signs depends on the location of the lymphoid masses, and diagnosis typically requires histopathology, supported by imaging techniques (Capello et al. 2005; Dharnidharka 2018; Glotz et al. 2012). Recipient EBV seronegativity (Raab-Traub 2012) and the intensity of immunosuppression are among the major risk factors (Grulich et al. 2007). Monitoring EBV levels in blood for pre-emptive intervention has emerged as the preferred strategy for PTLD prevention (Green 2001).

The treatment of established PTLD involves reducing immunosuppression, administering

rituximab (a B-cell-specific antibody against CD20) (Khalil et al. 2018), chemotherapy, and EBV-specific cytotoxic T cells.

Despite these interventions, mortality and morbidity rates remain high, and patient outcomes depend on the severity of the presentation, treatment-related complications, and the risk of allograft loss. Innovative treatment options hold promises for improving outcomes in the future.

The understanding of PTLD pathogenesis is incomplete. The cause of EBV-negative PTLD and non-B cell PTLD is unknown, and the factors that influence EBV-positive PTLD are not clear. It is also unclear whether the cumulative immunosuppression burden that triggers PTLD is related to maximal intensity at a point in time or based on a high burden over some period of time. Developing biomarkers to monitor immunosuppression may help prevent PTLD and improve therapy. Achieving transplant tolerance may also confer tolerance to EBV, which could be a very adverse outcome. Future studies of PTLD may unlock important pathways in other major disciplines of medicine and biology.

Table.2 Latent viral protein expression patterns in EBV-associated malignancy.

Tumor type	EBV protein expression
Burkitt lymphoma	EBNA1
Nasopharyngeal carcinoma	EBNA1, LMP2
Hodgkin lymphoma	EBNA1, LMP1, LMP2
Gastric carcinoma	EBNA1, LMP1, LMP2
Diffuse large B-cell lymphoma	EBNA1, LMP1, LMP2
Post-transplant lymphoproliferative	EBNA1, 2, 3A, 3B, 3C, LP, LMP1, LMP2

1.17 RAB11FIP1

RAB11FIP1 (also known as Rab-coupling protein, RCP) is a member of the Rab11 interacting proteins (RAB11FIPs) that influences Rab11-mediated recycling of vesicles and is involved in endosomal trafficking and receptor sorting (Baetz and Goldenring 2013; Jing et al. 2010; Rainero et al. 2012). Owing to the highly conserved C-terminal RBD (Rab11-binding domain), RAB11FIPs were initially characterized by their ability to bind Rab11 subfamily members. Rab11 is a small GTPase that plays a role in regulating membrane traffic from the endocytic recycling compartment, also known as recycling endosome (ERC) to either the plasma membrane or the trans-Golgi network (TGN) (Horgan and McCaffrey 2009).

Altogether, the RAB11FIP family has five members and is subdivided into Class I and Class II, based on domain organizations. Class I RAB11FIPs has three members, RAB11FIP1, RAB11FIP2, and RAB11FIP5. Class II RAB11FIPs consist of RAB11FIP3 and RAB11FIP4. Class I RAB11FIPs have a C2 domain in NH_2-terminal and associate with membranes through lipid binding (Lindsay and McCaffrey 2004; Machesky 2019). Class II RAB11FIPs have an ezrin-radixin-moesin domain at the C-terminal and a helix-loop-helix structural domain at the NH_2-terminal region (Lindsay and McCaffrey 2004).

RAB11FIPs bind and are localized to the ERC under steady-state conditions. Studies have identified that RAB11FIPs play key roles in the regulation of multiple distinct membrane trafficking events, which are currently subgrouped into three categories: recycling of cargoes to the cell surface, delivery of membrane to the cleavage furrow/midbody during cell division, association between Rab11 and molecular motor proteins (Horgan and McCaffrey 2009). Class I RAB11FIPs have been associated with the trafficking of multiple cargoes, for example, GLUT4-containing vesicles (Bruno et al. 2016), the water channel protein AQP2 (Nedvetsky et al. 2007), the chemokine receptor CXCR2 (Fan et al. 2003), and different integrin complexes (Eva et al. 2010). Class II RAB11FIPs, RAB11FIP3 and RAB11FIP4, have been shown to play key roles during cytokinesis during which they couple Rab11 and Arf6 during cell division (Ai and Skop 2009). RAB11FIP1 proteins segregate into distinct compartments within plasma membrane recycling systems (Horgan and McCaffrey 2009). Multiple RAB11FIP1 splice variants have been identified (Jin and Goldenring 2006). RAB11FIP1A was first discovered as an interactor of Rab11 (Hales et al. 2001), and RAB11FIP1C is an 80-kDa protein that interacts with GTP-bound Rab4 (Lindsay et al. 2002). RAB11FIP1 possesses a homologous C2 domain and a Rab binding domain (RBD) near the amino-terminus and the carboxyl terminus, respectively (Prekeris et al. 2000). RAB11FIP1 proteins are involved in controlling membrane trafficking along the phagocytic pathway as well as early endosomal trafficking into the recycling system (Schafer et al. 2016). Rab4, Rab11 and Rab5 have been known to bind RAB11FIP1 through their RBD domain (Lindsay et al. 2002). The C2 domain of the class I Rab11FIPs plays an important role in regulating the transport of cargo to the plasma membrane. Several studies have demonstrated that the expression of RAB11FIPs truncation mutants without C2 domain led to a significant inhibition in endosomal recycling (Lindsay et al. 2002; Lindsay and McCaffrey 2002; Prekeris et al. 2000). It is thought that the C2 domain of class I RAB11FIPs targets docking sites on the plasma membrane that are enriched in phosphatidylinositol-(3,4,5)-triphosphate and phosphatidic acid (Lindsay and McCaffrey 2004).

An abnormal RAB11FIP1 expression has been observed in several malignancies, including head and neck squamous cell carcinoma (Dai et al. 2012), breast cancer (Zhang et al. 2009; Zhang et al. 2016), and non-small cell lung carcinoma (NSCLC) (Balsara et al. 1997). Such overexpression was correlated with a progression of the disease and reduced survival of patients (Cho and Lee 2019). Among breast cancer tumors, expression of RAB11FIP1 was highest in estrogen receptor (ER)-positive luminal B type tumors and lowest in ER-negative basal-like tumors (Mitra et al. 2016). Recent studies have shown that RAB11FIP1, in combination with Rab14, influences human immunodeficiency virus (HIV-1) envelope complex incorporation onto particles in relevant human cells (Qi et al. 2013).

1.18 Aim of this study

EBV lytic replication, more generally described as EBV reactivation has been shown to occur in a subset of individuals with a variety of autoimmune diseases and cancers. Thus, modulation of EBV reactivation may be a target for disease prevention. Our comprehension of the interactions between endogenous cellular factors and the viral latency program, governing the expression of viral regulatory switch genes BZLF1 and BRLF1, remains constrained. Most experimental procedures that drive latent cells into lytic replication are based on treatment with chemicals that might act in a completely unphysiological manner.

Therefore, the objectives of this thesis are:

1) To use a spontaneously replicating LCL to identify the key cellular genes expressed during the spontaneous lytic replication of LCLs.
2) to explore the mechanisms through which these cellular proteins enhance spontaneous EBV replication in B lymphocytes.

2. Material and methods

2.1 Materials

2.1.1 Cells

Bacteria

Strain	Primary Use	Genotype
E. coli DH5α	Molecular cloning	F- Φ80lacZΔM15 Δ(lacZYA-argF) U169 recA1 endA1 hsdR17 (rk-, mk+) phoA supE44 λ-thi-1 gyrA96 relA1

Eukaryotic cells

Name	Description
HEK293	Human embryonic kindey cell line transformed with sheared Adenovirus 5 DNA
Producer cells	M81 EBV producer cell line was used in this study. M81 cell line was generated by transfecting HEK293 cells with BAC DNA and selecting with hygromycin (100 µg/mL)
B lymphocytes	Primary B cells isolated from blood samples

2.1.2 Cell culture media

Name	Source of supply
RPMI 1640	Invitrogen
Fetal calf serum (FCS)	Biochrom AG

2.1.3 Plasmids

Internal lab. Label	Description
p509	A plasmid with a PK5 backbone that contains BZLF1 from the B95-8 strain of EBV, controlled by a CMV promoter.
P2130	A plasmid with a PK5 backbone that contains BRLF1 from the B95-8 strain of EBV, controlled by a CMV promoter.

EBV-BACs

Internal lab. Label	Description
B110	Recombinant M81 wild-type virus
B1039	A recombinant M81 construct was generated by inserting rat CD2 into the BXLF1 locus.

2.1.4 Oligonucleotides

Aim	**Name**	**Sequence**
ATF3	fwd	GGGTAACTCATTCGACTGTGGA
	rev	ACGGTAACTGCTTTTCCCTGT
BAX	fwd	GTTTTCTGACGGCAACTTCAAC
	rev	GAAGTCCAATGTCCAGCCCA
BIN1	fwd	CAACACGTTCCAGAGCATCG
	rev	CGACCAGCACATCATTGAGG

BZLF1	fwd	CAGCAGCAGTGGTGTTGG
	rev	CGCATTCCTCCAGCGATTC
CARKD	fwd	TGCTAAGACTCAGCCAAGCC
	rev	TGTTTTCTGTGGTCCAGCAAG
CATSPER2	fwd	TGCCATTCGTTCACGTCTCA
	rev	TCCGGCCCACAAAGAAAGAG
CREBRF	fwd	CACTCTGGGGAAACCTGCTG
	rev	ATCCATTCCGCTTACACTAGGC
DKK4	fwd	TGGACTTCAACAACATCAGGAG
	rev	GGTATTGCAGTCCGTGTCAG
FAM175A	fwd	TCCACTGGTTTTAGCCGAGC
	rev	TGCCTGAATCTGTGCTCCTC
FOS	fwd	TTCAACGCAGACTACGAGGC
	rev	CGTGGGAATGAAGTTGGCAC
HILPDA	fwd	TGAGTTTTGTGGCGGGAAGC
	rev	ATGGCTGAAAGGACCCTACTC
ING1	fwd	CTCGCCTCTGGAAAAAGTGAC
	rev	ACGATCTGGATCTTCTCGTCG
	ING1 probe	5'FAM-TGAAGGAGCTAGACGAGTGC-3'TAMRA
KIDINS220	fwd	GGACAGCTCTTATGTGGGCA
	rev	CGTGCAGCCCAAACTAAAGG
MAGT1	fwd	GCGGTTTTGGTGTGTCTCTG
	rev	ATTTCTCGGTGGGGCTTTCA
MAL	fwd	TTCTCCTACATAGCCACTCTGC
	rev	GGGTTTTCAGCTCAAGTTCTACTG
MBD4	fwd	CCCCCACCGTCACCTCTA
	rev	AGCAAGGGATTACATTCACTGC
MIER2	fwd	GCGTCAGACCCCATTTCAGA
	rev	GTGAGGTCGTCAGCAGATGA
MINDY1	fwd	ACTGCCTCCTGTCCATCAAG
	rev	CGCACATTGACATCCAGACC
MTHFD2	fwd	GTTGGCGAGAATCCTGCAAG
	rev	AGGCAACTGAACAAGGAGGC
MXD1	fwd	GCTGAACATGGTTATGCCTCC
	rev	CAACTTCTCCAGGCACAAGC
NFATC1	fwd	ATGGAAGCGAAAACTGACCG
	rev	TTAGAAAAAGCACCCCACGC
PRMT1	fwd	AGCAGTGAGAAGCCCAACG
	rev	GGTTATGAAACATGGAGTTGCGG
PTGR2	fwd	CCGAATGGAAGAAGTCTATTTACCAG
	rev	TTGAGATAGCTGCCAAGGTGT
RAB11FIP1	fwd	AAAAAGTGCTGCTTCGTCCC
	rev	TCCGTACTCGCTGTTCTCTTG
RAB11FIP3	fwd	CTGAAGGCCAACATTGAGCG
	rev	AACTGGTGCCTCTCGTGACT
RASSF6	fwd	GCAAAGGAATGACACGCTGG
	rev	CCTTTGCATGTGGCTTCAGG
RGS1	fwd	TCTGGAAAAACTTCTTGCCAACC
	rev	TAGTCTTCACAAGCCAGCCAG
RGS2	fwd	CACAAGAGCGAGGAGAAGCG
	rev	GGGCTTCCCAGGAGTAGAGG
SAP130	fwd	AAGCAAGAGCCTGTTGTGGT
	rev	TAGAAGGTGGAGCAGGAGCA
SGK1	fwd	TGGGCTACCTGCATTCACTG
	rev	ATACAAGACAGCTCCCAGGC
SMYD4	fwd	ACAGCAGAGACCTTGAGGGA
	rev	CGAGTCCTTTCCCACCAAGT
TMEM106A	fwd	AGTTGGTGGCTCTCATTCCC
	rev	ATCAAAGGCCACTGTGGAGG
USP48	fwd	GCTTGGTTGGTATTGGTGAGC
	rev	AAGTAGAGTGCCTGCCGAAG
WSB1	fwd	GTGTTCAGTCGGAGCCAGTA
	rev	GCAGTAGCCAGTAATGCTCCA
ZNF84	fwd	CACAGTTTTGGGGCAGAAGC
	rev	TAGCTGCCACTCCTTTTGGG
ZNF483	fwd	GTTGGTGCTGTTTGCGGATG

	rev	AGTACAGTCCACCAACAGGC
HPRT	fwd	TGCTGAGGATTTGGAAAGGG
	rev	ACAGAGGGCTACAATGTGATG
TFRC	fwd	AATCCTGGGGGTTATGTGGC
	rev	GGTGATTTTCCCTGCTCTGAC

2.1.5 Antibodies

Name	Supplier
rat CD2	Hybridoma supernatant
α-gp350	Supernatant from hybridoma clone 72A1
Anti-rabbit lgG (HRP, secondary antibody)	Cell Signaling
Anti-mouse lgG (HRP, secondary antibody)	Promega
LMP1	Hybridoma supernatant
BZLF1	Hybridoma supernatant
RAB11FIP1	Cell Signaling
Rab9	Santa Cruz Biotechnology
Syntaxin7	Santa Cruz Biotechnology
Rab7	Santa Cruz Biotechnology
Lamin A	Santa Cruz Biotechnology
Vinculin	Santa Cruz Biotechnology
Tubulin	Sigma

2.1.6 Enzymes

Name	Company
Phusion High-Fidelity DANN polymerase	Thermo Scienfitic
Restriction Enzymes	Fermentas, New England Biolabs
Alkaline Phosphatase	Roche
T4 DNA Polymerase	Fermentas
RNase A	Roche
DNaseI	Fermentas
Proteinase K	Roche
AMV Reverse Transcriptase	Roche
RNAse inhibitor	Roche
T4 DNA Ligase	Fermentas
Taqman Universal Master Mix	Life technologies

2.1.7 Chemicals, reagents, and kits

Name	Source of supply
Acrylamide: 30% stock, with 0-8% bisacrylamide	Roche
Absolute Ethanol	Sigma
Acetic Acid	Sigma-Aldrich
Agarose	Sigma-Aldrich
Bromphenol blue	Serva
Chloroform	Carl Roth
DMSO	Sigma-Aldrich
Dynabeads CD19 Pan B	ThermoFischer
DETACHaBEAD CD19	ThermoFischer
dNTP mix (10mM)	Invitrogen
Ethanol	Sigma-Aldrich
Ethidiumbromide	Carl Roth
Fetal Bovine Serum	Biochrom
Glycerol	VWR International
Glycine	GERBU
GlycoBlue	Invitrogen
GlycoBlue	Invitrogen
Hygromycin B	Invitrogen
Isopropanol	Sigma aldrich
Metafectene	Biontex Laboratories
PBS tablets for cell culture	Gibco
Phenol	Carl Roth
Potassium acetate (KAc)	Carl Roth
Plasmid Midi Kit	QIAGEN
Protease inhibitor cocktail	Roche
Page Ruler Prestained Protein Ladder	Fermentas
Phenol/Chloroform/Isoamylalcohol	Roth
RNase inhibitor (RNasin)	Promega
Roti-Phenol	Roth
RNase free water	Invitrogen
Taqman microRNA Reverse Transcription Kit	Applied Biosystems

TRIzol reagent	Life Technologies
Tryptone	Sigma-Aldrich
Yeast extract	Sigma-Aldrich
1 kb DNA Ladder	Life Technologies
1-butanol	AppliChem
3 M sodium acetate, pH 5.5, Rnase free	Invitrogen
4% Paraformaldehyde (PFA)	AppliChem
6x DNA loading dye	Thermo Scientific
10 bp DNA ladder	Invitrogen

2.1.8 Buffers and solutions

Buffer	Composition
Antigen binding and washing	PBS+0.1% Tween 20
Blocking	buffer 5% Skim milk powder in PBST
Blotting buffer	25 mM Tris base, 150 mM Glycine and 20% Methanol
DNA gel extraction buffer	300mM NaCl, 10mM Tris (pH 8.0), 1mM EDTA
DNA loading buffer	0.25% Bromphenolblue, 40% (w/v) Sucrose, dissolved in H2O
ECL reagents	Enhanced Luminol Reagent and Oxidizing Reagent, store at 4°C
LB medium	(2:1:2) Tryptone, Yeast extract, NaCl in H2O pH7.0
LB agar	15g Bacto-Agar in 1L LB mudium
Lysis buffer (circle prep)	1% SDS, 2mM EDTA, 50mM NaCl, 40mM NaOH
Mounting buffer (IF)	90& Glycerol in PBS
PBS	137mM Nacl, 2.7mM KCl, 10mM Na2HPO4, 2mM KH2PO4, pH 7.4
PBS-T	0.1% Tween-20 in PBS
SDS loading buffer	100mM Tris-HCl pH=6.8, 4% (w/v) SDS (electrophoresis grade), 0.2% (w/v) bromphenol blue, 20% (v/v) glycerol, 200mM ß-merapto-Ethonal
Staining buffer (IF)	10% Heat-inactivated goat serum in PBS

Stacking gel buffer	2M Tris pH 6.8
Seperating gel buffer	2M Tris pH 8.9
1x bloting buffer	25mM Tris, 150mM glycine, 10% MetOH
2x SDS loading buffer	100mM Tris-HCl pH=6.8, 4% (w/v) SDS (electrophoresis grade), 0.2% (w/v) bromphenol blue, 20% (v/v) glycerol, 200mM ß-merapto-Ethonal
3% low fat milk	3% low-fat milk power in 1xPBST
5x RIPA lysis buffer	750mM NaCl, 2.5% NP40, 5% Sodium Deoxycholat, 0.5% SDS, 25mM EDTA, 100mM Tris HCl pH=7.5
10x PBST	1.37M Nacl, 27mM KCl, 100mM Na2HPO4, 20mM KH2PO4, 1% Tween 20
10x SDS running buffer	250mM Tris, 1.92M glycine, 1% SDS, pH 8.5-8.8

2.1.9 Consumables, software and equipment

Name	Source of supply
Software:	
BioRender	BioRender
MacVector Software 15.1.1	MacVector Inc.
Prism	GraphPad
Consumables:	
Amersham membrane HybondTM ECL	GE Healthcare Life Sciences
Cell culure plates	Techno Plastic Products
Disposable Scalpel	Feather
Falcon Tubes (15/50 mL)	Techno Plastic Products
Safe-Lock tubes (0.5/1.5/2.0 mL)	Eppendorf AG
Electroporation civettes (1 mm)	Carl Roth
12 well plates	Corning
Equipment:	
Incubator Hood TH 30	Edmund Buhler GmbH
Incubator for bacteria (B 5060)	Heraeus
Hera Cell 150 incubator	Thermo Scientific
Light inverted microscope, DMIL-Led	Leica

Fluorescent microscope DM5000B	Leica
pH-meter 766	Knick
Sonicator UW2070	Bandelin Electronics
Step One Plus™ qPCR machine system	Applied Biosystems
Applied Biosystems 7300 Real-time PCR	UVP
Magnetic rack	Applied Biosystems
Nanodrop	GE Healthcare Life Sciences

2.2 Methods

2.2.1 Culture conditions of bacteria

In order to grow E. coli strains, two different methods were used: shaking in low-salt Luria-Bertani (LB) medium or on LB-agar plates in an incubator, both supplemented with ampicillin (100 µg/ml) for culturing. The optimal temperature for bacterial growth was maintained at 37°C, except under special circumstances where other conditions were necessary. To ensure that the bacterial strains were preserved for future use, 10% glycerol was added before freezing the samples at -80°C, allowing for long-term storage.

2.2.2 Sequencing of plasmid DNA

Eurofins MWG Operon (Ebersberg, Germany) conducted the plasmid DNA sequencing. The samples that were sent for sequencing underwent a preparation process, which involved mixing 13.5 µL of template DNA (100 ng/µL) with 1.5 µL of the appropriate oligonucleotide (10 mM). The sequencing results were thoroughly analyzed with the help of MacVector software version 15.1.1, ensuring accurate and reliable interpretation of the data obtained.

2.2.3 Transformation of bacteria by heat shock of E. coli DH5α

To transform competent E. coli DH5α, a heat shock method was employed. First, the chemically competent cells were thawed on ice and mixed with 10 µL of ligation mixture on ice for 5 minutes. The ligation mixture contained the plasmid DNA of interest as well as other necessary components for successful transformation. Next, the cell-DNA mixture was incubated at 42°C for 2 minutes. The transformed cells were then mixed with 600 µL of LB

medium and incubated at 37°C with shaking at 180 rpm for 15-30 minutes after incubation, the cells were centrifuged at 3000 rpm for 10 minutes and the culture supernatant was removed. The pelleted bacterial cells were then resuspended on LB agar plate containing the appropriate antibiotic and incubated overnight.

2.2.4 HEK 293 cells transfection

To initiate the transfection process, cells were seeded at a concentration of 1.5 x 105 cells per well on a 12-well plate in 1 ml of RPMI medium containing 10% FBS, without any antibiotics. After three days, the transfection mixture was carefully prepared by resuspending 600 ng of candidate plasmid DNA and 500 ng of BZLF1 DNA in 100 µl of RPMI without any additions. 3.5 µl of Metafectene was also added and resuspended in 100 µl of RPMI without any additions. The two mixtures were combined gently by pipetting a few times and left to incubate at room temperature for 25 minutes. The plasmid-Metafectene mixture was then dropwise added to the cells and incubated at 37°C for 24 hours. Following this, the medium of the transfected cells was carefully removed, and the cells were collected for further analysis.

2.2.5 LCLs transfection

The introduction of plasmids into LCLs was achieved using the Neon Transfection System. The cells were carefully washed three times with PBS that did not contain Ca^{2+} and Mg^{2+} to remove any potential contaminants that could interfere with the transfection. They were then resuspended with buffer T to ensure optimal conditions for electroporation. The concentration of LCLs was determined to be 2.0x 107 cells/mL in a 1.5 mL tube to allow for efficient transfection. Appropriate amount of plasmid DNA in deionized water at concentration of 3-5 µg/µL was added into the 1.5 mL tube containing the cells. The cells and plasmid DNA were combined by gentle pipetting, ensuring that the mixture was homogenous before being subjected to electroporation. To perform electroporation, the mixture was transferred into the electroporation cuvette, and the cuvette was loaded into the Neon Transfection System. The parameters for the electroporation were set to 1.1 KV of pulse voltage, 30 ms of pulse width and 2 of pulse number. The transfected cells were then collected and used for downstream applications.

2.2.6 Immunofluorescence staining

To prepare the cells for staining, a fixative solution of 4% paraformaldehyde in PBS was used to immobilize the cells for 20 minutes at room temperature. Subsequently, the fixed cells were permeabilized with a solution of PBS containing 0.5% Triton X-100 for 2 minutes, with the exception of samples treated with an antibody specific for the viral glycoprotein gp350. To visualize the viral glycoprotein, the cells were incubated with the primary antibody at 37°C for 30 minutes, followed by washing in PBS three times. The cells were then incubated with a secondary antibody conjugated to Cy-3 for 30 minutes at 37°C. Once the staining was complete, the slides were embedded in 90% glycerol and stored at 4°C. To visualize the staining, pictures were taken with a camera attached to a fluorescence microscope (Leica).

2.2.7 Alkaline lysis minipreparation of plasmid

To obtain small quantities of DNA, an alkaline lysis minipreparation of plasmid was performed. First, bacteria were cultured on antibiotic agar plates overnight at 37°C. The resulting bacterial pellet was then resuspended in 200 µL of TE buffer containing 50 µg/mL of RNase. The bacterial suspension was then transferred to a clean 1.5 mL eppendorf tube and mixed with a freshly prepared lysis buffer consisting of 1% SDS and 0.2 M NaOH in water. After gently inverting the tube two times, the mixture was incubated at room temperature for 2 minutes. Next, a 200 µL aliquot of 3 M Potassium Acetate was added to the lysed cells, and the tube was inverted two times before being incubated on ice for 10 minutes. The mixture was then centrifuged at 13,000 x g for 10 minutes, and the resulting supernatant was transferred to a clean tube and centrifuged again. The supernatant was then mixed with 350 µL of isopropanol and the DNA was allowed to precipitate on ice for 10 minutes before being pelleted at 13,000 x g for 10 minutes. After removing the supernatant, the pellet was washed in 1 mL of 80% ethanol, air-dried for 5 minutes, and then resuspended in 50 µL of TE buffer. The resulting DNA was stored long-term at -20°C.

2.2.8 Restriction digestion

The experiment utilized restriction enzymes obtained from ThermoFisher Scientific, and all digestions followed the manufacturer's instructions. To minimize the occurrence of star activity due to excessive levels of glycerol, the restriction enzymes never made up more than 1/10 of the total reaction mixture.

2.2.9 Virus production

Cell lines stably transfected with BAC DNA were used to produce virus. These cells were continuously maintained with 100 µg/ml Hygromycin B selection in order to keep EBV BAC inside the cells in the long term. Viable cells were plated at 3.5 x 10^5 in a 6 well plate and incubated overnight at 37°C. EBV producer cell lines were transfected with 0.5 µg expression plasmids of the BZLF1 (p509) and BRLF1 (p2130) to induce lytic replication for virus production. Transfection mixes were set-up mixing 100 µL of RPMI 1640 containing DNA and 100 µL of RPMI 1640 containing metafectene. Transfection mixes were incubated at room temperature for 20 minutes and added to cells in a drop-wise fashion. Cells were incubated for 8 to 12 hours, and the metafectene-containing medium was replaced with fresh RPMI 1640 supplemented with 10% FBS. The cells were incubated at 37°C for three days and supernatants were collected. The supernatants were centrifuged at 400 x g for 10 minutes and filtered through a 0.44 µm cellulose filter and stored at 4 °C.

2.2.10 RNA extraction

To extract RNA from each sample, the TRIzol reagent was used. The cells were first pelleted and then lyzed with 1 ml TRIzol, followed by extraction with 0.2 ml CHCl3. After shaking the TRIzol lysate vigorously for at least 30 seconds at room temperature and incubating it for 2 minutes, the samples were centrifuged at 12000 g for 15 minutes at 4°C (cold room). The upper colorless aqueous phase was carefully transferred into a new tube containing 500 µl of 2-Propanol (iso-PrOH) and mixed by inverting the centrifuge tube. RNA was then precipitated at -20°C for at least 20 minutes and pelleted at 12000 g for 10 minutes at 4°C (cold room). The supernatant was removed, and the pellet was washed with 75% Ethanol (EtOH; prepared with nuclease-free water) and centrifuged at 8000 g for 5 minutes at 4°C (cold room). The RNA pellet was resuspended in 40 µl of pre-heated nuclease-free water (95°C) and incubated at 60°C for 10 minutes with vortex to dissolve the RNA pellet completely. Finally, the RNA concentration was determined at OD260 nm in a nanodrop photo spectrometer and stored at -80°C. This protocol is a modified version of the one shared in the F100 DKFZ folder.

2.2.11 SYBR Green real-time PCR

To prepare the cDNA, a reverse transcription reaction was performed on total RNA extracted from LCLs using AMV-reverse transcriptase (Roche) and a mix of random hexamers. 500 ng

of total RNA was used as input for the reverse transcription reaction.

An example is given below for a 20 µl reaction containing the following components:

4 µl	5x RT buffer
2 µl	2mM dNTPs
2 µl	random hexamers
4 µl	$MgCl_2$
0.8 µl	AMV reverse transcriptase
1 µl	RNA inhibitor
1.2 µl	water
15 µl in total	Mix

A total of 5 µl of RNA sample was added to the master mix and allowed to incubate on ice for 5 minutes. Subsequently, the RT reaction was initiated and run according to the following program:

25 ˚C	10 min
42 ˚C	60 min
90˚C	5 min
4˚C	hold

After completing the reverse transcription reaction, the final cDNA should be stored at -20 ˚C until needed. To use the cDNA in a PCR reaction, add 80 µl of water and use 5 µl of the resulting solution per reaction. Here's an example of a 20 µl reaction containing the required components:

10 µL	2×Power SYBR green PCR Mix
1 µL	Forward primer (target gene)
1 µL	Reverse primer (target gene)
3 µL	water
+5.0 µL	cDNA sample
20 µL in total	

Consider adding an Internal Reference PCR, such as GAPDH, to the protocol

10 µL	2x Power SYBR green PCR Mix
1 µL	forward primer GAPDH (10µM)
1 µL	reverse primer GAPDH (10µM)
3 µL	water
+5.0 µL	cDNA sample

20 µL in total

The qPCR was conducted using the following parameters:

50 °C for 2 min (initial denaturation)

95 °C for 10 min (denaturation)

40 cycles:

95 °C for 15 s

60 °C for 1 min

The relative expression levels of the qPCR results were obtained using the $2^{-\Delta\Delta Ct}$ method, which is a modified version of the protocol shared in the F100, DKFZ folder.

2.2.12 Cell culture conditions

To ensure optimal growth and viability, all eukaryotic cells used in this study were cultured in incubators maintained at 37°C with a stable atmosphere of 100% humidity and 5% CO2. LCLs were cultured in RPMI supplemented with 10% FBS and were regularly split at a ratio of 1:5 or 1:10 depending on their growth rate and overall state. Adherent HEK293 cells were also cultured in RPMI with 10% FBS, while HEK293 cells that stably transfected with recombinant EBV were supplemented with hygromycin (100 µg/mL) in their culture medium. When HEK293 cells reached about 80% confluence, they were split at a ratio of 1:10 using 0.05% trypsin at 37°C for 1 min. These stringent culture conditions were necessary to maintain the integrity and functionality of the cells and ensure reliable and reproducible results.

2.2.13 Determination of virus titre by quantitative PCR (qPCR)

The virus supernatants underwent qPCR analysis to determine their titre. Prior to qPCR, the supernatants underwent treatment with DNaseI and Proteinase K. DNaseI was used to remove free-floating viral DNA, while Proteinase K was used to release virus-associated DNA from capsids. For DNaseI digestion, 45 µL of virus supernatant was mixed with 5 µL of 10X reaction buffer (with $MgCl_2$) and 1 unit of RNase-free DNaseI, followed by incubation at 37°C for 1 hour and 70°C for 10 minutes. For Proteinase K treatment, 5 µL of DNaseI-treated supernatant was mixed with 5 µL of Proteinase K (100 µg/mL), incubated at 50°C for 1 hour, and then at 75°C for 20 minutes. After Proteinase K treatment, 90 µL of dH_2O water was added to each sample. To quantify the amount of virus genomes, qPCR was performed using primers that target the EBV DNA polymerase gene (BALF5). The following reaction

mixture was set up for each sample:

12,5 µL TaqMan Fast PCR Master mix (2x)

2.5 µL Forward primer

2.5 µL Reverse primer

1.0 µL Probe

1.5 µL H_2O

5 µL DNaseI and Proteinase K treated sample

25 µL Total

The following thermocycling conditions were utilized for all samples:

Step 1- 50°C 2 minutes

Step 2- 95°C 10 minutes

Step 3- 95°C 15 seconds

Step 4- 60°C 1 minute

The genomes per milliliter of virus supernatant were determined using the threshold cycle (Ct) values. This was accomplished by employing a standard curve, which established the linear correlation between Ct values and genome/mL.

2.2.14 Western Blot

To extract proteins from cells, a standard RIPA buffer was used on ice, which contained NaCl, NP-40, Sodium deoxycholate, SDS, EDTA, Tris-HCl pH7.5, and a proteinase inhibitor cocktail from Roche. The genomic DNA was sheared by performing sonication. The amount of proteins was measured by a Bradford assay, and then the proteins were denatured in Laemmli buffer, supplemented with β-mercaptoethanol, for 10 minutes at 95°C prior to separation on SDS-polyacrylamide gels for SD-PAGE. The electroblotting of proteins onto a wet 0.45 nm nitrocellulose membrane was performed at 25V for 90 minutes, followed by incubation in PBST-milk 5% for 60 minutes. The primary antibody was added against the target protein, and the membrane was incubated at 4°C overnight. Both primary and secondary antibodies were diluted in blocking buffer based on the suggested dilution rate of the purchased antibody sheets. After washing extensively in PBST, the blot was incubated with a suitable secondary antibody coupled to horseradish peroxidase for 1 hour, followed by three washes with PBST to remove unbound antibodies. Finally, bound antibodies were detected using the ECL detection reagent from Perkin Elmer.

2.2.15 Microarray analysis

For the microarray analysis, three independent samples of HEK 293 cells transfected with empty vector and RAB11FIP1 RBD domain deletion were utilized. To isolate RNA, each sample was treated with a TRIzol reagent and DNase to remove genome DNA and stored in a 1.5ml-tube on dry ice. A minimum concentration of 50 ng/µl and total volume of 10 µl were required for each sample. The samples were then sent to the Core Facility in DKFZ for further analysis. At the Core Facility, the experimental design, incoming QC to ensure quality and concentration of all samples, labeling and hybridization to the microarrays, quality monitoring at all steps, and basic data analysis were carried out. The IIIumina HT12 platform was utilized for the RNA sample analysis.

2.2.16 Proteomic analysis

Proteomic analyses were carried out at the DKFZ Genomics and Proteomics Core Facility. The samples were prepared and sent to the Core Facility for additional processing, and Dr. Martin Scheider provided the following techniques.

2.2.17 Sample Preparation

Proteins (10 µg) were run for 0.5 cm into an SDS-PAGE and the entire piece was cut out and digested using trypsin according to Shevchenko et al.

2.2.18 MS method Orbitrap Exploris 480

A LC-MS/MS analysis was carried out on an Ultimate 3000 UPLC system (Thermo Fisher Scientific) directly connected to an Orbitrap Exploris 480 mass spectrometer for a total of 150 min. Peptides were online desalted on a trapping cartridge (Acclaim PepMap300 C18, 5µm, 300Å wide pore; Thermo Fisher Scientific) for 3 min using 30 µl/min flow of 0.05% TFA in water. The analytical multistep gradient (300 nl/min) was performed using a nanoEase MZ Peptide analytical column (300Å, 1.7 µm, 75 µm x 200 mm, Waters) using solvent A (0.1% formic acid in water) and solvent B (0.1% formic acid in acetonitrile). For 132 min the concentration of B was linearly ramped from 4% to 30%, followed by a quick ramp to 78%, after two minutes the concentration of B was lowered to 2% and a 10 min equilibration step appended. Eluting peptides were analyzed in the mass spectrometer using data depend acquisition (DDA) mode. A full scan at 120k resolution (380-1400 m/z, 300% AGC target, 45

ms maxIT) was followed by up to 2 seconds of MS/MS scans. Peptide features were isolated with a window of 1.4 m/z, fragmented using 26% NCE. Fragment spectra were recorded at 15k resolution (100% AGC target, 54 ms maxIT). Unassigned and singly charged eluting features were excluded from fragmentation and dynamic exclusion was set to 35 s.

2.2.19 Data analysis

Data analysis was carried out by MaxQuant (version 2.1.4.0) using an organism specific database extracted from Uniprot.org (human containing 79038 entries from 03.02.2023), if not described otherwise default settings were used. Identification FDR cutoffs were 0.01 on peptide level and 0.01 on protein level. Match between runs (MBR) option was enabled to transfer peptide identifications across RAW files based on accurate retention time and m/z. Fractions were set in a way that MBR was only performed within each condition.

Quantification was done using a label free quantification approach based on the MaxLFQ algorithm. A minimum of 2 quantified peptides per protein was required for protein quantification.

In addition, iBAQ-values were generated via MaxQuant.

2.2.20 Statistical analysis

RNA expression files were all analyzed using the Limma package in R software (R version 4.2.2). After quality control and normalization, differential gene expression analysis was performed using the Limma package. Genes with an adjusted p-value < 0.05 and a log2 fold change > 1.5 (log2 fold change>1.4 in RAB11FIP1C transfection analysis) were considered as differentially expressed. To further understand the biological significance of the differentially expressed genes, KEGG enrichment analysis was conducted using the clusterProfiler package in R. Significantly enriched pathways and functions were identified using a threshold of p-value < 0.05. In addition, to explore specific pathways of interest, gene set enrichment analysis (GSEA) was performed using the GSEAbase package in R. Gene set of each pathway from the KEGG database were used as input, and the result of the endocytosis pathway analysis were visualized using a GSEA plot, which displayed the enrichment score for the gene set along with a running enrichment score (RES) curve and a normalized enrichment score (NES) that took into account the size and variability of the gene set.

Statistical analysis was performed using GraphPad Prism 5 software, unless otherwise

specified. Paired student t-tests were used for single comparisons, while One- or Two-way ANOVAs were utilized for multiple comparisons with default settings.

3. Results

3.1 Selection of replicating LCLs

M81 is an EBV strain derived from a NPC case and this strain induces a spontaneous virus replication in LCLs. In this study, a recombinant M81 EBV (B1039) was used to select the replicating LCLs. It contained a rat CD2 gene that was inserted into BXLF1 gene of the M81 EBV genome (Fig.4 A). Rat CD2 becomes transactivated under the early lytic viral EA-D promoter when LCLs are reactivated. Thus, CD2 is expressed on the cell surface of replicating cells, which can then be pulled down by a monoclonal antibody (OX34) coupled with anti-mouse lgG Dynabeads.

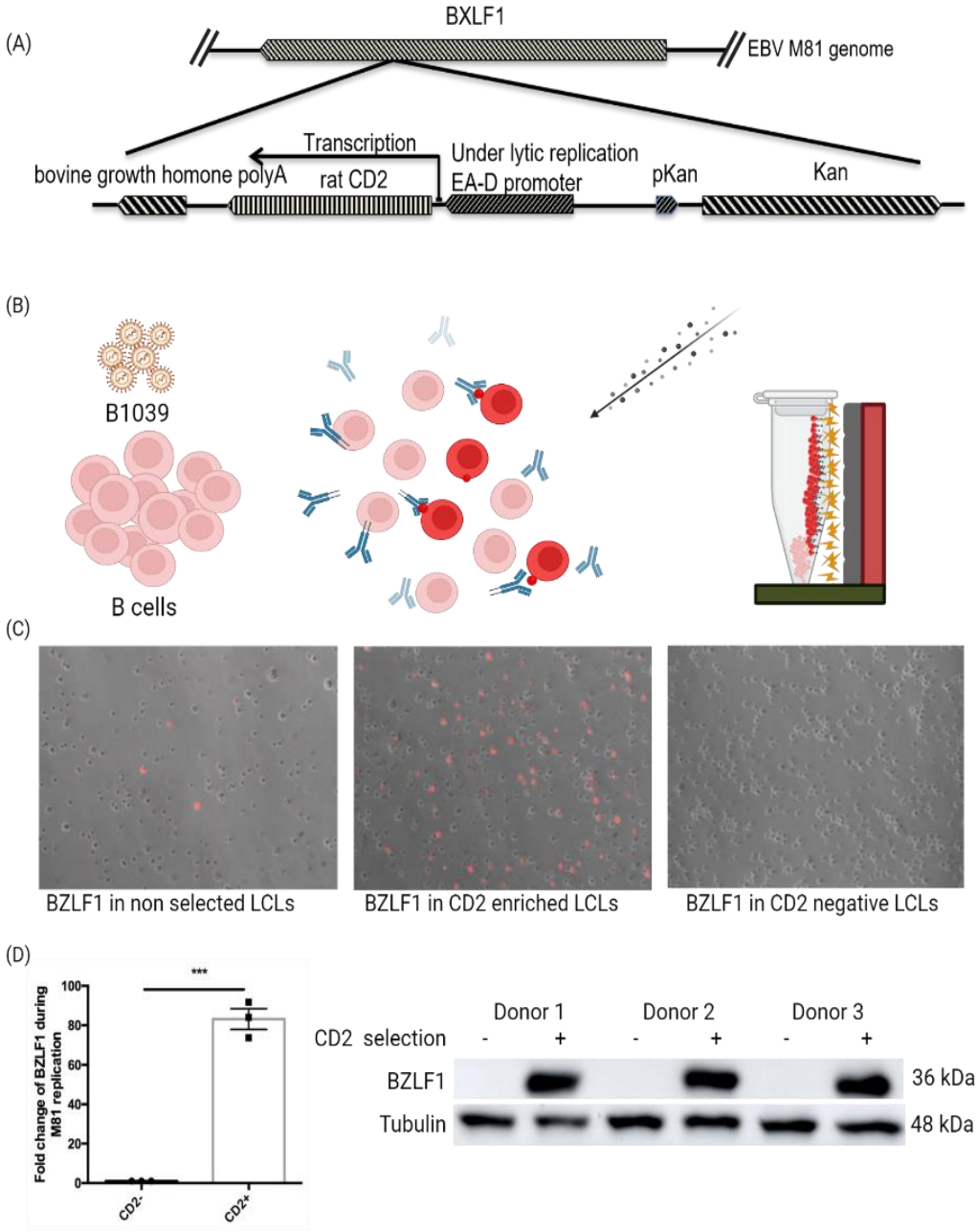

Fig.4 (A) General structure of the recombinant virus B1039: the rat CD2 gene is cloned under the control of an EA-D promoter that was inserted into the BXLF1 gene of the M81 genome (nucleotide 131044 to nucleotide 133362) by homologous recombination using a linear vector that included the kanamycin resistance cassette as a selection marker. Rat CD2 becomes transactivated in LCLs that initiate lytic replication. (B) Schematic representation of the workflow: the recombinant virus B1039 was used to infect B cells and the LCLs were then cultured for expansion. OX34 was used to attach the replicating LCLs and then beads were used to separate replicating LCLs from latent LCLs. (C) BZLF1 was stained in the non-selected LCLs, the rat CD2 enriched LCLs, and the rat CD2 negative LCLs. (D) RT- qPCR and Western blot were performed to detect BZLF1 changes in rat CD2-selected and rat CD2-negative LCLs.

LCLs were established by infecting primary B-cells with recombinant EBV (B1039). Then LCLs were expanded before being separated into replicating LCLs latent LCLs using the rat CD2 antibody (Fig.4 B). A BZLF1 staining was performed to detect the results of the enrichment procedure for infected cells undergoing replication (Fig.4 C). These cells were successfully enriched after selection with the rat CD2-specific antibody. Conversely, cells that were not selected by this antibody contained far fewer replicating cells when compared to untreated LCLs. Then RT-qPCR and Western blot were performed to detect BZLF1 mRNA level and protein level changes (Fig.4 D). The results revealed that in rat CD2 positive cells, BZLF1 mRNA and protein levels were significantly higher than in rat CD2-negative cells. Therefore, replicating cells can be efficiently separated from latently infected cells by selecting rat CD2. The purified replicating cells were then be subjected to protein and RNA extraction and analysis using microarrays combined to western blots (as exemplified in Fig.5).

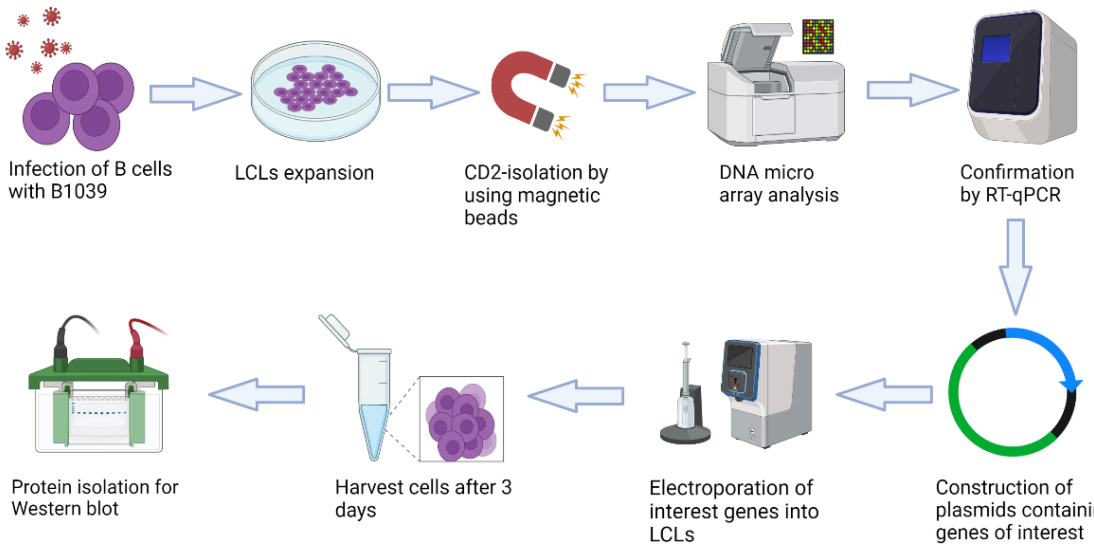

Fig.5 Workflow of various methodologies used to identify and characterize the events during EBV reactivation (Created with Biorender.com). Extracted samples of rat CD2-positive LCLs

and rat CD2-negative LCLs were subjected to a DNA microarray analysis to detect changes in cellular genes during EBV reactivation. Candidate cellular genes identified by this strategy were selected based on their fold changes and functions, then RT-qPCR was used to confirm their changes. Thereafter, the selected genes were cloned into a vector that encodes a tetracyclin-inducible promoter. These cloned genes were transfected into LCLs to evaluate their effects on spontaneous replication. Finally, the molecular impacts of these genes on EBV replication were investigated.

3.2 DNA Microarray analysis

A DNA microarray assay was performed to identify changes in the expression of cellular genes during LCL reactivation. To this end, replicating LCLs were separated from latent LCLs by rat CD2 selection. Then, synthesized cDNA from the rat CD2 positive and rat CD2 negative samples were subjected to DNA microarray. A total of three biological replicates were analyzed. The results of DNA microarray revealed that many genes were down regulated and upregulated (Fig.6). The genes with a fold change above 2 were selected for further confirmation.

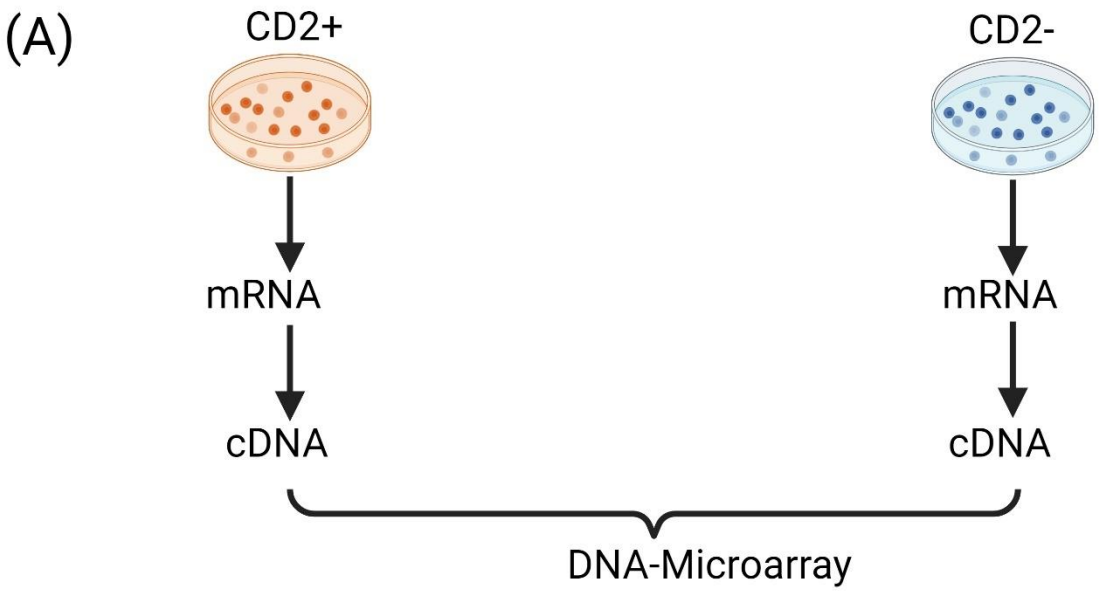

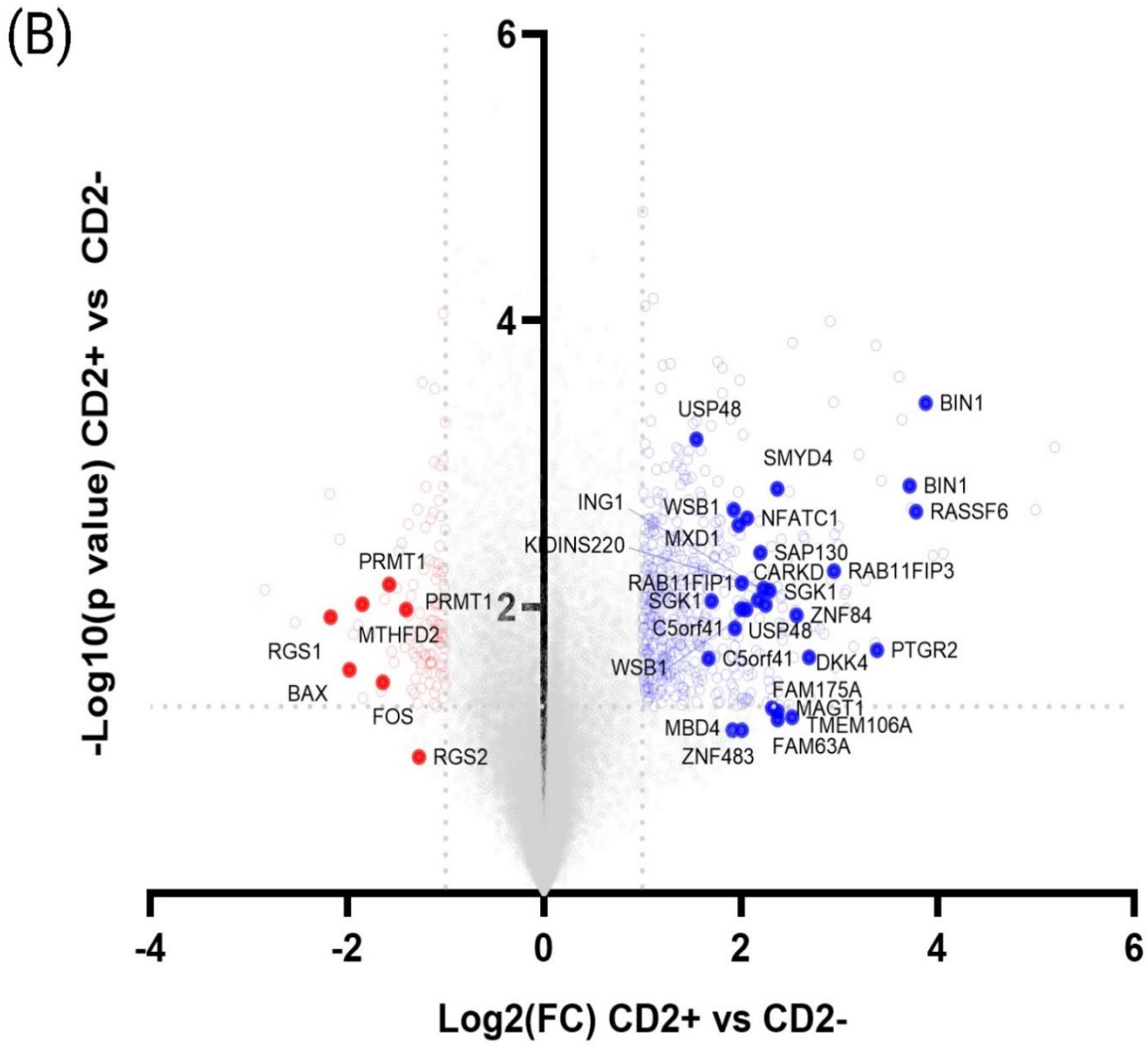

Fig.6 (A) Schematic representation of the workflow. Gene expression profiling was performed on reverse-transcribed mRNA from rat CD2+ and rat CD2- LCLs in three independent biological replicates. (B) Volcano plot representation of the differentially expressed transcripts. A two-tailed paired t-test was performed. Significantly upregulated (blue) or significantly downregulated (red) genes were selected when their p value was <0.05 (horizontal dotted line) and the absolute fold change versus the negative control was >2 (vertical dotted lines).

3.3 RT-qPCR analysis

Following the initial analysis using DNA microarray, the genes displaying a fold change above 2 were selected for further confirmation through RT-qPCR (Fig.7). Among the 31 candidate genes identified through the DNA microarray, the ones showing a significant upregulation of 2.5-fold change, as confirmed by qPCR results, were selected for further investigation. The aim was to explore the potential effects of these candidate genes on the replication process.

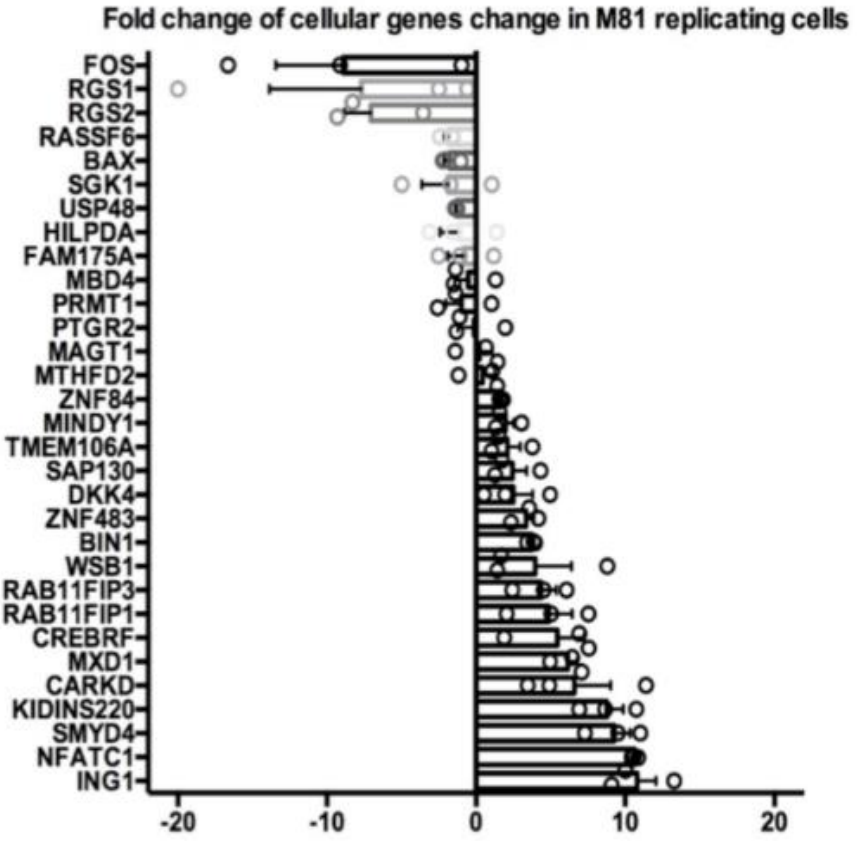

Fig.7 Results of RT-qPCR-based expression studies. The candidate cellular genes were selected based on their fold changes and functions from DNA array results. RT-qPCR were performed to confirm their fold changes in LCLs undergoing replication. A total of three biological replicates were tested.

The candidate genes from DNA array and RT-qPCR are summarized in Table.3. Their functions and fold changes are also displayed.

Table.3: Cellular genes fold change in LCLs undergoing EBV lytic replication.

Gene	Description	Fold change	Fold change

name		compared to nonlytic cells (Agilent DNA arrays)	compared to nonlytic cells(qPCR)
FOS	Interacting selectively with DNA of a specific nucleotide composition	-2,96±0,86	-8,91±7,84
RGS1	Increases the activity of a GTPase, an enzyme that catalyzes the hydrolysis of GTP	-4,39±1,15	7,70±10,69
RGS2	Increases the activity of a GTPase, an enzyme that catalyzes the hydrolysis of GTP	-2,20±1,34	-7,04±3,07
RASSF6	Interacting selectively with any protein or protein complex	13,95±2,25	-1,86±0,49
BAX	Interacting selectively with an identical protein to form a	-3,74±1,42	-1,78±0,65
SGK1	Catalysis of the transfer of a group	4,60±0,91	-1,89±3,02
USP48	Catalysis of the reaction	4,25±0,88	-1,33±0,09
HILPDA	Hypoxia-inducible lipid droplet-associated protein (HILPDA)	-6,94±1,70	-1,10±2,28
FAM175A	Interacting selectively with any protein or protein complex	6,14±3,73	-0,81±1,87
MBD4	Catalysis of the hydrolysis of ester linkages within deoxyribonucleic acid	4,37±2,44	-0,52±1,58
PRMT1	Catalysis of the transfer of a methyl group to the nitrogen atom of an acceptor molecule	-2,62±0,37	-0,97±1,84
PTGR2	Interacting selectively with zinc (Zn) ions	11,79±6,13	-0,15±1,83
MAGT1	Catalysis dolichyl diphosphooligosaccharide + protein L-asparagine	5,77±3,20	0,23±1,46
MTHFD2	Catalysis of the hydrolysis of various bonds	-3,54±0,64	0,44±1,41
ZNF84	Interacting selectively with zinc (Zn) ions	6,13±1,49	1,66±0,13
MINDY1	Has exodeubiquitinase activity and has a preference for long polyubiquitin chains	6,22±3,74	1,98±0,94
TMEM106A	May play a role in inhibition of proliferation and migration	7,10±4,78	2,10±1,46
SAP130	Catalysis of the hydrolysis of terminal 1,4-linked alpha-D-glucose residues	4,64±0,64	2,44±1,65
DKK4	Catalysis or binding, describing the actions of a gene product at the molecular level.	7,02±2,81	2,48±2,27
ZNF483	The function of binding to a specific DNA sequence in order to modulate transcription	4,74±2,72	3,35±0,93
BIN1	Interacting selectively with any protein or protein complex	14,74±1,07	3,74±0,27
WSB1	Elemental activities, such as catalysis or binding	4,09±0,83	3,97±4,19
RAB11FIP3	Plays a role in cytokinesis, endosomal recycling	7,89±1,63	4,34±1,82
RAB11FIP1	Interacting selectively with any protein or protein complex	4,08±0,67	4,87±2,75
CREBRF	The function of binding to a specific DNA sequence in order to modulate transcription	3,94±0,84	5,46±3,11
MXD1	The function of binding to a specific DNA	3,96±0,40	6,16±1,09

	sequence in order to modulate transcription		
CARKD	NAXD (NAD(P)HX Dehydratase	4,78±0,94	6,59±4,22
KIDINS220	scaffold for MAPK-cascade, enhancement of JAK/STAT with SNTA1 activates p21	4,88±1,12	8,77±1,91
SMYD4	Interacting selectively with zinc (Zn) ions	5,19±0,48	9,27±1,87
NFATC1	Nuclear factor of activated T cells, cytoplasmic 1	4,20±0,41	10,64±0,22
ING1	Elemental activities, such as catalysis or binding	4,99±0,97	10,80±2,20

(The expression fold change between cells undergoing lytic replication and the controls is provided along with the mean value and standard deviation of three independent experiments conducted with separate samples.)

3.4 Cotransfection of selected genes with BZLF1 in M81 producer cells

The first step in studying the effects of the selected genes on the replication process was to transfect them into B110 293 cells, which are M81 EBV producer cells. However, it was found that none of these genes induced lytic replication in B110 293 cells when tested alone. To further investigate the potential effects of these candidate genes on the replication process, they were co-transfected with BZLF1 into B110 293 cells. The aim was to examine any changes in the expression of BZLF1, gp350 and gp220 proteins induced by these genes, and to gain a better understanding of how these genes may impact the replication process.

When introduced along with BZLF1, the genes BIN1, MXD1, SMYD4, WSB1, ZNF483, RAB11FIP1, RAB11FIP3, and KIDINS220 were observed to have an enhancing effect on the expression of BZLF1. Similarly, with regards to gp350 and gp220, the genes BIN1, MXD1, SMYD4, WSB1, ZNF483, CARKD, CREBRF, RAB11FIP1, KIDINS220, and ING1 demonstrated increased effects on the expression of gp350 and gp220 when co-transfected with BZLF1 (Fig.8). These findings suggest a potential role for these genes in regulating the replication process of EBV.

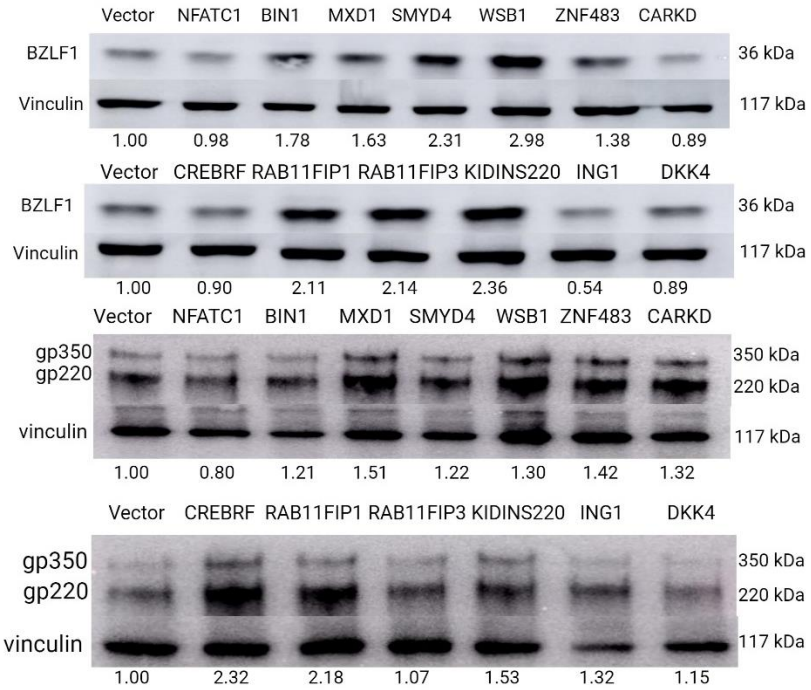

Fig.8 This figure shows the results of the co-transfection experiment, where 500ng of BZLF1 was co-transfected with 600ng of candidate target genes into B110 293 cells. After 24 hours, cells were collected and subjected to western blot analysis to detect the expression of BZLF1. The results demonstrate the effects of the candidate genes on BZLF1 expression. The expression levels of BZLF1, gp350, and gp220 were normalized to vinculin expression for accurate comparison. Additionally, the fold change of BZLF1, along with the combined gp350 and gp220, resulting from the overexpression of target genes was provided beneath the blot for clarity.The figure includes representative western blot images and quantification of protein expression levels. The data supports the conclusion that some of the candidate genes have an impact on the replication process in EBV-infected cells.

3.5 Electroporation of candidate genes into LCLs to study their effects on BZLF1 expression

The selected genes described above were cloned into a vector containing multiple genetic elements such as OriP, the latent origin of EBV replication GFP, NGFR, rat CD2, and the gene of interest whose expression was driven by a tetracycline-inducible promoter. The presence of OriP on the plasmid allows its attachment to the host genome. LCL cells transfected with this plasmid were then selected twice by using the antibody against rat CD2 and induced to express the genes of interest using tetracycline. LCLs expressing the target genes were collected after 3 days to evaluate their impact on BZLF1 expression.

Based on the findings of the study, it was observed that the expression of certain genes had varying effects on the expression of BZLF1. Specifically, the expression of WSB, CREBRF,

and DKK4 resulted in a slight decrease in BZLF1 expression. On the other hand, the expression of BIN1, RAB11FIP1, and RAB11FIP3 led to an increase in BZLF1 expression (Fig.9). These results provided insight into the potential roles of these genes in the replication process of EBV.

Due to the promising up-regulation of BZLF1 expression shown after RAB11FIP1 expression, it was selected as a prime candidate for further investigation of its effects on BZLF1 expression.

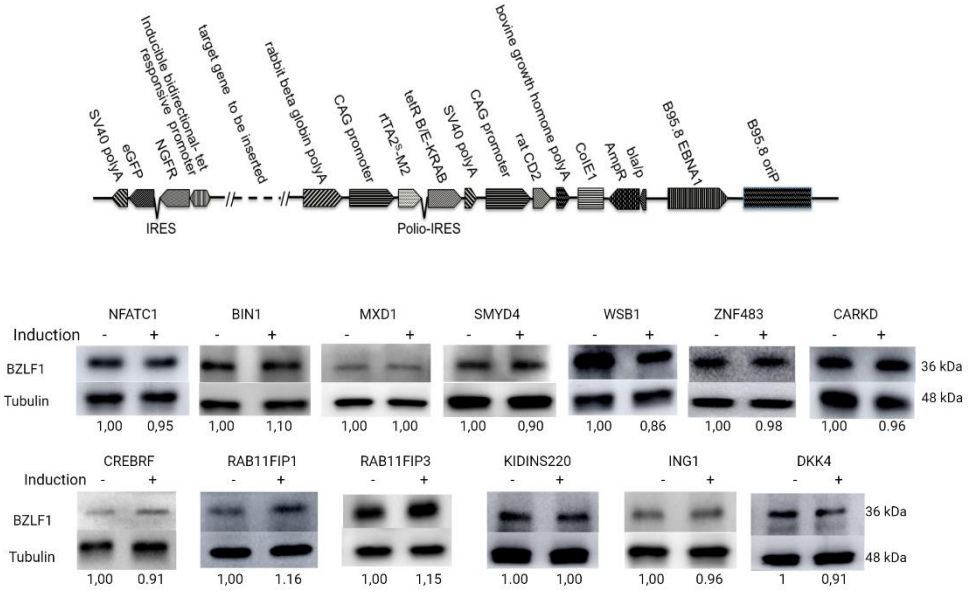

Fig.9 The schematic graph shows the structure of the vector used to electroporate LCLs and the elements it encodes. The vector encodes GFP, NGFR, rat CD2, and a tetracycline-inducible promoter to drive the expression of candidate genes. To further examine the long-term effects of candidate target genes on BZLF1 expression in LCLs, the genes of interest were cloned into this vector, which was then used for electroporation of the LCLs. After selection of the transfected cells using rat CD2, tetracycline was used to induce the expression of the target genes. Three days later, the LCLs with the target genes were collected to detect their effects on BZLF1 expression. The expression levels of BZLF1 were normalized to tubulin expression for accurate comparison. Additionally, the fold change of BZLF1 resulting from the overexpression of target genes was provided beneath the blot for clarity.

3.6 Identification of differentially expressed genes and pathways in EBV replication using KEGG analysis

To identify signaling pathways differentially regulated by EBV replication, the global results of the DNA array data was analysed by multiple programs. Pathway enrichment analysis was performed using the Kyoto Encyclopedia of Genes and Genomes (KEGG) database.

Differentially expressed genes identified by DNA microarray were mapped onto the KEGG (Fig.10). The analysis of gene expression changes in LCLs during replication reveals significant alterations in key genes involved in the HSV-1 pathway, which encompasses the complex interplay between viral and host factors necessary for the virus to successfully infect, replicate, and persist within host cells.

For instance, the protein SP100 (Speckled 100) has been identified as having a pivotal role in HSV-1 replication (Everett et al. 2008). HSV-1 can disrupt the TSC1/TSC2 complex, leading to the activation of the mTOR pathway, which promotes cell growth and creates a favourable environment for viral replication and spread (Minami et al. 2007). However, the specific functions of SP100 and the TSC1/TSC2 complex in EBV replication have not been explored yet.

These results suggest that these enriched pathways may play important roles in the biological processes affected by the replication of LCLs, and provide valuable insights into the underlying mechanisms of these processes.

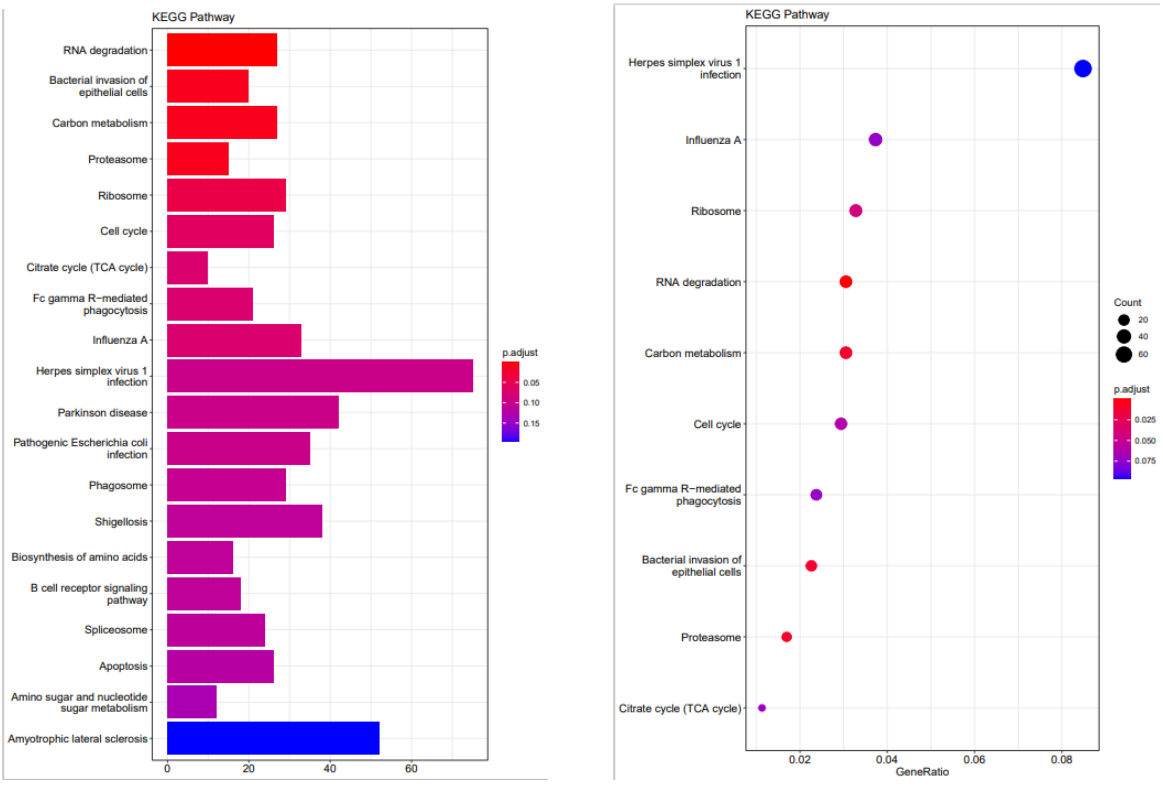

Fig.10 Bar chart depicting the results of the KEGG pathway enrichment analysis of differentially expressed genes in latent and replicating LCLs. The presented bar graph displays the top 20 KEGG enrichment pathways from the analysis of differentially expressed genes (DEGs) between latent LCLs and replicating LCLs. The x-axis represents the numbers of DEGs mapped to each pathway, while the y-axis lists the enriched KEGG pathways.

Bubble chart for KEGG enrichment of cluster-specific marker gene transcripts that are upregulated in LCLs replication. The size of each circle next to the pathway name represents the number of DEGs mapped to that pathway. The x-axis represents the ratio of numbers of DEGs in each pathway to the total number of DEGs. The colour of each bar indicates p values, with redder shades indicating lower p values.

3.7 GSEA analysis of endocytosis pathway in LCLs: comparison of latent and replicating LCLs

Among the tested genes, RAB11FIP1 exhibited the most significant effect on the expression of BZLF1. This gene is recognized for its role in regulating endocytosis and is a Rab GTPase effector that plays a role in regulating endocytic recycling. It has been shown to regulate endocytosis of several membrane receptors, including transferrin receptor, EGFR, and β1-integrin (von Grabowiecki et al. 2021). Therefore, a GSEA analysis for the endocytosis pathway was conducted between replicating LCLs and latent LCLs, using the gene set compiled from previously published KEGG data (Fig.11). The colors indicate upregulated (red) and downregulated (blue) genes. Interestingly, the replication of LCLs did not appear to have any significant effect on the endocytosis pathway, as indicated by a non-significant p-value of 0.3018.

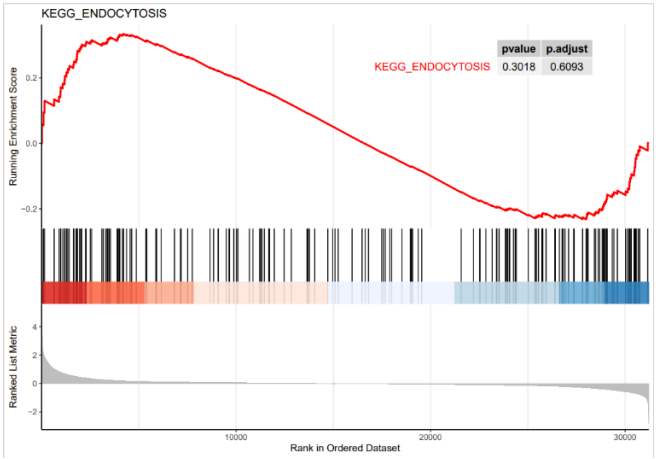

Fig.11 GSEA analysis of endocytosis pathway in replicating vs. Latent LCLs with non-significant effect on replication.

3.8 The expression of RAB11FIP1 was found to be altered in replicating LCLs

I first monitored expression of the two main RAB11FIP1 isoforms (Fig.12 A), RAB11FIP1C and RAB11FIP1B, after transfection into HEK293 cells. After 24 hours, the expression of each isoform was detected by Western blot analysis. The size of RAB11FIP1C is approximately 85kDa, and the size of RAB11FIP1B is approximately 280kDa (Fig.12 B).

This information is important for subsequent experiments that investigate the effects of these isoforms on gene expression.

(A)

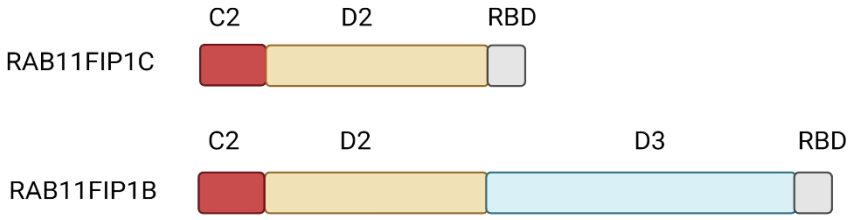

(B)

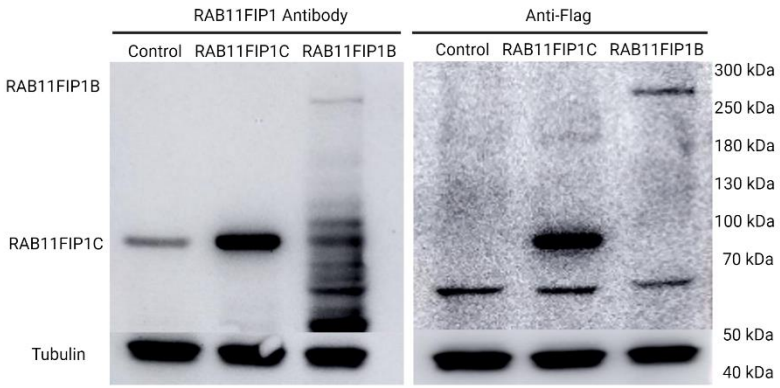

Fig.12 The proteins RAB11FIP1C and RAB11FIP1B have been FLAG-tagged to facilitate observation of their respective sizes via western blot analysis. (A) This figure depicts a schematic representation of the structure of RAB11FIP1C and RAB11FIP1B, two main isoforms of RAB11FIP1. Both contain several functional domains, including a coiled-coil domain, a C2 domain, and a RBD domain, which are involved in various cellular processes. In contrast, RAB11FIP1C has a shorter length and lacks the D3 domain. (B) This figure also depicts the results of a Western blot analysis performed on HEK 293 cells to determine the RAB11FIP1C and RAB11FIP1B. The bands observed on the blot correspond to the size of the RAB11FIP1C and RAB11FIP1B isoforms, allowing for the identification and localization of the endogenous RAB11FIP1 proteins.

The current study aimed to investigate the effects of RAB11FIP1C and RAB11FIP1B on the expression of BZLF1. To achieve this, B110 293 cells were co-transfected with 500ng BZLF1 and 600ng of either RAB11FIP1C or RAB11FIP1B, and the levels of BZLF1 were measured using Western blotting after 24 hours. According to the quantification results from

the Western blot analysis, both RAB11FIP1C and RAB11FIP1B exhibited a substantial impact on BZLF1 expression, leading to an approximate 3-fold increase (Fig.13). These findings suggest that RAB11FIP1 may play a crucial role in regulating the lytic cycle of EBV.

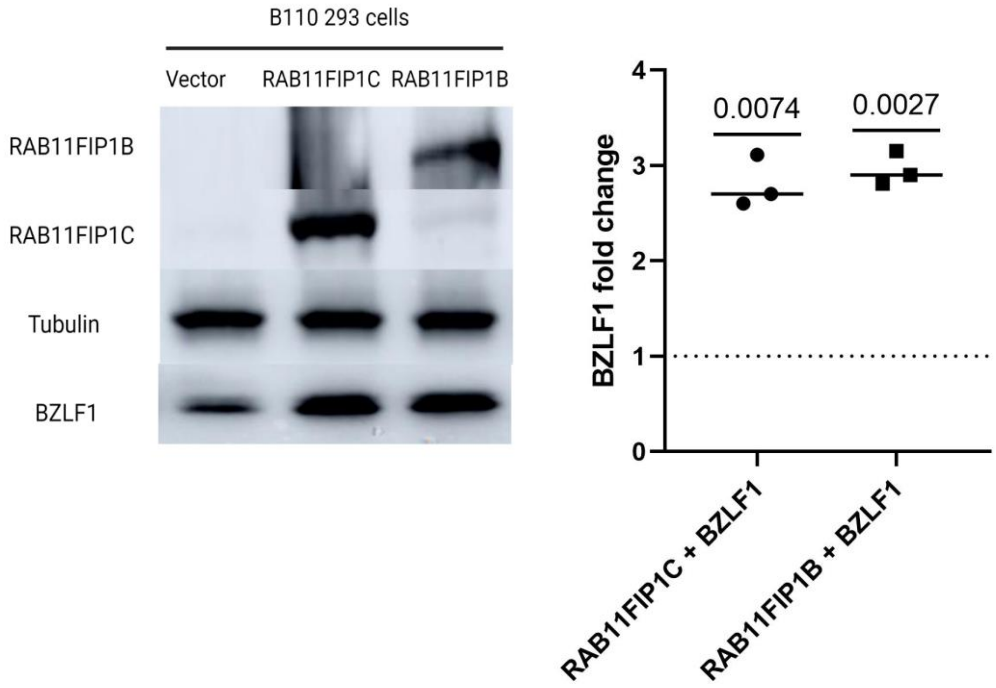

Fig.13 This figure displays the results of a Western blot analysis of B110 293 cells co-transfected with BZLF1 and RAB11FIP1C or RAB11FIP1B. The analysis shows the effects of RAB11FIP1C and RAB11FIP1B on the expression of BZLF1.The graph presents the quantification results of the Western blot analysis, indicating the effects of RAB11FIP1C and RAB11FIP1B on BZLF1 expression. The expression levels of BZLF1 were normalized to tubulin expression for accurate comparison. Both RAB11FIP1C and RAB11FIP1B were found to upregulate the expression of BZLF1 with an approximate 3-fold change. A one sample t test ($\mu=1$) was performed, and the p-value is indicated above the comparison. $P<0.05$ was considered statistically significant.

To further investigate the increase in BZLF1 expression observed in B110 293 cells after RAB11FIP1C transfection, a comparison of expression levels for RAB11FIP1B and RAB11FIP1C was conducted in latent and replicating cells derived from LCLs infected with the recombinant virus expressing CD2 under the regulation of the EA promoter. The higher expression levels of both proteins in replicating cells compared to latent cells confirms a potential link between RAB11FIP1B and RAB11FIP1C expression and the induction of EBV replication (Fig.14). These findings are consistent with results obtained from earlier analyses, such as DNA microarray and RT-qPCR, which have also shown increased expression of

RAB11FIP1B and RAB11FIP1C in replicating LCLs. Overall, these results provide important insights into the potential mechanisms underlying EBV replication and shed light on the role of RAB11FIP1B and RAB11FIP1C in this process.

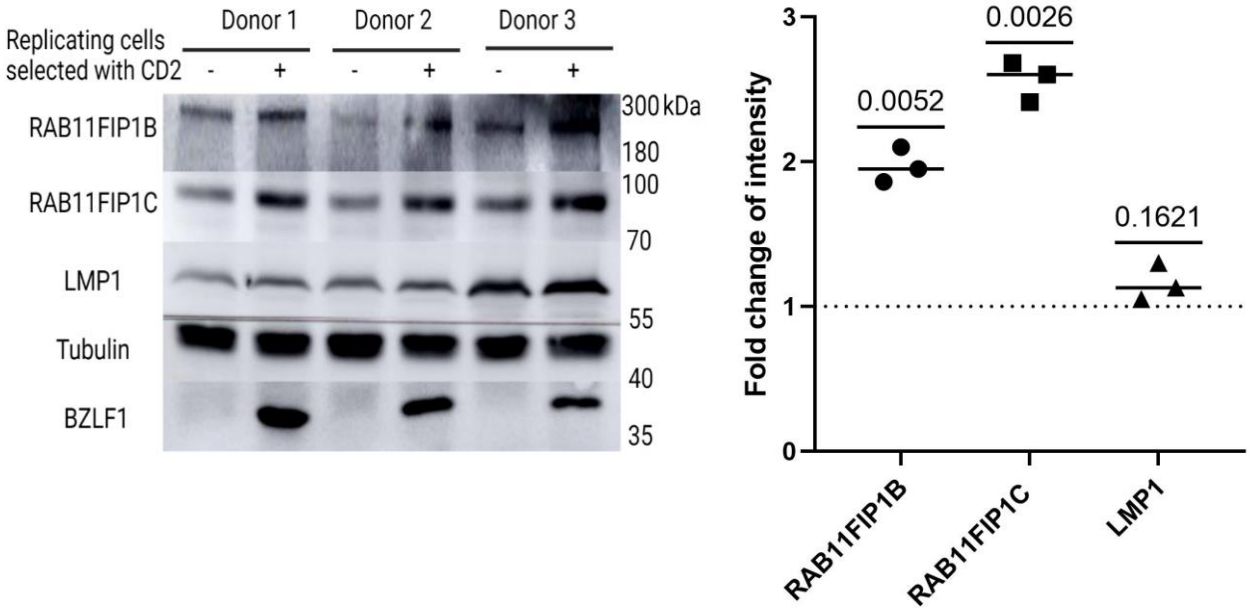

Fig.14 This figure displays the Western blot analysis of the expression levels of RAB11FIP1B, RAB11FIP1C, and LMP1 in both latent and replicating LCLs. The expression levels of BZLF1 were normalized to tubulin expression for accurate comparison. The quantification of RAB11FIP1B, RAB11FIP1C, and LMP1 expression changes is presented in this panel. A one sample t test ($\mu=1$) was performed, and the p-value is indicated above the comparison. $P<0.05$ was considered statistically significant.

In light of the fact that both RAB11FIP1C and RAB11FIP1B were found to be capable of upregulating BZLF1 expression, and since RAB11FIP1C is the predominant isoform expressed in LCLs, the research further focused mainly on investigating the role of RAB11FIP1C in regulating BZLF1. Here the expression of RAB11FIP1C in B110 293 cells was monitored after BZLF1 induction over a period of 5 days. It was observed that the expression of RAB11FIP1C gradually increased over time (Fig.15). This fits with a significant role for RAB11FIP1C in facilitating EBV replication.

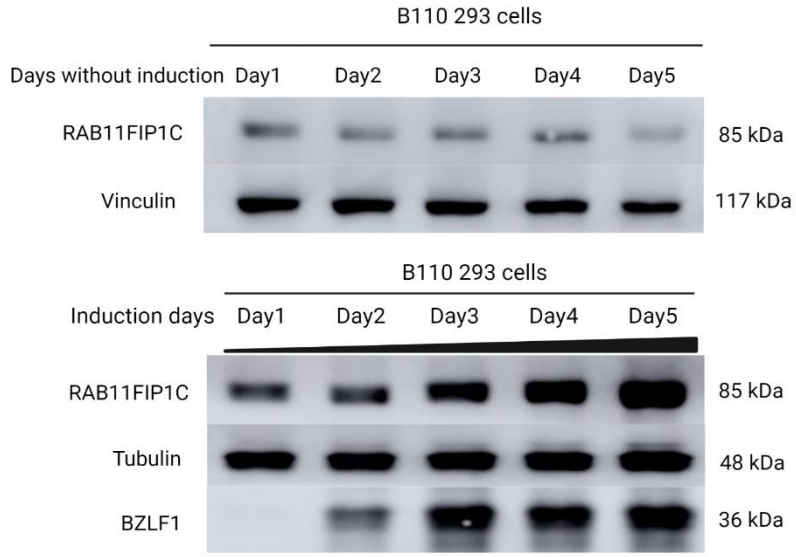

Fig.15 The figure depicts the changes in RAB11FIP1C expression levels over a period of 5 days, both with and without the induction of BZLF1. The bar above the western blot signifies the increasing amount of RAB11FIP1C.

To determine whether downregulation of RAB11FIP1C would alter the expression of BZLF1, shRNA targeting RAB11FIP1C was transfected into B110 293 cells. After 2 days, BZLF1 was transfected into the same cells, followed by cell collection 1 day later for Western blot analysis to assess changes in BZLF1 expression. This assay showed a down regulation of BZLF1 expression after RAB11FIP1C knockdown, confirming that this protein potentiates BZLF1 expression (Fig.16).

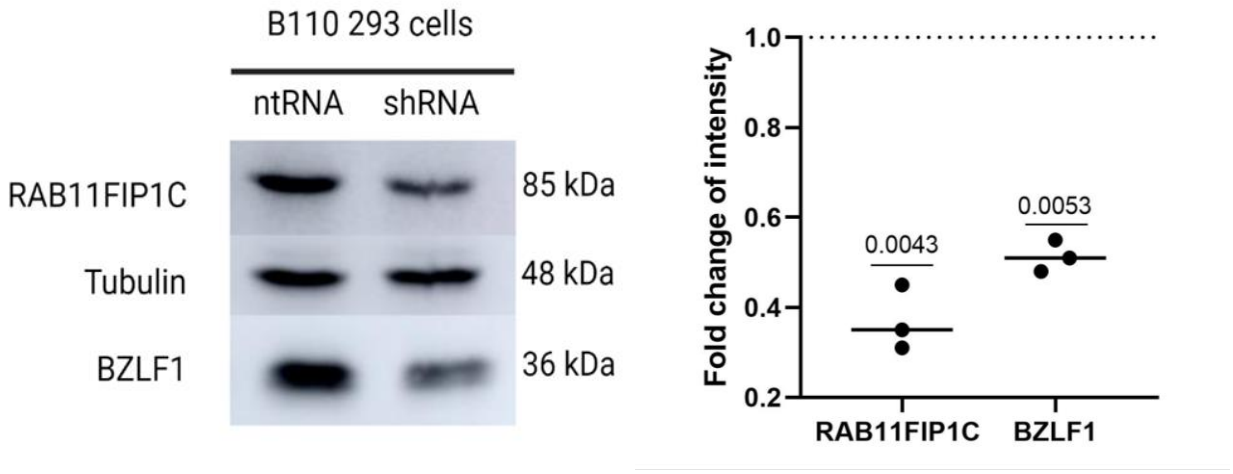

Fig.16 The figure illustrates the alteration in BZLF1 expression resulting from a two-day transfection of RAB11FIP1C shRNA in B110 293 cells. The expression levels of RAB1FIP1C and BZLF1 were normalized to tubulin expression for accurate comparison. The graph presents the quantification results, showing the fold change in BZLF1 expression upon a two-day transfection of RAB11FIP1C shRNA in B110 293 cells. A one sample t test (μ=1) was performed, and the p-value is indicated above the comparison. P<0.05 was considered statistically significant.

3.9 RAB11FIP1C modulates gene expression independently of EBV: evidence from co transfection experiments in HEK293 cells

To investigate whether the ability of RAB11FIP1C to potentiate BZLF1 expression extended to other genes, RAB11FIP1C was co-transfected with GFP into HEK 293 cells, with a total of 600ng of RAB11FIP1C and 500ng of GFP being used. After 24 hours, cells were collected for western blot analysis to determine if there was any change in GFP expression (Fig.17).

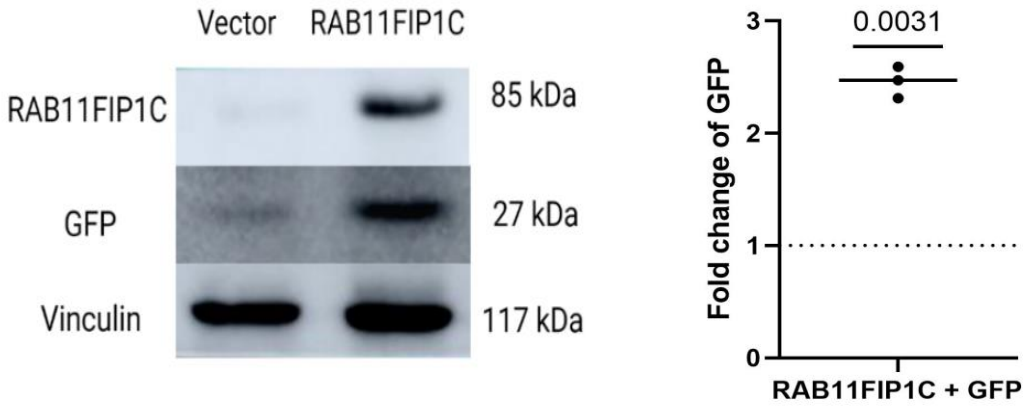

Fig.17 This figure illustrates the outcome of a Western blot analysis conducted on HEK293 cells co-transfected with vector and RAB11FIP1C along with GFP for 24 hours. The expression levels of GFP were normalized to vinculin expression for accurate comparison. The graph depicts the quantification of Western blot analysis performed on three replicates of HEK 293 cells co-transfected with vector and RAB11FIP1C along with GFP. A one sample t test (μ=1) was performed, and the p-value is indicated above the comparison. P<0.05 was considered statistically significant.

The results of the experiment showed that GFP expression was increased in cells co-transfected with RAB11FIP1C, indicating that the increasing effects of RAB11FIP1C were not limited to EBV proteins. This suggests that RAB11FIP1C may have a general effect on protein expression and is not specific to EBV replication (Fig.18).

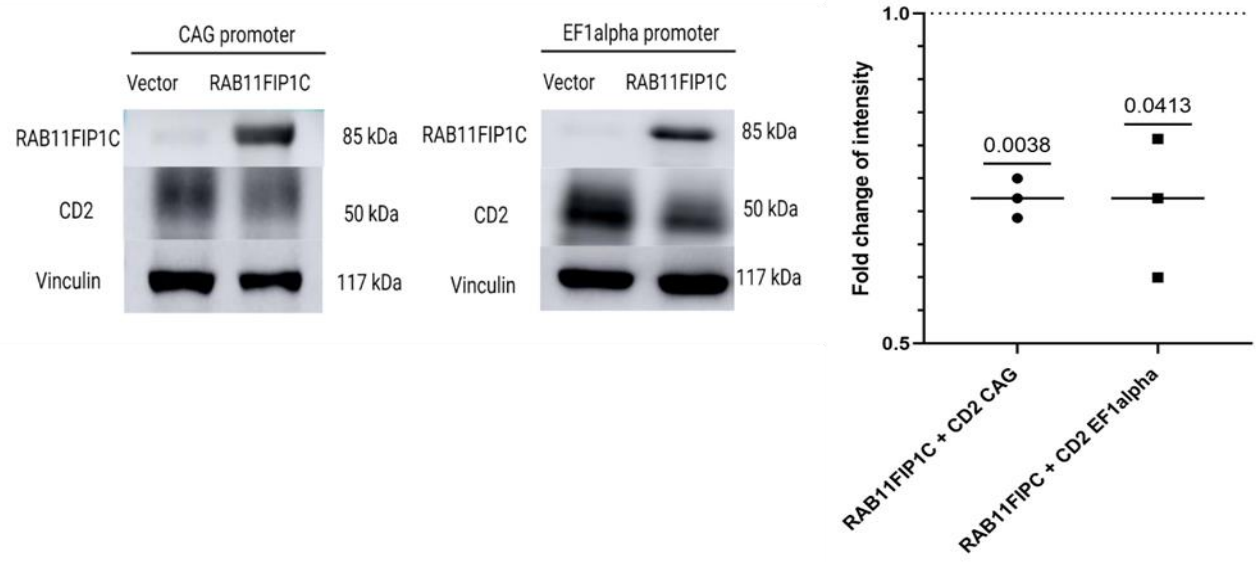

Fig.18 This figure shows the results of a Western blot analysis performed on HEK 293 cells co-transfected with vector and RAB11FIP1C, along with rat CD2 under the control of the EF1alpha promoter and the CAG promoter. The expression levels of CD2 were normalized to vinculin expression for accurate comparison. The graph displays the quantification results obtained from three replicates of co-transfection of vector and RAB11FIP1C along with rat CD2 using the EF1alpha promoter and CAG promoter into HEK293 cells. A one sample t test ($\mu=1$) was performed, and the p-value is indicated above the comparison. $P<0.05$ was considered statistically significant.

The regulation of gene expression is a complex process that involves various factors, including promoters. Therefore, two different promoters of CD2, namely EF1alpha promoter and CAG promoter, were co-transfected with RAB11FIP1C into HEK 293 cells. It was observed that CD2 expression decreased significantly when co-transfected with RAB11FIP1C. Interestingly, the two different promoters did not alter the decreasing effect of RAB11FIP1C on CD2 expression, indicating that the effect of RAB11FIP1C is not dependent on the type of promoter used.

The results suggest that RAB11FIP1C can have both stimulating and dampening effects on gene expression, and these effects are not limited to specific promoters.

3.10 Relationship between LMP1 and RAB11FIP1

Latent membrane protein 1 (LMP1), an EBV oncoprotein activates several signaling

pathways, such as cell death and survival, cell motility, and dynamics of actin filaments (DeKroon et al. 2018).

LMP1 has been reported to impact the recycling endosome by activating Rab11/RAB11FIP1(DeKroon et al. 2018). Furthermore, many studies have demonstrated that LMP1 can influence cellular biological characteristics and gene expressions. Specifically, LMP1 has been found to impact proteasome subunits, conjugating enzymes, ubiquitin-specific peptidases, vesicle trafficking proteins, and mitogen-activated protein kinase signaling proteins (Mainou et al. 2005). Recent research has suggested that the activation of the canonical NF-κB pathway by the carboxy-terminal activation domain 2 (CTAR2) of LMP1 is primarily responsible for the majority of LMP1-induced effects on cellular transcription (Edwards et al. 2015; Gewurz et al. 2011). In contrast, CTAR1 activates the noncanonical NF-κB pathway and induces minimal changes in gene transcription (Edwards et al. 2015; Luftig et al. 2004). Nevertheless, CTAR1 has a significant impact on cellular biological properties and can activate phosphatidylinositol 3-kinase (PI3-kinase)/Akt and induce the expression of epidermal growth factor receptor (EGFR) (Edwards et al. 2015; Mainou et al. 2005). The impact of LMP1 on the cellular proteome is achieved by altering the levels of certain proteins through the proteasome-mediated mechanism. Upon analyzing the effects of LMP1 on vesicle trafficking pathways, it was found that the regulation of numerous signaling complexes is also influenced by its ability to impact vesicle formation and trafficking.

To investigate the effects of LMP1 on RAB11FIP1C expression, the same amount of empty vector and LMP1-encoding plasmid were co-transfected with RAB11FIP1C into HEK293 cells. After 24 hours, cells were collected and lysed for western blot analysis. Our results showed a significant increase in RAB11FIP1C expression in cells co-transfected with LMP1 compared to cells co-transfected with the empty vector ($p<0.01$), suggesting that LMP1 may upregulate RAB11FIP1C expression in HEK293 cells (Fig.19).

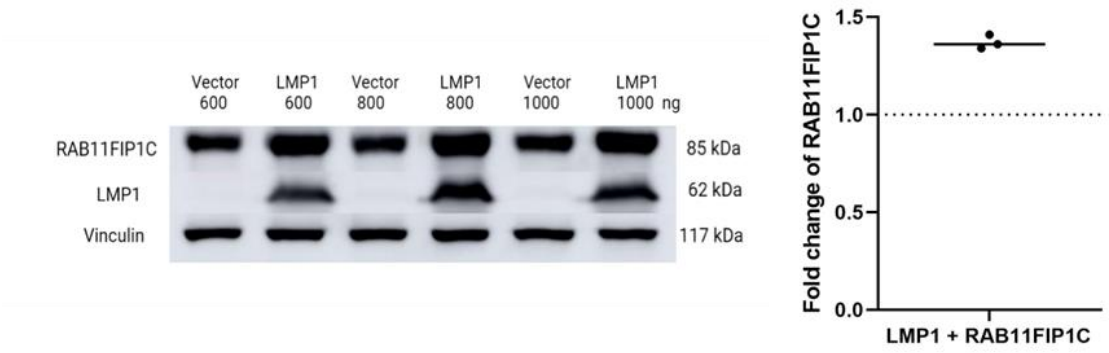

Fig.19 This figure demonstrates the effect of LMP1 on RAB11FIP1C expression. LMP1was co-transfected with RAB11FIP1C or control vector in HEK 293 cells. As determined by Western blot analysis, LMP1 increased RAB11FIP1C expression. The expression levels of RAB11FIP1C were normalized to vinculin expression for accurate comparison. The quantification of the Western blot analysis is presented in the graph, showing the fold change in RAB11FIP1C expression in the presence of LMP1 compared to the control. A one sample t test ($\mu=1$) was performed, and the corresponding p-value is shown above the comparison. A p-value less than 0.05 was deemed statistically significant.

In contrast, to explore the impact of RAB11FIP1C on LMP1 expression, equal quantities of vector and RAB11FIP1C were co-transfected with LMP1 into HEK 293 cells. Following a 24-hour incubation period, the cells were collected and subjected to western blot analysis to evaluate the effects of RAB11FIP1C on LMP1 expression (Fig.20). The statistical analysis revealed a significant decrease in LMP1 expression by RAB11FIP1C ($p<0.5$), indicating that RAB11FIP1C may play a role in modulating LMP1 expression.

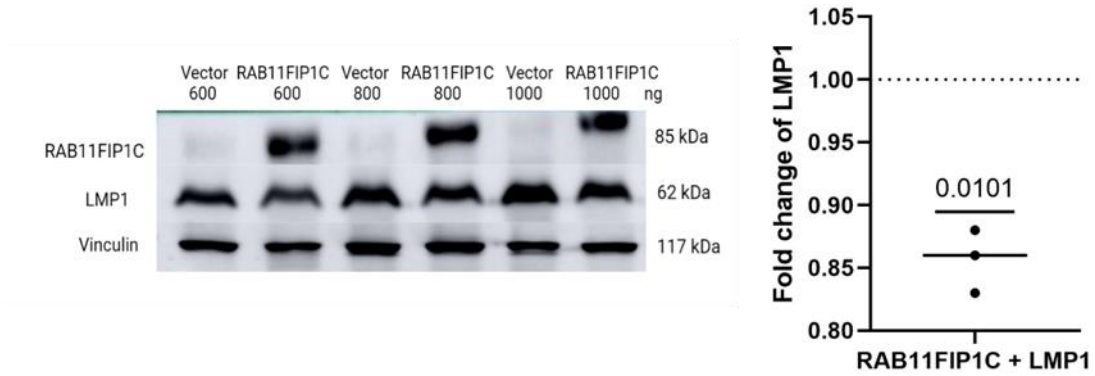

Fig.20 This Western blot analysis depicts the impact of co-transfecting different quantities of vector and RAB11FIP1C, along with LMP1, into HEK293 cells. The varying expression levels were determined by Western blot analysis, and the results illustrate that LMP1 expression decreased as the amount of RAB11FIP1C increased, suggesting that

RAB11FIP1C has a negative regulatory effect on LMP1 expression. The expression levels of LMP1 were normalized to vinculin expression for accurate comparison. The graph shows the fold change of LMP1 expression in the presence of RAB11FIP1C compared to the control, indicating that LMP1 expression was significantly decreased in the presence of RAB11FIP1C. A one sample t test (μ=1) was performed, and the corresponding p-value is shown above the comparison. A p-value less than 0.05 was deemed statistically significant.

To investigate the effect of LMP1 on the transcriptional level of RAB11FIP1C, equal amounts of empty vector and LMP1 were co-transfected into HEK 293 cells along with RAB11FIP1C. After 24 hours, cells were collected, and RT-qPCR was performed (Fig.21). The results showed no significant change in the mRNA level of RAB11FIP1C ($p>0.05$).

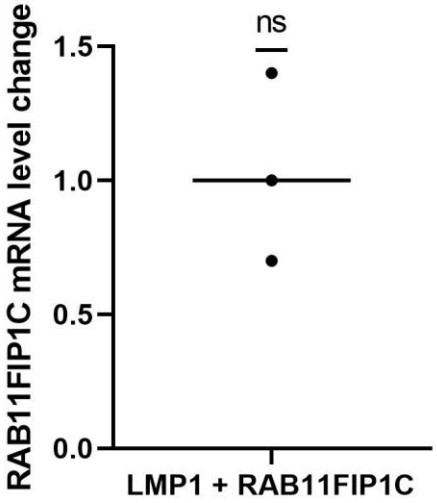

Fig.21 The graph depicts the quantification results of the RT-qPCR analysis of the effects of LMP1 overexpression on the transcriptional level of RAB11FIP1C. The results show that there was no significant change in the mRNA level of RAB11FIP1C in the presence of LMP1, as determined by a one sample t test (μ=1).

3.11 Investigating the role of RAB11FIP1C domains in regulating viral gene expression in B110 293 cells

In order to further investigate the specific domain of RAB11FIPC that may be involved in the regulation of the observed decreasing and increasing effects on LMP1 and BZLF1 expression, a more targeted approach was employed. Specifically, two truncated versions of RAB11FIP1C, namely RAB11FIP1C ΔRBD and RAB11FIP1C ΔRBD ΔC, were generated and co-transfected with LMP1 and BZLF1 into B110 293 cells. The RAB11FIP1 ΔRBD lacks the RAB binding domain, which is known to be important for RAB11 binding, while the RAB11FIP1 ΔRBD ΔC lacks both the RAB binding domain and the C-terminal domain. By

comparing the effects of these truncated versions with the full-length RAB11FIP1C on LMP1 and BZLF1 expression, a better understanding of the specific regions of RAB11FIP1C that are responsible for its observed effects on viral gene expression can be gained (Fig.22).

Upon investigating the role of different domains of RAB11FIP1C in regulating the expression of LMP1, it was observed that even when co-transfected with RAB11FIP1C ΔRBD, there was still a significant decrease in LMP1 expression. However, when RAB11FIP1 ΔRBD ΔC was co-transfected, the observed decrease in LMP1 expression was no longer present. This suggests that the presence of the C-terminal domain of RAB11FIP1 is necessary for the observed effects on LMP1 expression. Further analysis of the specific regions within the C-terminal domain responsible for these effects may provide valuable insights into the precise mechanism of action of RAB11FIP1C in regulating viral gene expression.

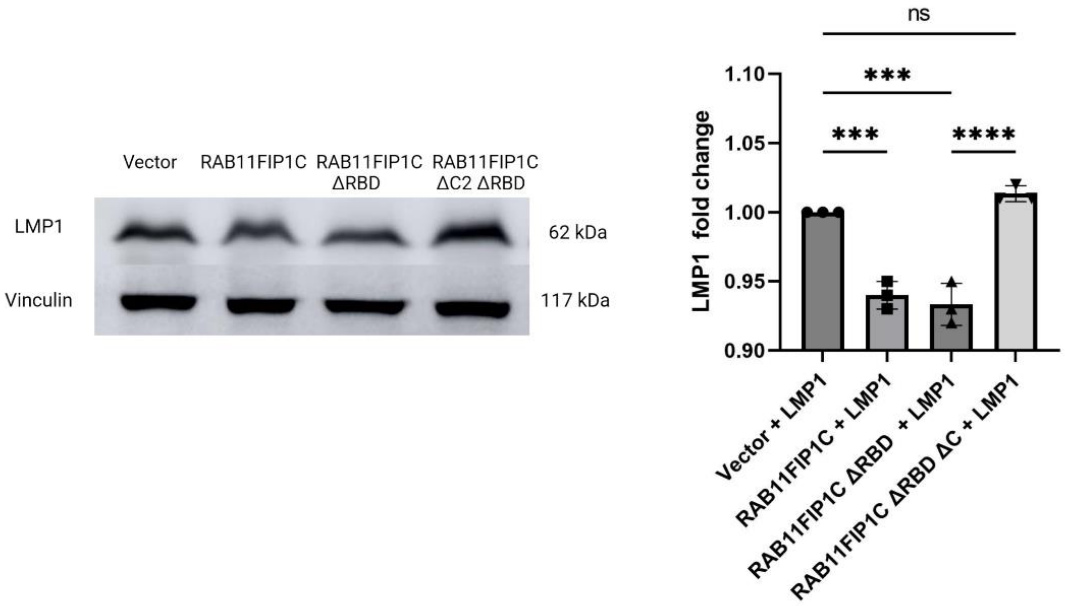

Fig.22 This figure depicts the effects of co-transfecting RAB11FIP1C and its truncated variants, RAB11FIP1C ΔRBD and RAB11FIP1 ΔRBD ΔC, with LMP1 into B110 293 cells. The graph quantifies the co-transfection results of RAB11FIP1C and its truncation variants, RAB11FIP1C ΔRBD and RAB11FIP1 ΔRBD ΔC, with LMP1 into B110 293 cells. The expression levels of LMP1 were normalized to vinculin expression for accurate comparison. Statistical significance is indicated by asterisks denoting the p value.

Similar results were obtained after co-transfection of truncated versions of RAB11FIP1C together with BZLF1 into B110 293 cells. Here again, deletion of the RBD domain, did not impair RAB11FIP1C's ability to increase BZLF1 expression. However, when RAB11FIP1C ΔRBD ΔC was co-transfected, the observed increase in BZLF1 expression was significantly

reduced. This points towards the C region as being essential to modulate BZLF1 and LMP1 expression, albeit in opposite directions (Fig.23).

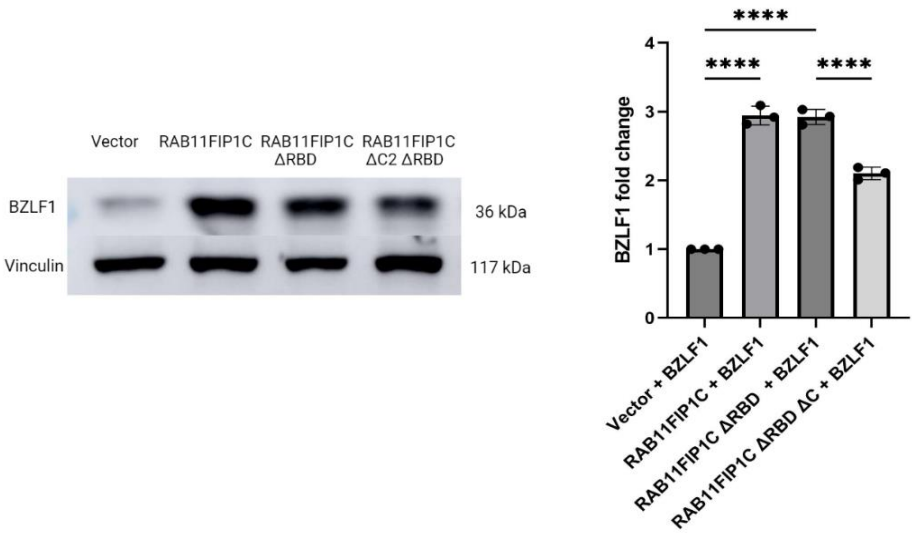

Fig.23 This figure shows the effects of co-transfecting B110 293 cells with BZLF1 and RAB11FIP1C, as well as its truncated forms, RAB11FIP1C ΔRBD and RAB11FIP1C ΔRBD ΔC. The graph illustrates the quantification of the co-transfection results on BZLF1. The expression levels of BZLF1 were normalized to vinculin expression for accurate comparison. The significance level of the data is indicated by asterisks, representing the p value.

3.12 A time course study reveals optimal time point for RAB11FIP1C's contribution to the regulation of BZLF1 expression.

To further explore the potential role of RAB11FIP1C in regulating BZLF1 expression, a time course study was conducted to examine whether its increasing effects on BZLF1 expression were sustained over time. B110 293 cells were co-transfected with RAB11FIP1C and BZLF1 for 24, 36, and 48 hours, respectively. Subsequently, cells were collected and subjected to detection to evaluate the effects of RAB11FIP1C on BZLF1 expression at each time point. By analyzing the temporal changes in the effects of RAB11FIP1C on BZLF1 expression, a better understanding of the optimal time point for RAB11FIP1C in the regulation of BZLF1 may be achieved (Fig.24). The results indicated that the peak contribution of RAB11FIP1C to BZLF1 expression occured at 24 hours. Subsequently, the presence of RAB11FIP1C no

longer significantly contributed to BZLF1 expression. Therefore, the 24-hour time point was selected for further investigation.

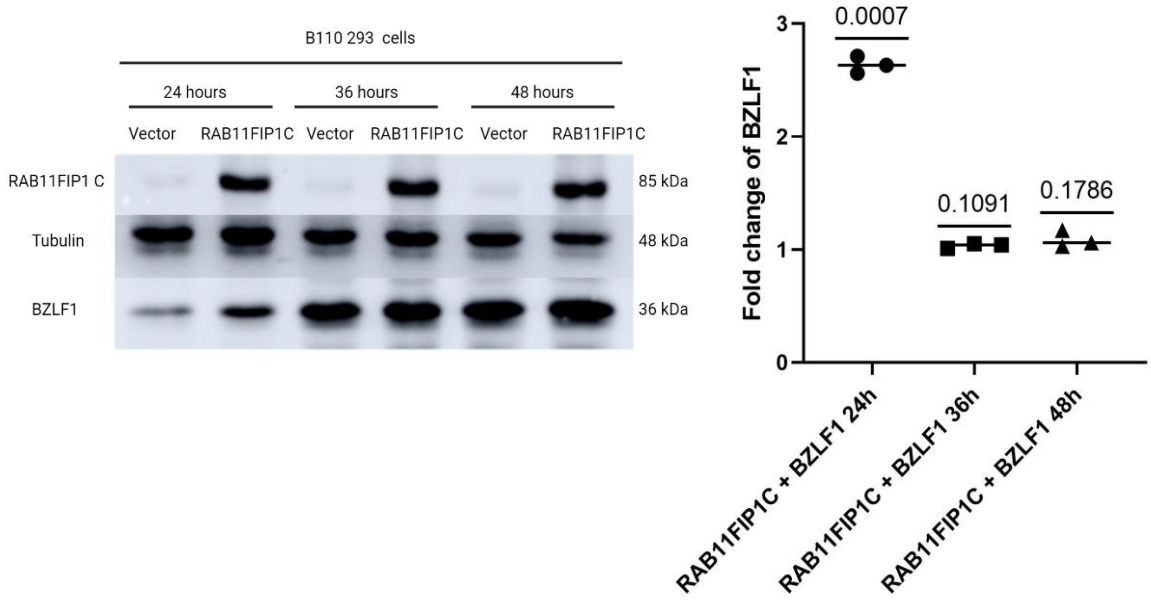

Fig.24 This figure depicts the co-transfection experiment of RAB11FIP1C with BZLF1 into B110 293 cells at different time points, namely 24, 36, and 48 hours. The results indicate that RAB11FIP1C overexpression leads to an increase in BZLF1 expression at 24 hours post-transfection, but this effect diminishes over time, with no significant increase observed at 36 or 48 hours. This graph represents the quantification results of BZLF1 fold change in response to RAB11FIP1C overexpression at the different time points. The expression levels of RAB11FIP1C were normalized to tubulin expression for accurate comparison. The statistical significance of the results is indicated by p values, with a significant difference ($p < 0.05$) and "ns" indicating no significance ($p > 0.05$).

3.13 Comparison of cellular transcripts in vector versus RAB11FIP1C ΔRBD transfected HEK293 cells

In the study, as it was observed that the RAB11FIP1C exhibited an increase in BZLF1 expression in B110 293 cells, with the effect being the most pronounced at 24 hours. These findings suggest that RAB11FIP1C may play a crucial role in regulating BZLF1 expression, and the RBD domain may not be necessary for this effect. To further investigate this phenomenon, RAB11FIP1C ΔRBD was overexpressed in HEK 293 cells to detect whether it may cause changes in cellular transcripts, leading to an increase in BZLF1 expression. In this experiment, 600ng of RAB11FIP1C ΔRBD was transfected into 293 cells. After 24 hours, cells were collected for DNA microarray analysis. The resulting heatmap generated from the

DNA microarray revealed that there were barely any gene changes when RAB11FIP1C ΔRBD was overexpressed (Fig.25). This finding suggests that the up regulation of BZLF1 is not due to the transcriptional change incurred by the overexpression of RAB11FIP1C ΔRBD. These findings suggest that RAB11FIP1C may play an important role in regulating the lytic cycle of EBV through mechanisms other than transcriptional regulation.

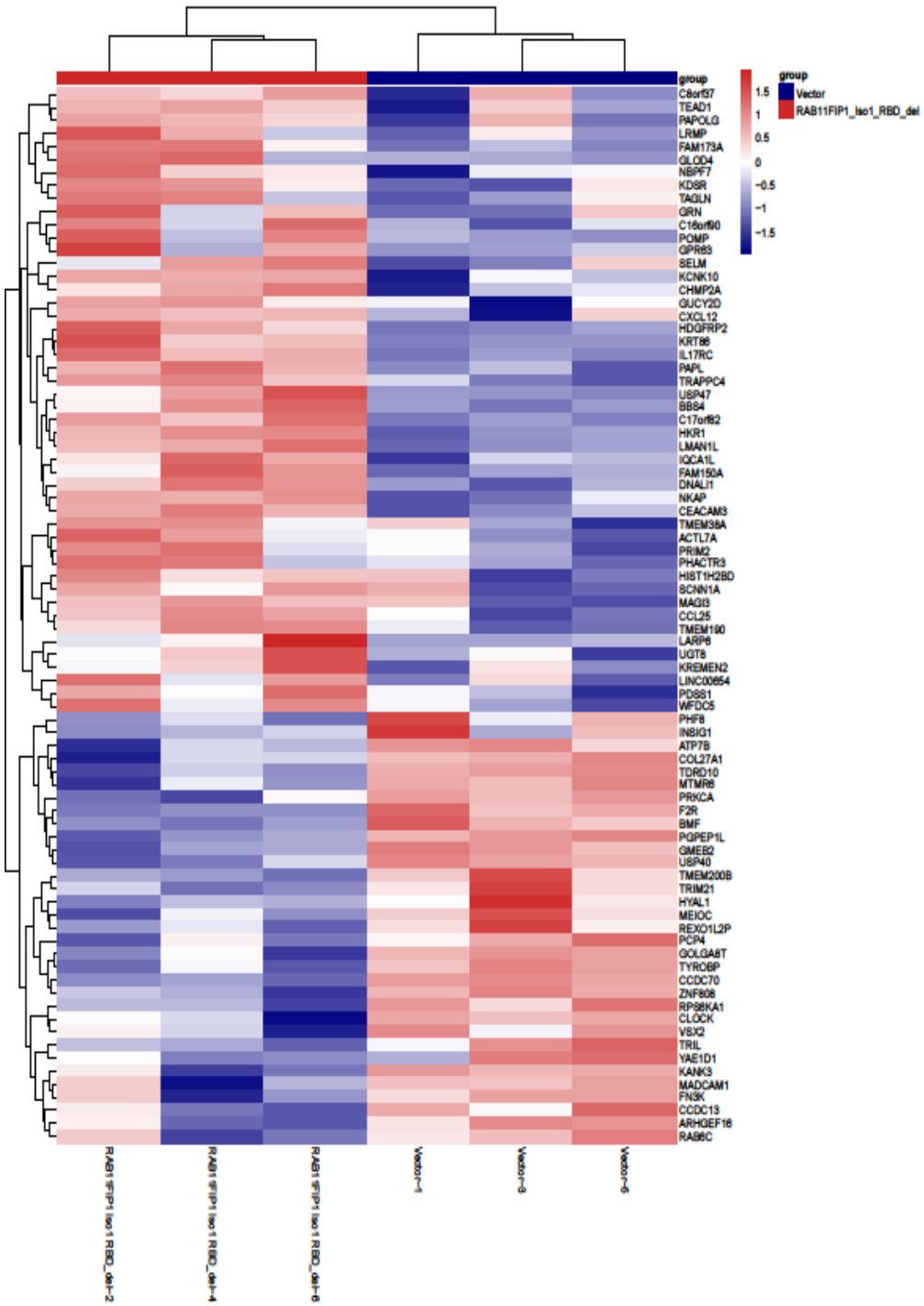

Fig.25 This heatmap presents the transcriptome analysis results of RNA samples extracted from HEK 293 cells that were transfected with either vector or RAB11FIP1C ΔRBD. Differential gene expressions were determined using log2Fold Change and a P value

threshold of less than or equal to 0.05. Genes with log2Fold values greater than or equal to 1.4 were considered up-regulated and shown in red, while those with log2Fold values less than or equal to -1.4 were considered down-regulated and shown in blue. The analysis revealed the impact of RAB11FIP1C ΔRBD on gene expression in HEK 293 cells.

For a deeper investigation into the potential signaling pathways influenced by RAB11FIP1C ΔRBD overexpression, an analysis of the differentially expressed genes detected via DNA microarray was performed, and these genes were subsequently aligned with the KEGG pathway database (Fig.26). However, our findings revealed that barely any genes were enriched in any pathway. These results suggest that the overexpression of RAB11FIP1C ΔRBD may not have a significant impact on specific signaling pathways. Further investigation is needed to elucidate the underlying mechanisms of the observed effects of RAB11FIP1C ΔRBD overexpression.

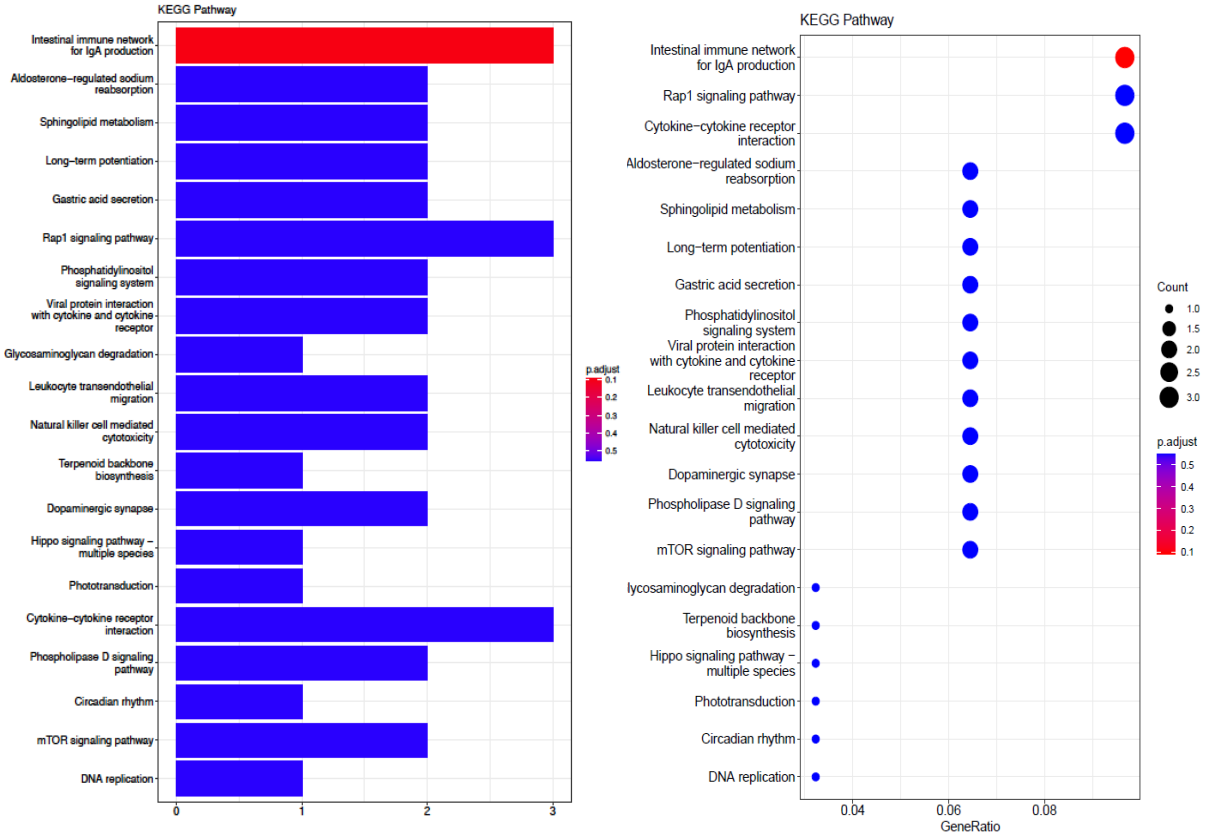

Fig.26 In this figure, a bar chart is presented, showing the top 20 KEGG enrichment pathways in the differentially expressed genes between control and RAB11FIP1C ΔRBD over-expressed HEK 293 cells. The x-axis represents the number of differentially expressed genes mapped to each pathway, while the y-axis lists the enriched KEGG pathways. This bubble chart is presented to show the KEGG enrichment of cluster-specific marker gene transcripts that are upregulated in RAB11FIP1C ΔRBD over-expressed HEK 293 cells. The size of each circle next to the pathway name represents the number of differentially expressed genes mapped to that pathway. The x-axis represents the ratio of the number of differentially expressed genes in each pathway to the total number of differentially expressed genes. The colour of each bar indicates the p-value, with redder shades indicating lower p-values.

3.14 Proteomic analysis of RAB11FIP1C ΔRBD overexpression in HEK 293 cells

Following the observation that overexpression of RAB11FIP1C ΔRBD in HEK 293 cells did not lead to any significant changes in transcriptional levels, a proteomic analysis was carried out to detect possible alterations in cellular protein levels that could play a role in EBV replication. Specifically, HEK 293 cells were transfected with RAB11FIP1C ΔRBD or with an empty vector control to investigate any changes in protein levels. The objective was to identify specific molecular events induced by RAB11FIP1C ΔRBD overexpression that may be involved in the process of EBV replication. Despite performing a comprehensive proteomic analysis, it was surprising to discover that the overexpression of RAB11FIP1C ΔRBD did not result in any significant changes in the cellular proteome (Fig.27). However, a small subset of genes did display minor alterations. The genes with the most significant changes in expression have been compiled and presented in Table 4, along with their corresponding fold changes and functional associations.

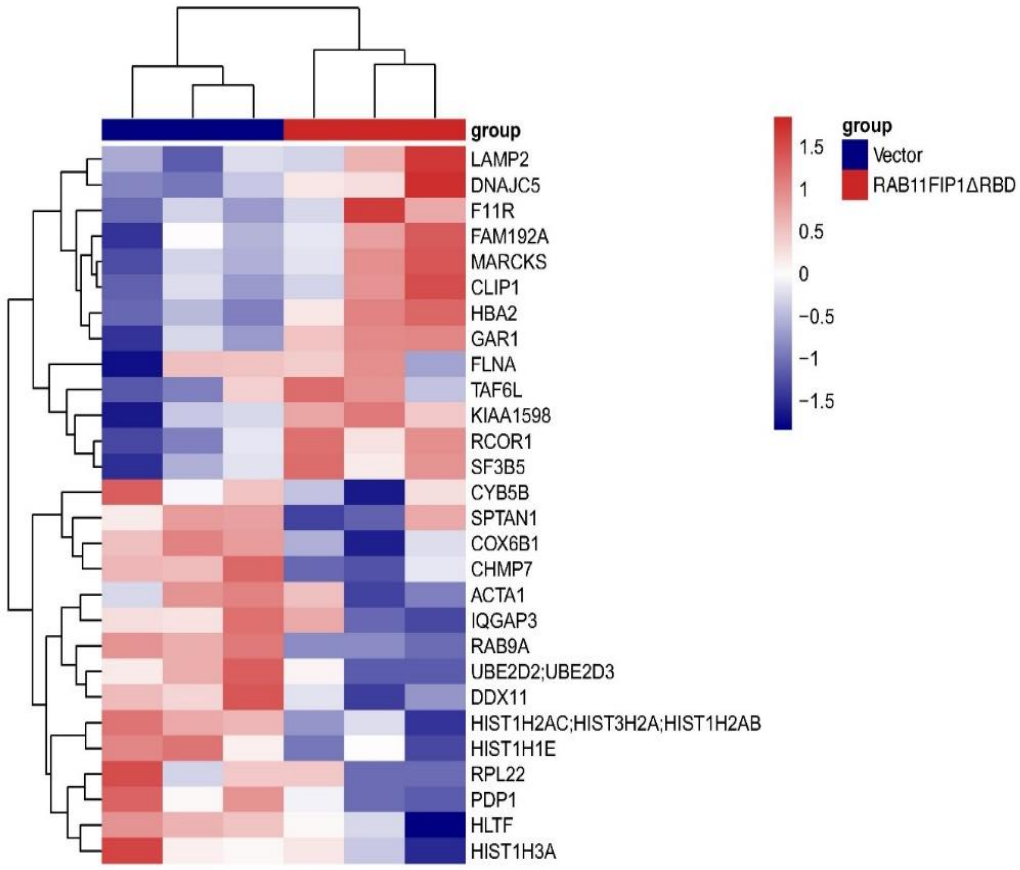

Fig.27 provides a visual representation of the differential gene expressions determined based on log2Fold Change and P value less than <0.05. The analysis provides a comprehensive overview of the impact of RAB11FIP1C ΔRBD on protein expression in HEK 293 cells.

Table.4: Gene expression changes induced by RAB11FIP1C ΔRBD overexpression.

Gene name	Regulation	Fold change	Description
LAMP2	up	1.57	Encodes a lysosomal membrane protein that is involved in the transport of lysosomal enzymes.
DNAJC5	up	1.57	Plays a role in the regulation of synaptic vesicle endocytosis and recycling.
F11R	up	1.23	Encodes a cell adhesion molecule that is involved in the regulation of tight junctions and the maintenance of epithelial integrity.
FAM192A	up	1.21	The function of this gene is not well understood, but it has been suggested to play a role in cell proliferation and differentiation.
MARCKS	up	1.33	Regulates cell motility, adhesion, and signaling by interacting with the plasma membrane and cytoskeleton.
CLIP1	up	1.57	Binds to microtubules and regulates their dynamics.
GAR1	up	1.30	Encodes a protein that is involved in the assembly and processing of ribosomes.
TAF6L	up	1.18	Part of the transcription factor IID complex, which is involved in the initiation of transcription by RNA polymerase II.
KIAA1598	up	1.62	The function of this gene is not well understood, but it has been suggested to play a role in the regulation of transcription.
RCOR1	up	1.29	Plays a role in gene regulation by acting as a transcriptional co-repressor
SF3B5	up	1.32	Part of the spliceosome, a complex that is involved in the processing of pre-mRNA into mature mRNA.
FLNA	down	-1.46	Encodes filamin A, a protein involved in linking the actin cytoskeleton to the cell membrane and organizing cellular structures.
CYB5B	down	-1.52	Encodes a cytochrome b5 protein involved in lipid metabolism and electron transfer reactions.
SPTAN1	down	-1.94	Encodes alpha-II spectrin, a protein involved in cytoskeletal organization and stability.
COX6B1	down	-1.31	Encodes a subunit of cytochrome c oxidase, which is important in the electron transport chain for cellular respiration.
CHMP7	down	-1.30	Encodes a protein involved in endosomal sorting and transport.
ACTA1	down	-1.49	Encodes alpha-skeletal muscle actin, a protein involved in muscle contraction and cytoskeletal organization.
IQGAP3	down	-1.19	Encodes a protein that interacts with a variety of cellular components and is involved in cytoskeletal

			organization, cell adhesion, and signaling.
RAB9A	down	-1.48	Encodes a protein involved in regulating intracellular vesicular transport and protein trafficking.
UBE2D2; UBE2D3	down	-1.58	Encode ubiquitin-conjugating enzymes, which play a role in protein degradation and regulation.
DDX11	down	-1.24	Encodes a DNA helicase that also plays a role in DNA repair and replication.
RPL22	down	-1.33	Encodes a ribosomal protein that is part of the large subunit of the ribosome and plays a role in protein synthesis.
PDP1	down	-1.31	Encodes a pyruvate dehydrogenase phosphatase that regulates the activity of the pyruvate dehydrogenase complex in cellular energy metabolism.
HLTF	down	-1.27	Encodes a DNA helicase that plays a role in DNA repair and replication.
HIST1H3A	down	-1.40	Encodes a histone protein that plays a role in DNA packaging and gene expression regulation.

The table presents a summary of the genes that were minimally affected upon overexpression of RAB11FIP1C ΔRBD, along with their corresponding fold change and functional annotations.

3.15 BioID-based map of human cell identifies potential candidates for RAB11FIP1C interaction

A community resource called humancellmap.org has been created based on this dataset, which provides online tools for localization analysis of user BioID data and offers insights into the results obtained from BioID experiments. The authors of this study (Go et al. 2021) presented a BioID-based map of a human cell and defined the intracellular locations of thousands of unique proteins. This map exceeded the specificity of previous approaches and enabled the discovery of proteins crucial for mitochondrial homeostasis.

Utilizing this data source, a list of potential candidates was generated with the aim of identifying proteins that could potentially interact with RAB11FIP1C (Table.5).

Bait	Bait localization	SC	SAINT
RAB11A	recycling endosome	143	1
STX7	late endosome, lysosome	99	1
RHOB	late endosome, lysosome, plasma membrane	26.5	1
KRAS	plasma membrane	26.5	1
RAB9A	Golgi apparatus, late endosome, lysosome	21.5	1
RAB35	plasma membrane, recycling endosome	19	0.98
OCLN	cell junction	14	0.99
STX6	Golgi membrane, early endosome	13	1
ZFPL1	Golgi membrane	13	0.99
EBAG9	Golgi membrane	11.5	1
CAV1	caveola, plasma membrane	11.5	1
MARCKS	cytoskeleton, plasma membrane	12	0.96
LYN	plasma membrane	11.5	0.95
LAMP2	late endosome, lysosome	11	0.96
RAB4A	early endosome, recycling endosome	10	0.95
FLOT1	caveola, plasma membrane	9.5	0.94
LCK	plasma membrane	9	0.91
CXADR	cell junction	9	0.93
LAMTOR1	late endosome, lysosome	8.5	0.9
LAMP3	late endosome, lysosome	8.5	0.92
MARCKS	plasma membrane	8	0.9
RAB5A	early endosome	6	0.9

Table.5: Summary table of the publicly available Bio-ID interactome dataset for RAB11FIP1 from Cell Map, showing average spectral counts (SC) and SAINT score for interactors (https://cell-map.org/; Table 5).

Syntaxin7, Rab9, and Rab7 are important proteins involved in intracellular trafficking and lysosomal biogenesis. Syntaxin7 is a SNARE protein that mediates the fusion of late endosomes with lysosomes, while Rab9 and Rab7 are small GTPases that regulate the transport of endocytic vesicles from early to late endosomes and from late endosomes to the trans-Golgi network, respectively. These proteins were selected due to their known involvement in vesicle trafficking and the endocytic pathway, which may be critical for the replication of LCLs.

The expression levels of Syntaxin7, Rab9, and Rab7 were analyzed in both replicating and latent LCLs to investigate any potential changes (Fig.28). However, the results did not reveal any significant changes between the two groups, indicating that these proteins may not play a major role in regulating the transition from latent to replicating state in LCLs.

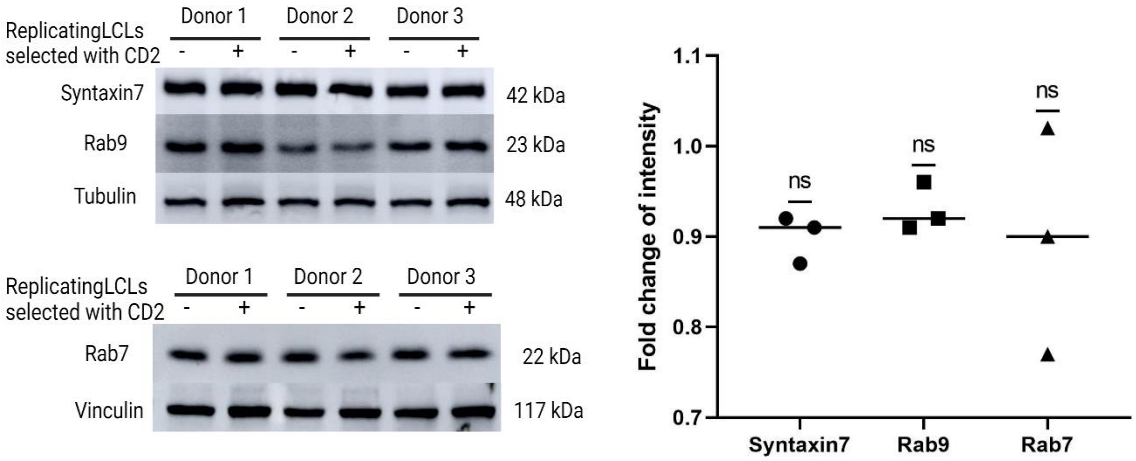

Fig.28 The expression changes of Syntaxin7, Rab9, and Rab7 were examined in both latent and replicating LCLs. The expression levels of Syntaxin7, Rab9, and Rab7 were normalized to vinculin expression for accurate comparison. The quantification results of Syntaxin7, Rab9, and Rab7 were presented for both latent and replicating LCLs. ("ns" was used to indicate the cases where there was no significant difference between the two groups.)

3.16 RAB11FIP1C transfection leads to increased BZLF1 expression in B110 293 cells independently of cell proliferation

B110 293 cells were co-transfected with vector and RAB11FIPC1, and immunofluorescence was performed to quantify the variations in BZLF1 protein expression.. The results showed a significant increase in the BZLF1 expression rate (Fig.29 A and B). To determine if the upregulation of BZLF1 was due to a change in its transcriptional level induced by RAB11FIP1C overexpression, BZLF1 was co-transfected with vector and RAB11FIP1C into B110 293 cells. The expression of BZLF1 was then measured using RT-qPCR to determine if there was any change in its transcriptional level in response to RAB11FIP1C overexpression. Surprisingly, the results showed that there was no significant change in the transcriptional level of BZLF1 in response to RAB11FIP1C overexpression, suggesting that the increase in BZLF1 expression was not caused by RAB11FIP1C did not result from variations in transcription .

Previous studies have reported that RAB11FIP1 recruitment to the midbody is crucial for proper Rab35 function in actin removal during cytokinesis. In the absence of Rab11FIP1C, Rab35 drops from the midbody, leading to defects in cytokinesis, such as cytokinetic delays and binucleation due to the overaccumulation of actin at the intercellular bridge (Iannantuono

and Emery 2021). Thus, to determine whether the observed increase in BZLF1 expression was due to an increase in cell numbers after RAB11FIP1C transfection, cell numbers were counted for both control and RAB11FIP1C transfected B110 293 cells. However, the results indicated that there was no significant increase in cell number, suggesting that the observed increase in BZLF1 expression was not simply a result of increased cell proliferation (Fig.29 C and D).

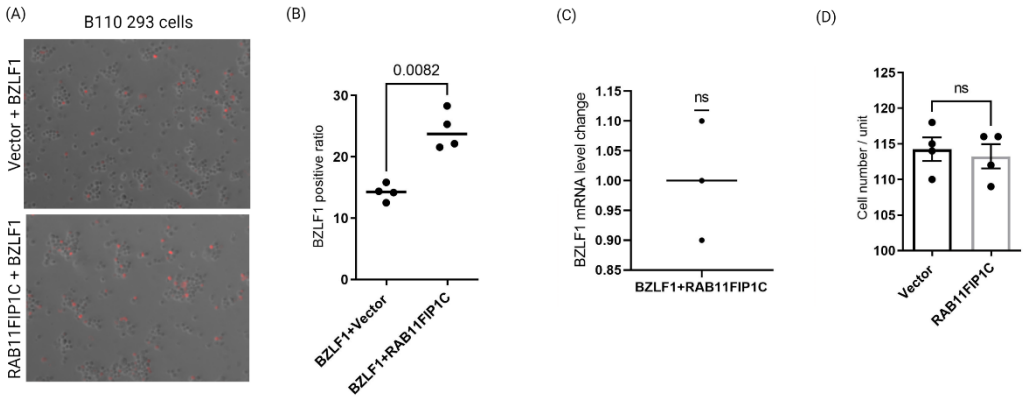

Fig.29 (A) BZLF1 staining was performed 24 hours after co-transfection with BZLF1 into B110 293 cells. (B) Panel B shows the quantification of BZLF1 positive cells in B110 293 cells that were transfected with Vector + BZLF1 and RAB11FIP1C + BZLF1, respectively. (C) The mRNA level of BZLF1 was detected by RT-qPCR in panel C to determine if there were any transcriptional effects of BZLF1. (D) In panel D, cells were counted to determine whether RAB11FIP1C could increase the population after its transfection into B110 293 cells. A p-value less than 0.05 was deemed statistically significant and "ns" indicates not significant).

3.17 Suppression of autophagy inhibits BZLF1 expression as well as RAB11FIP1C

Autophagy, a cellular process responsible for the degradation and recycling of damaged or unnecessary cellular components, plays a vital role in maintaining intracellular balance. Endosomes play a role in the regulation of autophagy by influencing the trafficking and fusion events involved in autophagosome formation. Because RAB11FIP1C is involved in the transportation of endosomes, my hypothesis was that RAB11FIP1C prevented endosome degradation and promoted recycling. This, in turn, would reduce the fusion of endosomes with autophagosomes and subsequently leads to decreased degradation of BZLF1.To investigate the potential degradation of BZLF1 through autophagy, an autophagy inhibitor known as MRT68921 was used to assess its impact on BZLF1 levels change. MRT68921 has been documented to exhibit inhibitory effects on autophagy by targeting specific proteins involved in the process, such as ULK1 and ULK2 (Unc-51-like autophagy-activating kinases).

Through the inhibition of these proteins, MRT68921 interferes with the initiation of autophagy, leading to disruption of the autophagy process. Unexpectedly, the administration of the autophagy inhibitor MRT68921 resulted in a reduction in the expression level of BZLF1(Fig.30). These findings suggest that the degradation of BZLF1 probably does not occur through modulation of the autophagy process.

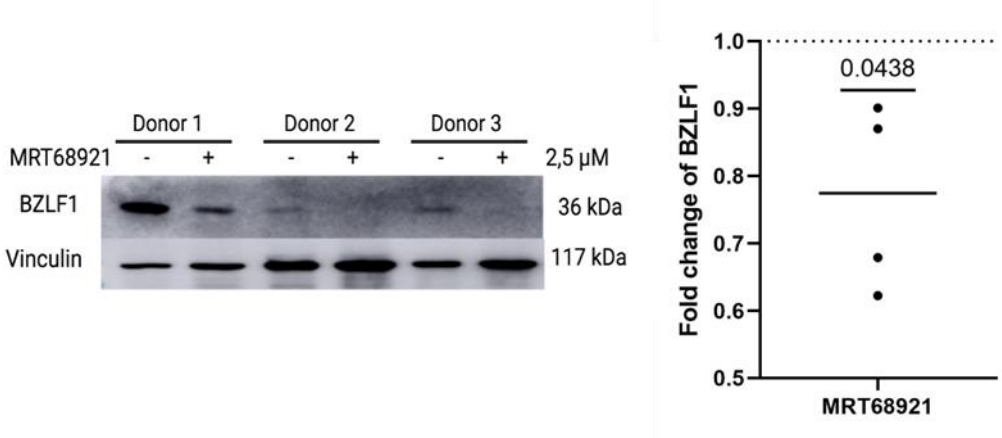

Fig.30 The figure illustrates the change in BZLF1 expression following a 24-hour treatment of MRT68921. The expression levels of BZLF1 were normalized to vinculin expression for accurate comparison. The graph presents the results of BZLF1 quantification upon a 24-hour treatment of MRT68921 and its resulting fold change in expression. The significance level of the data is indicated the corresponding p-value.

The impact of the autophagy inhibitor MRT68921 on the expression of RAB11FIP1C was also investigated. Interestingly, the expression of RAB11FIP1C was also found to decrease upon treatment with MRT68921(Fig.31). Based on my previous experimental findings, it appears that elevated expression of RAB11FIP1C plays a role in upregulating BZLF1, while a decrease in RAB11FIP1C expression leads to a subsequent reduction in BZLF1 levels. Therefore, the downregulation of BZLF1 induced by MRT68921 could also be attributed to the decrease of RAB11FIP1C.

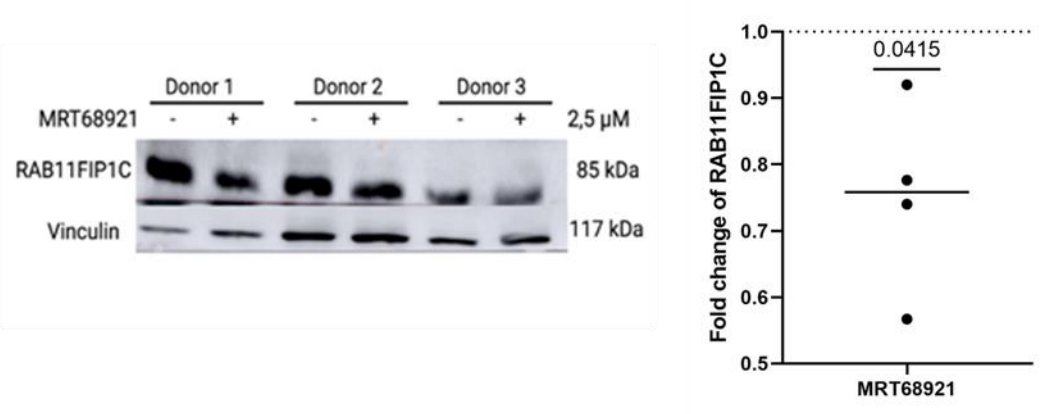

Fig.31 The figure illustrates the change in RAB11FIP1C expression following a 24-hour treatment of MRT68921. The expression levels of RAB11FIP1C were normalized to vinculin expression for accurate comparison. The graph presents the quantification results of the fold change in RAB11FIP1C expression upon a 24-hour treatment of MRT68921. The significance level of the data is indicated the corresponding p-value.

3.18 The role of RAB11FIP1C and its C2 domain in cellular localization and EBV replication

In the present study, it was found that the C2 domain of RAB11FIP1C plays a crucial role in both its enhancing and inhibitory effects. C2 domains, which are approximately 130 amino acid motifs, are present in numerous proteins involved in cell signaling, such as phosphoinositide-3-kinase (PI-3-kinase) and PTEN, as well as membrane trafficking proteins like rabphilin-3A and synaptotagmin. These domains were initially discovered in protein kinase C (PKC) (Cho 2001). Multiple research studies have provided evidence showing that the expression of truncated versions of RAB11FIPs, lacking their C2 domains, leads to a notable decrease in the rate of endosomal recycling. The recycling of transferrin to the plasma membrane is hindered, implying a key regulatory role of the C2 domain in class I Rab11FIPs for the transportation of ligands and their receptors back to the plasma membrane (Lindsay et al. 2002; Lindsay and McCaffrey 2002; Prekeris et al. 2000).

C2 domains exhibit a preference for binding to PtdIns(3,4,5)P_3 and phosphatidic acid (PA). Stimulation of A431 cells with epidermal growth factor (EGF) or with a phorbol ester leads to the synthesis of PtdIns(3,4,5)P_3 or PA, followed by relocation of endogenous RAB11FIP1C from the endosomal-recycling compartment (ERC) to the plasma membrane. This translocation is effectively blocked when cells are pre-treated with wortmannin, a PI3K inhibitor. Notably, the presence of the C2 domain within RAB11FIP1C is of utmost importance for this plasma membrane translocation event. Truncation mutants lacking this

domain fail to undergo translocation even when subjected to the same treatments in cells (Lindsay and McCaffrey 2004).

The quantification of RAB11FIP1C's distinct morphological features was conducted in latent and replicating LCLs. In LCLs, around 45% of cells showed RAB11FIP1 localized in the perinuclear region, forming a characteristic dot-like formation. However, during replication, there was a significant change in the formation of RAB11FIP. Specifically, the dot-like formation observed in LCLs became more diffuse in replicating LCLs. These findings suggest that the behavior of RAB11FIP1 is affected by EBV replication and could potentially play a role in the regulation of cellular processes during this stage of EBV replication (Fig.32 and 33).

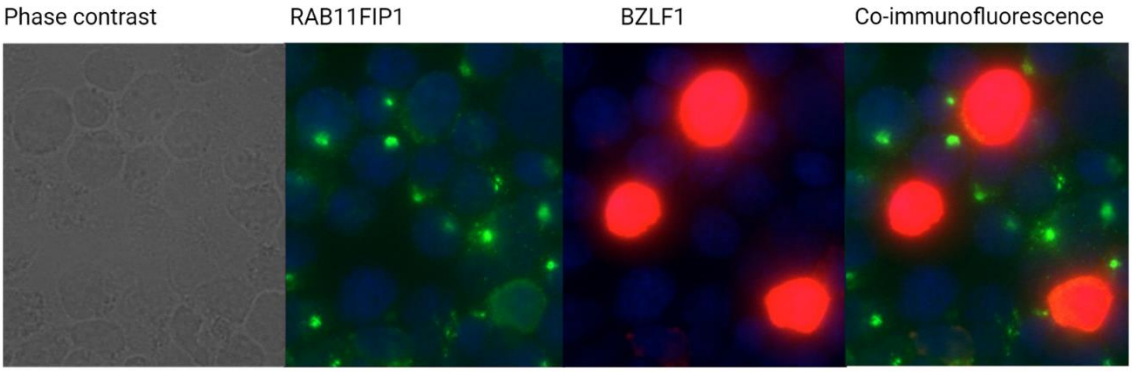

Fig.32 The images presented here depict the staining results of RAB11FIP1 (shown in green) and BZLF1 (shown in red), with the nuclei labelled using DAPI (shown in blue).

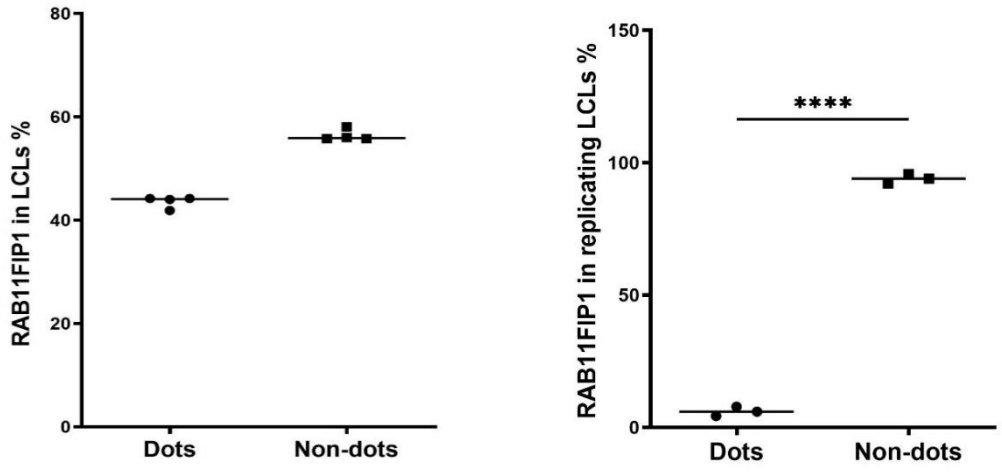

Fig.33 The image displays the counting results of RAB11FIP1 formations in LCLs, categorized as Dots-like and Non-dots-like. The image also presents the counting results of

RAB11FIP1C formations in replicating LCLs, classified as Dots-like and Non-dots-like. The significance level of the data is indicated by asterisks, representing the corresponding p-value.

3.19 The role of RAB11FIP1C and its C2 domain in cellular localization and EBV replication

Therefore, the effects of wortmannin, a PI3K inhibitor, on RAB11FIP1C and BZLF1 was investigated. Treatment with the PI3K inhibitor resulted in a slight decrease in the expression of RAB11FIP1C and a significant reduction in BZLF1 expression (Fig.34).

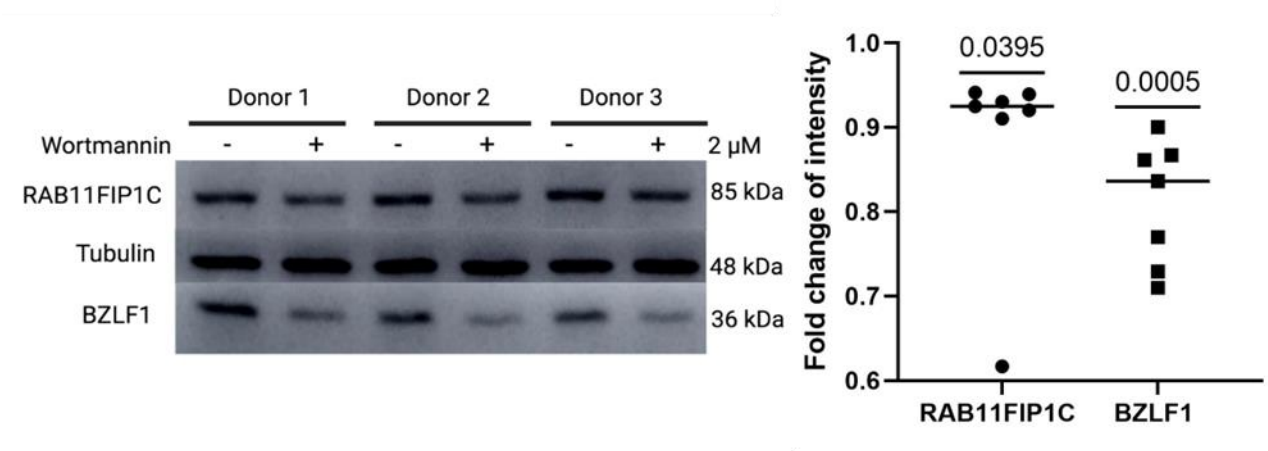

Fig.34 The figure depicts the change in BZLF1 expression observed in LCLs following treatment with wortmannin. The expression levels of RAB11FIP1C and BZLF1 were normalized to tubulin expression for accurate comparison. The graph displays the quantification data, presenting the fold change in BZLF1 expression after a 24-hour wortmannin treatment in LCLs. The significance level of the data is indicated the corresponding p-value.

To further investigate the potential involvement of the AKT/PI3K pathway in EBV replication, Recilisib, an activator of AKT and PI3K, was utilized. However, the results depicted in the graph indicate that treatment of LCLs with Recilisib for a 24-hour incubation period did not induce any significant changes in the expression levels of RAB11FIP1C and BZLF1 (Fig.35).

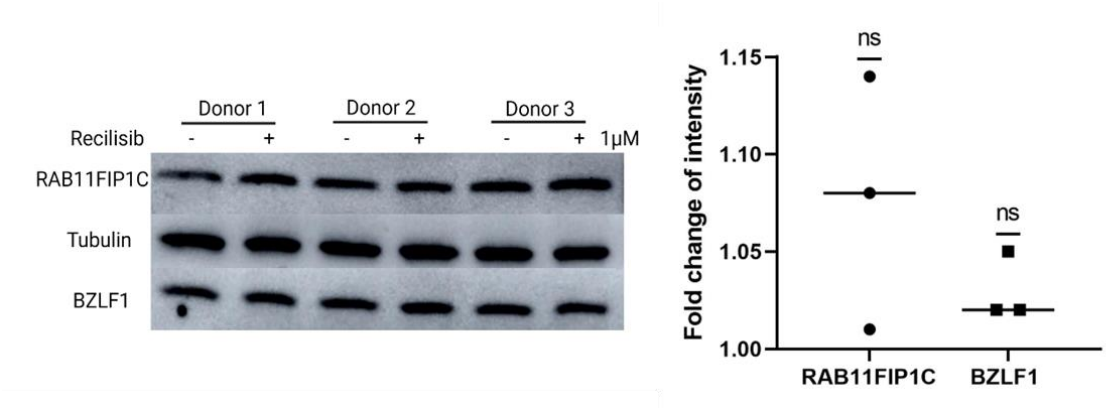

Fig.35 The figure illustrates the alteration in BZLF1 expression observed in LCLs upon treatment with Recilisib. The expression levels of RAB11FIP1C and BZLF1 were normalized to tubulin expression for accurate comparison. The graph showcases the quantified results, demonstrating the fold change in BZLF1 expression following a 24-hour treatment of Recilisib in LCLs.

EGF triggers the activation of PI3K, subsequently leading to the activation of AKT. Through its activation, AKT plays a crucial role in governing a wide range of cellular processes by phosphorylating specific target proteins (Liu et al. 2009).Then the effects of EGF treatment on HEK293 cells were assessed by performing staining for RAB11FIP1 to observe any alterations in its formation. Staining was conducted at 15, 30 minutes and 3-hour time points. The results of the staining revealed significant changes in the intensity and distribution of RAB11FIP1. Specifically, the staining intensity of RAB11FIP1 exhibited a stronger signal, indicating an upregulation. Additionally, the formation of RAB11FIP1 shifted from its original perinuclear localization to the plasma membrane (Fig.36). These observations provide compelling evidence of the dynamic changes induced by EGF treatment in the localization and abundance of RAB11FIP1.

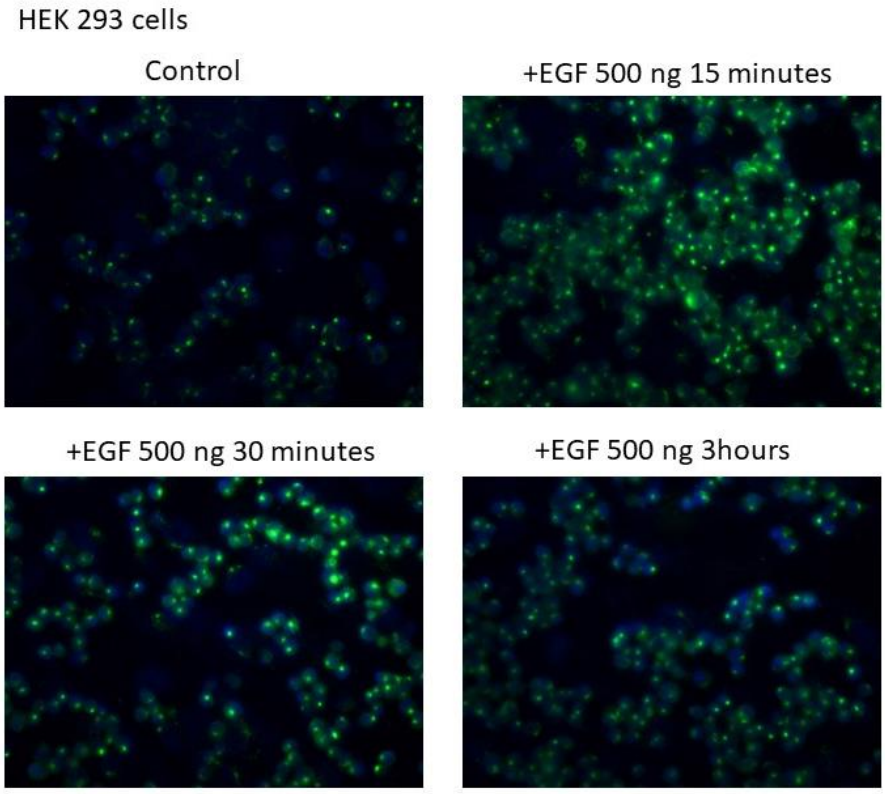

Fig.36 These images illustrate the staining outcomes of RAB11FIP1, visualized in green, captured at various time intervals. Additionally, the nuclei are clearly labelled using DAPI, indicated by blue coloration.

After transfecting BZLF1 into B110 293 cells, 500 ng of EGF was added 12 hours later. Following a 12-hour incubation, cells were collected for Western blot analysis. The results revealed an increase in BZLF1 expression upon EGF treatment (Fig.37).

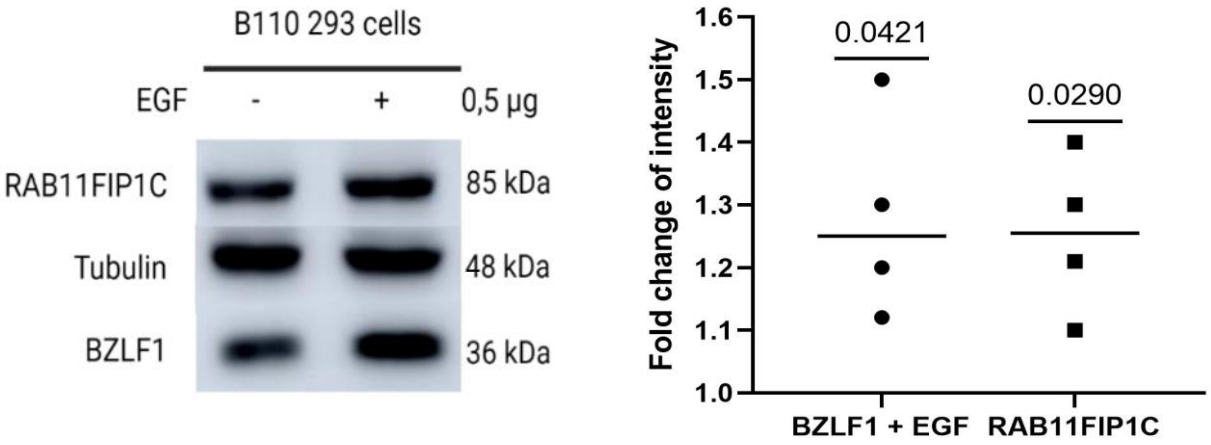

Fig.37 The figure demonstrates the change in BZLF1 expression observed in B110 293 cells following EGF treatment. The expression levels of RAB11FIP1C and BZLF1 were normalized to tubulin expression for accurate comparison. The graph displays the quantification data, presenting the fold change in BZLF1 expression after a 24-hour EGF treatment in B110 293 cells. The significance level of the data is indicated the corresponding p-value.

4. Discussion

The M81 strain, isolated from a patient with nasopharyngeal carcinoma, has been previously found to induce robust spontaneous virus production in infected B cells. Moreover, it has been observed that M81 lytic replication is closely associated with chromosome instability, indicating a direct link between the two phenomena. As such, investigating the mechanisms that underlie M81's ability to replicate is crucial for understanding its oncogenic properties. However, despite its significance, much less is known about the spontaneous replication of M81 compared to replication induced by chemical agents. Thus, there is a need for further research to elucidate the mechanisms involved in M81's spontaneous replication, which may shed light on the development and progression of virus-associated malignancies. Understanding the mechanisms of EBV replication is important for developing treatments for EBV-associated diseases, as well as for developing vaccines to prevent infection with this virus.

However, lytic replication of Gammaherpesviruses is notoriously difficult to study as there are no fully permissive cellular systems available. For this reason, all investigators in the field use rare cell lines that support virus replication but are completely artificial. For the first time in our lab, a physiological experimental system has been developed in infected primary B cells, in which replicating cells are rescued using the CD2 purification system encoded onto the virus. However, only 5% of the infected B cells produce the virus and their purification is very time- and work intensive. Moreover, investigators in the laboratory have developed a very complex plasmid that allows expression of transgenes in infected B cells. This plasmid remains as an episome in infected B cells independently of the viral genome and requires an origin of replication as well as two surface markers, an inactive rat CD2 or an inactive NGF-receptor. This very complex system is necessary because EBV-infected B cells are difficult to transfect and the small percentage of the cell population that receives the plasmid needs to be sequentially purified by antibodies specific to CD2 or to the NGF-receptor. As previously mentioned, only approximately 1% to 5% of the LCL population consists of actively replicating cells. Consequently, the effects of the candidate genes can only be very limited when studying the whole population. They remain nevertheless substantial. Moreover, taking the low number of replicating cells into consideration, the candidate genes are expected to have a notably more substantial impact in replicating cells than what is currently observed in the blots. Thus, not all experiments can be performed in LCLs and need to be performed in B110 293 cells. Another advantage of the B110 293 cells is that we can initiate the EBV lytic

replication with high efficiency by co-transfecting BZLF1, which is not possible with the LCLs. Thus, our experiment systems go well beyond the state-of-the-art in the field and allow identification of previously unknown molecular mechanisms, but they need to be completed with more conventional experimental systems.

4.1 Exploring cellular genes and their role in EBV replication

To explore the replicating process of LCLs and identify the cellular genes involved, the following experimental strategy was employed. The rat CD2 gene was introduced into the BXLF1 gene of EBV M81 genome, enabling the isolation of replicating LCLs from latent LCLs. A comparative analysis was performed between replicating and latent EBV-infected B cells to identify cellular genes specifically associated with LCL replication. This comparative study offered an opportunity to explore the changes in gene expression patterns during the replication process, thereby gaining valuable insights into the functional roles of these genes in LCL replication.

The study initially focused on cellular genes that exhibited significant changes in DNA microarray assays, that could be confirmed by qPCR. These candidate genes were then transfected into B110 293 cells to investigate whether they could trigger the initiation of EBV replication. However, this functional approach showed that they cannot induce EBV replication in isolation. Therefore, they were subsequently co-transfected with BZLF1 to assess their impact on BZLF1 expression and on the whole replication cycle as assessed by gp350 expression. Furthermore, the genes were stably transfected into LCLs to evaluate their effects on spontaneous production of BZLF1. Interestingly, the study identified RAB11FIP1 as a crucial component influencing the replication process of EBV. This discovery prompted further exploration into the specific mechanisms by which RAB11FIP1 may contribute to driving viral replication, leading to a comprehensive investigation and subsequent discussion.

4.2 Genes that exhibited differential expression were evaluated using bulk RNA-seq analysis

There are two types of EBV, Type 1 (T1) and Type 2 (T2), that infect humans and cause different phenotypes in B cells due to substantial differences in their EBNA2 and EBNA3A/B/C latency proteins. In vitro experiments have shown that T1 EBV is more efficient at transforming B cells, while B cells infected with T2 EBV exhibit higher levels of lytic activity. In a recent study (Bristol et al. 2022), the researchers used bulk RNA-seq to analyze the gene expression of both cellular and viral genes in early-passage lymphoblastoid

cell lines (LCLs) infected with either T1 or T2 EBV strains. The analysis revealed that T2 LCLs exhibit distinct gene expression profiles compared to T1 LCLs and our focus shifted towards identifying genes that showed upregulation in both this screening process and our study. The examination of our DNA micro array results indicated an upregulation of the following genes: NFATC1, BIN1, MXD1, WSB1, SMYD4, ZNF483, CARKD, CREBRF, RAB11FIP1, RAB11FIP3, KIDINS220, ING1, and DKK4 were upregulated. Within this list, RAB11FIP1 and DKK4 were upregulated both in our screen and in T2 EBV-infected LCLs compared to T1 EBV-infected LCLs, with adjusted p-values of 0.054 and 0.060, respectively. Thus, RAB11FIP1 may play a crucial role in the replication process of T2 LCLs and of M81 LCLs. Notably, another study found that RAB11FIP1 remains continuously activated upon treatment with thapsigargin, a chemical agent that induces EBV lytic replication (Taylor et al. 2011) (Fig.38). Altogether, these data suggested that the elevated expression of RAB11FIP1 is an important event during EBV lytic replication in multiple cellular systems.

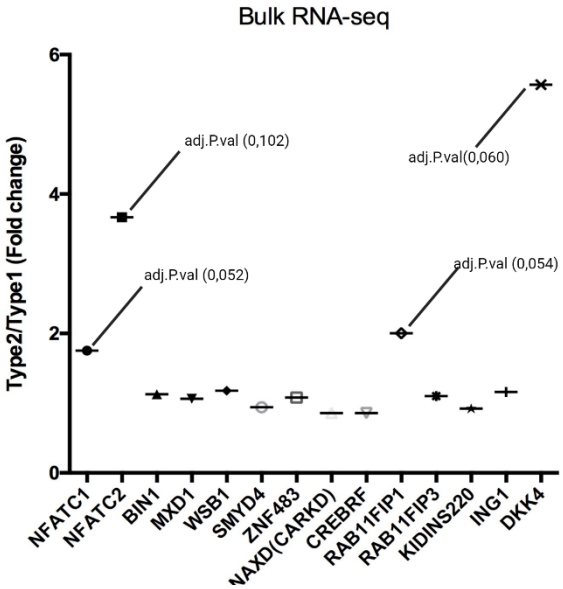

Fig. 38 The authors utilized bulk RNA-seq data to compare the gene expression patterns of T1 EBV- and T2 EBV-infected LCLs. Their goal was to identify the specific cellular gene expression program that is associated with the lytically-infected cell population(s). The bulk RNA-seq data was used to summarize the observed changes in upregulated candidate genes from the RT-qPCR results. The adjusted p-values for the differentially expressed genes were also reported (https://doi.org/10.1371/journal.ppat.1010453).

4.3 Enhanced BZLF1 expression by RAB11FIP1 is independent of transcription and translation

In this study, it was observed that both RAB11FIP1C and RAB11FIP1B exhibited increased

expression levels in replicating LCLs. This suggests that their higher expression potentially plays a facilitative role in the replication process. Transfecting either RAB11FIP1C or RAB11FIP1B along with BZLF1 resulted in an elevation of BZLF1 expression. Given that RAB11FIP1C is the predominant isoform expressed in LCLs, its specific role in the regulatory process was further investigated. RAB11FIP1C has the ability to upregulate the expression of genes such as BZLF1 and GFP, while also downregulating the expression of others, such as LMP1.

The functional roles of different domains of RAB11FIP1C isoform were investigated by analyzing the effects of forms of the proteins that lack the RBD and/or the C2 domain. These truncated forms were co-transfected with LMP1 and BZLF1 to assess their impact on gene upregulation and downregulation. Based on the findings, it was observed that the ability of RAB11FIP1C to modulate the expression of other proteins was primarily influenced by the C2 domain rather than the RBD domain. For a detailed examination of the effects of the RAB11FIP1C isoform without the RBD domain on transfected cells, alterations in transcriptional levels resulting from its overexpression were assessed. Surprisingly, the overexpression of the RAB11FIP1C isoform lacking the RBD domain had minimal effects on transcriptional level changes. This observation suggests that the upregulation of BZLF1 may not be attributed to transcriptional modifications caused by the overexpression of RAB11FIP1C RBD deletion isoform.

Subsequently, the RAB11FIP1C isoform lacking the RBD domain was once again overexpressed in HEK293 cells to investigate potential alterations in cellular proteomics. This analysis aimed to identify any cellular proteomic changes that could potentially contribute to the expression of BZLF1. Here again, the overexpression of the RAB11FIP1C isoform lacking the RBD domain did not induce any significant changes in cellular proteomics.

Consequently, a BioID-based mapping strategy was utilized to uncover potential protein interactions associated with RAB11FIP1C. Notably, the expression of Syntaxin7, Rab9, and Rab7, key proteins involved in intracellular trafficking and lysosomal biogenesis, was examined in replicating LCLs. However, Western blot analysis revealed that their expression levels in replicating LCLs remained unchanged when compared to latent LCLs.

RAB11FIP1 actively participates in the intricate dynamics and crucial functions of endosomes within the cell. Moreover, endosomes and autophagy exhibit a close interconnection, working in coordination to regulate various cellular processes. To investigate whether BZLF1 undergoes degradation through this pathway, an autophagy inhibitor was

employed. Surprisingly, treatment with this inhibitor resulted in a decrease in both BZLF1 levels and the expression of RAB11FIP1C.

The findings suggest that BZLF1 is not subjected to degradation via the autophagy pathway. Additionally, the downregulation of RAB11FIP1C using its specific shRNA leads to a decrease in BZLF1 expression. Therefore, it can be inferred that the inhibitory effects of the autophagy inhibitor on BZLF1 expression are likely mediated by its suppression of RAB11FIP1C.

4.4 The role of RAB11FIP1 in endosomal recycling and its intriguing distribution patterns in LCLs

In eukaryotic cells, the internalization of cell surface proteins occurs through the essential process of endocytosis. Once internalized, these proteins are directed to specialized organelles known as early or sorting endosomes (EEs). Within these multifunctional organelles, a critical decision is made regarding the fate of the proteins: either they are recycled back to the plasma membrane or transported to late endosomes and lysosomes for degradation. Many ligands, receptor-ligand complexes, and other substances that are meant to be degraded are transported from sorting endosomes to late endosomes, and ultimately to lysosomes, where they are broken down by hydrolytic enzymes. The precise mechanisms underlying the sorting and recycling of endocytosed proteins remain largely elusive, despite their fundamental importance in maintaining proper cellular function and promoting growth (Mellman 1996; Robinson et al. 1996).

RAB11FIP1 is an important protein involved in regulating endosomal recycling, a critical process for the transportation and sorting of various molecules within cells (Jin and Goldenring 2006; Peden et al. 2004). Recent research has indicated that RAB11FIP1 may also play a key role in virus-host interactions, particularly in the entry and replication of certain viruses such as influenza virus and HIV (Bruce et al. 2010; Fernandez-de Céspedes et al. 2022). Studies have shown that RAB11FIP1 interacts with the HIV envelope protein, facilitating the movement of the virus from endosomes to the plasma membrane (Qi et al. 2013).

Notably, RAB11FIP1 plays a critical role in intracellular sorting processes by accommodating various cargo, such as receptor tyrosine kinases, integrins, and other membrane receptors or molecules. In particular, the RAB11FIP1-Rab11 complex assumes a pivotal role in controlling the sorting of transferrin receptors. This dynamic complex

facilitates the transition of transferrin receptors from the degradative pathway to the recycling pathway, ensuring their proper cellular recycling and function (Peden et al. 2004).

The subcellular localization of RAB11FIP1C in LCLs was investigated, demonstrating its distribution in two distinct regions. It was primarily observed in the perinuclear region, while also exhibiting cytoplasmic localization near the membrane. This localization pattern was confirmed by the colocalization analysis with markers such as Lamin A and CD27.

The positioning of RAB11FIP1C within LCLs displays distinct patterns, which are associated with its formation. In the perinuclear region, RAB11FIP1C exhibits a dot-like configuration, whereas its relocation to the membrane results in a more diffuse distribution. Previous studies have proposed that these changes in formation are reliant on the C2 domain of RAB11FIP1C. Our findings align with this notion, as the C2 domain-dependent effects of RAB11FIP1C on BZLF1 expression were observed, emphasizing the significance of this domain in mediating its regulatory role.

Furthermore, the distribution of RAB11FIP1 throughout the cytoplasm appeared to be well-balanced, as indicated by a relatively stable ratio of dot-like formations to non-dot-like formations. In the context of replicating LCLs, a noticeable change occurred in the dot-liking formation ratio of RAB11FIP1, demonstrating a significant decrease compared to latent LCLs. This shift was accompanied by a distinct alteration in the subcellular localization pattern of RAB11FIP1. Specifically, RAB11FIP1 underwent a transition from dot-like formations primarily located in the perinuclear region to a more diffused distribution throughout the cytoplasm. These observations indicate a dynamic reorganization of RAB11FIP1 within replicating LCLs, suggesting its involvement in specific cellular processes associated with LCL replication.

4.5 Interplay of RAB11FIP1, PI3K/AKT, mTOR, and EGFR Signaling in EBV replication

One study has proposed a potential link between the positional shift of RAB11FIP1 and its involvement in the PI3K/AKT pathway. Furthermore, multiple studies have demonstrated the impact of the mTOR pathway on the replication of EBV. Inhibition of mTOR signaling has emerged as a promising strategy to effectively suppress the lytic replication of EBV in infected cells (Adamson et al. 2014; Wang et al. 2020). The combination of rapamycin, a specific inhibitor of the mTOR pathway, with inhibition of PI3K and Akt has demonstrated synergistic effects in reducing the growth of EBV positive PTLD cells (Furukawa et al. 2013;

Sang et al. 2019).

In this study, LCLs were treated with both a PI3K/AKT pathway activator and an inhibitor to assess the impact on BZLF1 and RAB11FIP1C.The inhibition of the PI3K/AKT pathway led to a decrease in BZLF1 expression, accompanied by a reduction in RAB11FIP1C levels. Conversely, treatment with the PI3K/AKT pathway activator did not result in any noticeable changes in BZLF1 and RAB11FIP1C expression.

Previous studies have noted the ability of EGF to induce changes in the localization of RAB11FIP1C, prompting an investigation into its functional effects in the present study. Intriguingly, upon treating HEK 293 cells with EGF, substantial alterations were observed in both the position and intensity of RAB11FIP1, underscoring the dynamic nature of its cellular behavior in response to EGF stimulation. Additionally, when BZLF1 was transfected into B110 293 cells and subjected to EGF treatment to explore its impact on BZLF1 expression, a noteworthy outcome emerged with an increase in BZLF1 expression levels. These findings shed light on the intricate relationship between EGF, RAB11FIP1C, and BZLF1, highlighting the potential regulatory role of EGF in modulating BZLF1 expression.

EGF and estrogens are recognized as important mitogens that play a role in promoting cellular proliferation, particularly in the breast and reproductive tract (O'Malley et al. 1991). In the context of breast cancer, the expression of RAB11FIP1 varies among different tumor subtypes, with the highest levels observed in estrogen receptor (ER) positive luminal B tumors and the lowest levels in ER-negative basal-like tumors. Interestingly, studies have demonstrated that estrogen can upregulate both EGF and its receptor levels in the uterine environment (Das et al. 1994; DiAugustine et al. 1988; Mukku and Stancel 1985). Intriguingly, the excessive production of estrogen within the tumor, driven by the enzyme aromatase, may exert stimulatory effects on BZLF1 expression and trigger the reactivation of EBV, thereby potentially contributing to the progression NPC (Dochi et al. 2022).

In NPC, it has been observed that EGFR is highly expressed in epithelial cells (Miller et al. 1995). Interestingly, RAB11FIP1C plays a crucial role in the cellular process of recycling the EGFR/α5β1-integrin complex, directing it back to the plasma membrane and thereby promoting cell invasion (Caswell et al. 2007). Notably, in breast cancer, overexpression of RAB11FIP1 has been shown to enhance extracellular signal-regulated kinase (ERK) phosphorylation and activate Ras, emphasizing its impact on intracellular signaling. Furthermore, an intriguing finding from the study revealed that RAB11FIP1C can form a complex with the H-RAS proto-oncogene, resulting in the potent activation of the downstream target MAPK (Zhang et al. 2009). These signaling pathways have implications

for EBV-related processes. Inhibitors targeting the ERK and nuclear factor (NF)-κB pathways have demonstrated the ability to impede both EBV transmission and lytic induction (Nanbo et al. 2012). Additionally, it has been demonstrated that activated RAS plays a crucial role in the disruption of viral latency induced by BRLF1 and BZLF1, occurring at a stage downstream of the transcription of BZLF1 and BRLF1 (Darr et al. 2001). The initiation of EBV reactivation cascade involves the activation of protein kinase C (PKC) by TPA, subsequently stimulating the mitogen-activated protein kinase (MAPK)/extracellular signal-regulated kinase (ERK) pathway (Davies et al. 1991; Liu et al. 1997). These interconnected findings highlight the intricate relationships between EGFR, RAB11FIP1C, intracellular signaling pathways, and EBV reactivation.

5. Summary

In replicating LCLs, both isoforms of RAB11FIP1 exhibited increased expression compared to latent LCLs. Notably, both RAB11FIP1C and RAB11FIPB were found to enhance BZLF1 expression, and this effect was shown to be dependent on the C2 domain. The increasing effects of RAB11FIP1C on BZLF1 were observed regardless of any transcriptional or proteomic changes induced by RAB11FIP1. Furthermore, the dynamic shift in the localization of RAB11FIP1 from the perinuclear region to the plasma membrane may contribute to an increased presence of EGFR in the plasma membrane. Consequently, the activation of MAPK/ERK pathway by EGF triggered by EGF, facilitating the replication of EBV. Moreover, the overexpression of RAB11FIP1 in replicating LCLs has the potential to enhance ERK phosphorylation and activate RAS, leading to the activation of the MAPK pathway and, consequently, an enhancement of EBV replication. These interconnected findings underscore the multifaceted role of RAB11FIP1 in influencing BZLF1 expression, cellular localization, EGFR signaling, and downstream MAPK pathway activation, ultimately contributing to the replication of EBV in LCLs.

6. Zusammenfassung

In replizierenden LCLs zeigten beide Isoformen von RAB11FIP1 im Vergleich zu latenten LCLs eine erhöhte Expression. Beachtenswert ist, dass sowohl RAB11FIP1C als auch RAB11FIPB die BZLF1-Expression verstärkten und dieser Effekt auf der C2-Domäne abhängig war. Die zunehmende Wirkung von RAB11FIP1C auf BZLF1 wurde unabhängig

von transkriptionellen oder proteomischen Veränderungen beobachtet, die durch RAB11FIP1 hervorgerufen wurden. Darüber hinaus kann der dynamische Wechsel der Lokalisierung von RAB11FIP1 von der perinuklearen Region zur Plasmamembran zu einer erhöhten Anwesenheit von EGFR in der Plasmamembran beitragen. Daraus resultiert die Aktivierung des MAPK/ERK-Signalwegs durch EGF, der die Replikation des EBV erleichtert. Darüber hinaus hat die Überexpression von RAB11FIP1 in replizierenden LCLs das Potenzial, die Phosphorylierung von ERK zu verstärken und RAS zu aktivieren, was zur Aktivierung des MAPK-Signalwegs und somit zur Verbesserung der EBV-Replikation führt. Diese verbundenen Erkenntnisse unterstreichen die vielschichtige Rolle von RAB11FIP1 bei der Beeinflussung der BZLF1-Expression, der zellulären Lokalisierung, der EGFR-Signalgebung und der Aktivierung des nachgeschalteten MAPK-Signalwegs, was letztendlich zur Replikation von EBV in LCLs beiträgt.

References

Adams, J. M., Harris, A. W., Pinkert, C. A., Corcoran, L. M., Alexander, W. S., Cory, S., Palmiter, R. D. and Brinster, R. L. (1985). **The c-myc oncogene driven by immunoglobulin enhancers induces lymphoid malignancy in transgenic mice**. Nature *318 (6046)*, 533-538, doi: 10.1038/318533a0.

Adamson, A. L., Le, B. T. and Siedenburg, B. D. (2014). **Inhibition of mTORC1 inhibits lytic replication of Epstein-Barr virus in a cell-type specific manner**. Virology Journal *11 (1)*, 110, doi: 10.1186/1743-422X-11-110.

Aghsaeifard, Z. and Alizadeh, R. (2022). **Clinical Post-Transplant Lymphoproliferative Disorders**. Cardiovasc Hematol Disord Drug Targets *22 (2)*, 96-103, doi: 10.2174/1871529x22666220804155810.

Aguayo, F., Boccardo, E., Corvalan, A., Calaf, G. M. and Blanco, R. (2021). **Interplay between Epstein-Barr virus infection and environmental xenobiotic exposure in cancer**. Infect Agent Cancer *16 (1)*, 50, doi: 10.1186/s13027-021-00391-2.

Ai, E. and Skop, A. R. (2009). **Endosomal recycling regulation during cytokinesis**. Commun Integr Biol *2 (5)*, 444-447, doi: 10.4161/cib.2.5.8931.

Alaggio, R., Amador, C., Anagnostopoulos, I., Attygalle, A. D., Araujo, I. B. d. O., Berti, E., Bhagat, G., Borges, A. M., Boyer, D. and Calaminici, M. (2022). **The 5th edition of the World Health Organization classification of haematolymphoid tumours: lymphoid neoplasms**. Leukemia *36 (7)*, 1720-1748.

Allday, M. J., Bazot, Q. and White, R. E. (2015). **The EBNA3 family: two oncoproteins and a tumour suppressor that are central to the biology of EBV in B cells**. Epstein Barr Virus Volume 2: One Herpes Virus: Many Diseases, 61-117.

Altmann, M. and Hammerschmidt, W. (2005). **Epstein-Barr virus provides a new paradigm: a requirement for the immediate inhibition of apoptosis**. PLoS biology *3 (12)*, e404.

Anonymous (2014). **Comprehensive molecular characterization of gastric adenocarcinoma**. Nature *513 (7517)*, 202-209, doi: 10.1038/nature13480.

Anonymous (2020). **Erratum: Global cancer statistics 2018: GLOBOCAN estimates of incidence and mortality worldwide for 36 cancers in 185 countries**. CA Cancer J Clin *70 (4)*, 313, doi: 10.3322/caac.21609.

Aurer, I., Zing, N. and Federico, M. (2020). **Hodgkin Lymphoma: Comments on ESMO Clinical Practice Guidelines**. Hemasphere *4 (4)*, e458, doi: 10.1097/HS9.0000000000000458.

Babcock, G. J., Decker, L. L., Volk, M. and Thorley-Lawson, D. A. (1998). **EBV persistence in memory B cells in vivo**. Immunity *9 (3)*, 395-404, doi: 10.1016/s1074-7613(00)80622-6.

Badoual, C. (2022). **Update from the 5th Edition of the World Health Organization Classification of Head and Neck Tumors: Oropharynx and Nasopharynx**. Head Neck Pathol *16 (1)*, 19-30, doi: 10.1007/s12105-022-01449-2.

Baer, R., Bankier, A. T., Biggin, M. D., Deininger, P. L., Farrell, P. J., Gibson, T. J., Hatfull, G., Hudson, G. S., Satchwell, S. C., Seguin, C. and et al. (1984). **DNA sequence and expression of the B95-8 Epstein-Barr virus genome**. Nature *310 (5974)*, 207-211, doi: 10.1038/310207a0.

Baetz, N. W. and Goldenring, J. R. (2013). **Rab11-family interacting proteins define spatially and temporally distinct regions within the dynamic Rab11a-dependent recycling system**. Mol Biol Cell *24 (5)*, 643-658, doi: 10.1091/mbc.E12-09-0659.

Balsara, B. R., Sonoda, G., du Manoir, S., Siegfried, J. M., Gabrielson, E. and Testa, J. R. (1997). **Comparative genomic hybridization analysis detects frequent, often high-level, overrepresentation of DNA**

sequences at 3q, 5p, 7p, and 8q in human non-small cell lung carcinomas. Cancer Res *57 (11)*, 2116-2120.

Bass, A. J., Thorsson, V., Shmulevich, I., Reynolds, S. M., Miller, M., Bernard, B., Hinoue, T., Laird, P. W., Curtis, C., Shen, H., Weisenberger, D. J., Schultz, N., Shen, R., Weinhold, N., Kelsen, D. P., Bowlby, R., Chu, A., Kasaian, K., Mungall, A. J., Robertson, A. G., Sipahimalani, P., Cherniack, A., Getz, G., Liu, Y., Noble, M. S., Pedamallu, C., Sougnez, C., Taylor-Weiner, A., Akbani, R., Lee, J.-S., Liu, W., Mills, G. B., Yang, D., Zhang, W., Pantazi, A., Parfenov, M., Gulley, M., Piazuelo, M. B., Schneider, B. G., Kim, J., Boussioutas, A., Sheth, M., Demchok, J. A., Rabkin, C. S., Willis, J. E., Ng, S., Garman, K., Beer, D. G., Pennathur, A., Raphael, B. J., Wu, H.-T., Odze, R., Kim, H. K., Bowen, J., Leraas, K. M., Lichtenberg, T. M., Weaver, S., McLellan, M., Wiznerowicz, M., Sakai, R., Getz, G., Sougnez, C., Lawrence, M. S., Cibulskis, K., Lichtenstein, L., Fisher, S., Gabriel, S. B., Lander, E. S., Ding, L., Niu, B., Ally, A., Balasundaram, M., Birol, I., Bowlby, R., Brooks, D., Butterfield, Y. S. N., Carlsen, R., Chu, A., Chu, J., Chuah, E., Chun, H.-J. E., Clarke, A., Dhalla, N., Guin, R., Holt, R. A., Jones, S. J. M., Kasaian, K., Lee, D., Li, H. A., Lim, E., Ma, Y., Marra, M. A., Mayo, M., Moore, R. A., Mungall, A. J., Mungall, K. L., Ming Nip, K., Robertson, A. G., Schein, J. E., Sipahimalani, P., Tam, A., Thiessen, N., Beroukhim, R., Carter, S. L., Cherniack, A. D., Cho, J., Cibulskis, K., DiCara, D., Frazer, S., Fisher, S., Gabriel, S. B., Gehlenborg, N., Heiman, D. I., Jung, J., Kim, J., Lander, E. S., Lawrence, M. S., Lichtenstein, L., Lin, P., Meyerson, M., Ojesina, A. I., Sekhar Pedamallu, C., Saksena, G., Schumacher, S. E., Sougnez, C., Stojanov, P., Tabak, B., Taylor-Weiner, A., Voet, D., Rosenberg, M., Zack, T. I., Zhang, H., Zou, L., Protopopov, A., Santoso, N., Parfenov, M., Lee, S., Zhang, J., Mahadeshwar, H. S., Tang, J., Ren, X., Seth, S., Yang, L., Xu, A. W., Song, X., Pantazi, A., Xi, R., Bristow, C. A., Hadjipanayis, A., Seidman, J., Chin, L., Park, P. J., Kucherlapati, R., Akbani, R., Ling, S., Liu, W., Rao, A., Weinstein, J. N., Kim, S.-B., Lee, J.-S., Lu, Y., Mills, G., Laird, P. W., Hinoue, T., Weisenberger, D. J., Bootwalla, M. S., Lai, P. H., Shen, H., Triche Jr, T., Van Den Berg, D. J., Baylin, S. B., Herman, J. G., Getz, G., Chin, L., Liu, Y., Murray, B. A., Noble, M. S., Arman Askoy, r. B., Ciriello, G., Dresdner, G., Gao, J., Gross, B., Jacobsen, A., Lee, W., Ramirez, R., Sander, C., Schultz, N., Senbabaoglu, Y., Sinha, R., Onur Sumer, S., Sun, Y., Weinhold, N., Thorsson, V., Bernard, B., Iype, L., Kramer, R. W., Kreisberg, R., Miller, M., Reynolds, S. M., Rovira, H., Tasman, N., Shmulevich, I., Ng, S., Haussler, D., Stuart, J. M., Akbani, R., Ling, S., Liu, W., Rao, A., Weinstein, J. N., Verhaak, R. G. W., Mills, G. B., Leiserson, M. D. M., Raphael, B. J., Wu, H.-T., Taylor, B. S., Black, A. D., Bowen, J., Ann Carney, J., Gastier-Foster, J. M., Helsel, C., Leraas, K. M., Lichtenberg, T. M., McAllister, C., Ramirez, N. C., Tabler, T. R., Wise, L., Zmuda, E., Penny, R., Crain, D., Gardner, J., Lau, K., Curely, E., Mallery, D., Morris, S., Paulauskis, J., Shelton, T., Shelton, C., Sherman, M., Benz, C., Lee, J.-H., Fedosenko, K., Manikhas, G., Potapova, O., Voronina, O., Belyaev, D., Dolzhansky, O., Kimryn Rathmell, W., Brzezinski, J., Ibbs, M., Korski, K., The Cancer Genome Atlas Research, N., Analysis Working Group: Dana-Farber Cancer, I., Institute for Systems, B., University of Southern, C., Memorial Sloan Kettering Cancer, C., Agency, B. C. C., The, E., Edythe, L. B. I., Center, M. D. A. C., Harvard Medical, S., University of North, C., Vanderbilt, U., Asan Medical, C., University of, M., National Cancer, I., Case Western Reserve, U., University of California at Santa, C., Duke, U., University of, M., University of, P., Brown, U., Brigham, Women's, H., National Cancer, C., Nationwide Children's, H., Washington, U., Greater Poland Cancer, C., Leuven, K. U., Genome Sequencing Center: The, E., Edythe, L. B. I., Washington University in St, L., Genome Characterization Centers, B. C. C. A., Harvard Medical, S. B., Women's Hospital, M. D. A. C. C., University of Southern California Epigenome, C., The Sidney Kimmel Comprehensive Cancer Center at Johns Hopkins, U., Genome Data Analysis Centers: The, E., Edythe, L. B. I., Memorial Sloan-Kettering Cancer, C., University of California, S. C., University of California San, F., Biospecimen Core Resource: The Research Institute at Nationwide Children's, H., International Genomics, C., Tissue Source Sites: Buck Institute for Research on, A., Chonnam National University Medical, S., City Clinical Oncology, D., Cureline and Center, U. N. C. L. C. C. (2014). **Comprehensive molecular characterization of gastric adenocarcinoma**. Nature *513 (7517)*, 202-209, doi: 10.1038/nature13480.

Bernheim, A., Berger, R. and Lenoir, G. (1981). **Cytogenetic studies on African Burkitt's lymphoma cell lines: t(8;14), t(2;8) and t(8;22) translocations**. Cancer Genet Cytogenet *3 (4)*, 307-315, doi: 10.1016/0165-4608(81)90039-x.

Bertrand, S., Berger, R., Philip, T., Bernheim, A., Bryon, P. A., Bertoglio, J., Dore, J. F., Brunat-Mentigny, M. and Lenoir, G. M. (1981). **Variant translocation in a non endemic case of Burkitt's lymphoma: t (8;22) in an Epstein--Barr virus negative tumour and in a derived cell line**. Eur J Cancer (1965) *17 (5)*, 577-584,

doi: 10.1016/0014-2964(81)90060-8.

Billaud, M., Busson, P., Huang, D., Mueller-Lantzch, N., Rousselet, G., Pavlish, O., Wakasugi, H., Seigneurin, J. M., Tursz, T. and Lenoir, G. M. (1989). **Epstein-Barr virus (EBV)-containing nasopharyngeal carcinoma cells express the B-cell activation antigen blast2/CD23 and low levels of the EBV receptor CR2**. J Virol *63 (10)*, 4121-4128, doi: 10.1128/JVI.63.10.4121-4128.1989.

Binne, U. K., Amon, W. and Farrell, P. J. (2002). **Promoter sequences required for reactivation of Epstein-Barr virus from latency**. J Virol *76 (20)*, 10282-10289, doi: 10.1128/jvi.76.20.10282-10289.2002.

Birkenbach, M., Tong, X., Bradbury, L. E., Tedder, T. F. and Kieff, E. (1992). **Characterization of an Epstein-Barr virus receptor on human epithelial cells**. J Exp Med *176 (5)*, 1405-1414, doi: 10.1084/jem.176.5.1405.

Boll, B., Hansen, H., Heuck, F., Reiners, K., Borchmann, P., Rothe, A., Engert, A. and Pogge von Strandmann, E. (2005). **The fully human anti-CD30 antibody 5F11 activates NF-{kappa}B and sensitizes lymphoma cells to bortezomib-induced apoptosis**. Blood *106 (5)*, 1839-1842, doi: 10.1182/blood-2005-01-0427.

Borchmann, P., Eichenauer, D. A. and Engert, A. (2012). **State of the art in the treatment of Hodgkin lymphoma**. Nat Rev Clin Oncol *9 (8)*, 450-459, doi: 10.1038/nrclinonc.2012.91.

Bristol, J. A., Brand, J., Ohashi, M., Eichelberg, M. R., Casco, A., Nelson, S. E., Hayes, M., Romero-Masters, J. C., Baiu, D. C., Gumperz, J. E., Johannsen, E. C., Dinh, H. Q. and Kenney, S. C. (2022). **Reduced IRF4 expression promotes lytic phenotype in Type 2 EBV-infected B cells**. PLoS Pathog *18 (4)*, e1010453, doi: 10.1371/journal.ppat.1010453.

Bruce, E. A., Digard, P. and Stuart, A. D. (2010). **The Rab11 pathway is required for influenza A virus budding and filament formation**. J Virol *84 (12)*, 5848-5859, doi: 10.1128/jvi.00307-10.

Bruno, J., Brumfield, A., Chaudhary, N., Iaea, D. and McGraw, T. E. (2016). **SEC16A is a RAB10 effector required for insulin-stimulated GLUT4 trafficking in adipocytes**. J Cell Biol *214 (1)*, 61-76, doi: 10.1083/jcb.201509052.

Bu, G. L., Xie, C., Kang, Y. F., Zeng, M. S. and Sun, C. (2022). **How EBV Infects: The Tropism and Underlying Molecular Mechanism for Viral Infection**. Viruses *14 (11)*, doi: 10.3390/v14112372.

Burke, A. P., Yen, T. S., Shekitka, K. M. and Sobin, L. H. (1990). **Lymphoepithelial carcinoma of the stomach with Epstein-Barr virus demonstrated by polymerase chain reaction**. Mod Pathol *3 (3)*, 377-380.

Bustami, R. T., Ojo, A. O., Wolfe, R. A., Merion, R. M., Bennett, W. M., McDiarmid, S. V., Leichtman, A. B., Held, P. J. and Port, F. K. (2004). **Immunosuppression and the risk of post-transplant malignancy among cadaveric first kidney transplant recipients**. Am J Transplant *4 (1)*, 87-93, doi: 10.1046/j.1600-6135.2003.00274.x.

Cai, L., Ye, Y., Jiang, Q., Chen, Y., Lyu, X., Li, J., Wang, S., Liu, T., Cai, H. and Yao, K. (2015). **Epstein–Barr virus-encoded microRNA BART1 induces tumour metastasis by regulating PTEN-dependent pathways in nasopharyngeal carcinoma**. Nature communications *6 (1)*, 7353.

Camargo, M. C., Murphy, G., Koriyama, C., Pfeiffer, R. M., Kim, W. H., Herrera-Goepfert, R., Corvalan, A. H., Carrascal, E., Abdirad, A., Anwar, M., Hao, Z., Kattoor, J., Yoshiwara-Wakabayashi, E., Eizuru, Y., Rabkin, C. S. and Akiba, S. (2011). **Determinants of Epstein-Barr virus-positive gastric cancer: an international pooled analysis**. Br J Cancer *105 (1)*, 38-43, doi: 10.1038/bjc.2011.215.

Capello, D., Rossi, D. and Gaidano, G. (2005). **Post-transplant lymphoproliferative disorders: molecular basis of disease histogenesis and pathogenesis**. Hematol Oncol *23 (2)*, 61-67, doi: 10.1002/hon.751.

Caswell, P. T., Spence, H. J., Parsons, M., White, D. P., Clark, K., Cheng, K. W., Mills, G. B., Humphries, M. J., Messent, A. J., Anderson, K. I., McCaffrey, M. W., Ozanne, B. W. and Norman, J. C. (2007). **Rab25**

associates with alpha5beta1 integrin to promote invasive migration in 3D microenvironments. Dev Cell *13 (4)*, 496-510, doi: 10.1016/j.devcel.2007.08.012.

Chabay, P. (2021). **Advances in the pathogenesis of EBV-associated diffuse large B cell lymphoma**. Cancers *13 (11)*, 2717.

Chan, A. S., To, K. F., Lo, K. W., Ding, M., Li, X., Johnson, P. and Huang, D. P. (2002). **Frequent chromosome 9p losses in histologically normal nasopharyngeal epithelia from southern Chinese**. Int J Cancer *102 (3)*, 300-303, doi: 10.1002/ijc.10689.

Chan, A. S., To, K. F., Lo, K. W., Mak, K. F., Pak, W., Chiu, B., Tse, G. M., Ding, M., Li, X., Lee, J. C. and Huang, D. P. (2000). **High frequency of chromosome 3p deletion in histologically normal nasopharyngeal epithelia from southern Chinese**. Cancer Res *60 (19)*, 5365-5370.

Chesnokova, L. S. and Hutt-Fletcher, L. M. (2011). **Fusion of Epstein-Barr virus with epithelial cells can be triggered by αvβ5 in addition to αvβ6 and αvβ8, and integrin binding triggers a conformational change in glycoproteins gHgL**. J Virol *85 (24)*, 13214-13223, doi: 10.1128/jvi.05580-11.

Chiu, S. H., Wu, C. C., Fang, C. Y., Yu, S. L., Hsu, H. Y., Chow, Y. H. and Chen, J. Y. (2014). **Epstein-Barr virus BALF3 mediates genomic instability and progressive malignancy in nasopharyngeal carcinoma**. Oncotarget *5 (18)*, 8583-8601, doi: 10.18632/oncotarget.2323.

Cho, K. H. and Lee, H. Y. (2019). **Rab25 and RCP in cancer progression**. Arch Pharm Res *42 (2)*, 101-112, doi: 10.1007/s12272-019-01129-w.

Cho, W. (2001). **Membrane targeting by C1 and C2 domains**. J Biol Chem *276 (35)*, 32407-32410, doi: 10.1074/jbc.R100007200.

Chodosh, J., Gan, Y., Holder, V. P. and Sixbey, J. W. (2000). **Patterned entry and egress by Epstein-Barr virus in polarized CR2-positive epithelial cells**. Virology *266 (2)*, 387-396, doi: 10.1006/viro.1999.0082.

Choy, E. Y.-W., Siu, K.-L., Kok, K.-H., Lung, R. W.-M., Tsang, C. M., To, K.-F., Kwong, D. L.-W., Tsao, S. W. and Jin, D.-Y. (2008). **An Epstein-Barr virus–encoded microRNA targets PUMA to promote host cell survival**. The Journal of experimental medicine *205 (11)*, 2551-2560.

Coiffier, B., Lepage, E., Briere, J., Herbrecht, R., Tilly, H., Bouabdallah, R., Morel, P., Van Den Neste, E., Salles, G., Gaulard, P., Reyes, F., Lederlin, P. and Gisselbrecht, C. (2002). **CHOP chemotherapy plus rituximab compared with CHOP alone in elderly patients with diffuse large-B-cell lymphoma**. N Engl J Med *346 (4)*, 235-242, doi: 10.1056/NEJMoa011795.

Connolly, S. A., Jackson, J. O., Jardetzky, T. S. and Longnecker, R. (2011). **Fusing structure and function: a structural view of the herpesvirus entry machinery**. Nat Rev Microbiol *9 (5)*, 369-381, doi: 10.1038/nrmicro2548.

Countryman, J., Jenson, H., Seibl, R., Wolf, H. and Miller, G. (1987). **Polymorphic proteins encoded within BZLF1 of defective and standard Epstein-Barr viruses disrupt latency**. J Virol *61 (12)*, 3672-3679, doi: 10.1128/JVI.61.12.3672-3679.1987.

Cristescu, R., Lee, J., Nebozhyn, M., Kim, K. M., Ting, J. C., Wong, S. S., Liu, J., Yue, Y. G., Wang, J., Yu, K., Ye, X. S., Do, I. G., Liu, S., Gong, L., Fu, J., Jin, J. G., Choi, M. G., Sohn, T. S., Lee, J. H., Bae, J. M., Kim, S. T., Park, S. H., Sohn, I., Jung, S. H., Tan, P., Chen, R., Hardwick, J., Kang, W. K., Ayers, M., Hongyue, D., Reinhard, C., Loboda, A., Kim, S. and Aggarwal, A. (2015). **Molecular analysis of gastric cancer identifies subtypes associated with distinct clinical outcomes**. Nat Med *21 (5)*, 449-456, doi: 10.1038/nm.3850.

Crombie, J. L. and LaCasce, A. S. (2019). **Epstein Barr Virus Associated B-Cell Lymphomas and Iatrogenic Lymphoproliferative Disorders**. Front Oncol *9*, 109, doi: 10.3389/fonc.2019.00109.

Curtis, R. E., Travis, L. B., Rowlings, P. A., Socié, G., Kingma, D. W., Banks, P. M., Jaffe, E. S., Sale, G. E., Horowitz, M. M., Witherspoon, R. P., Shriner, D. A., Weisdorf, D. J., Kolb, H. J., Sullivan, K. M., Sobocinski, K. A., Gale, R. P., Hoover, R. N., Fraumeni, J. F., Jr. and Deeg, H. J. (1999). **Risk of lymphoproliferative disorders after bone marrow transplantation: a multi-institutional study**. Blood *94 (7)*, 2208-2216.

Dai, Y., Liu, Y., Huang, D., Yu, C., Cai, G., Pi, L., Ren, C., Chen, G. Z., Tian, Y. and Zhang, X. (2012). **Increased expression of Rab coupling protein in squamous cell carcinoma of the head and neck and its clinical significance**. Oncol Lett *3 (6)*, 1231-1236, doi: 10.3892/ol.2012.652.

Darr, C. D., Mauser, A. and Kenney, S. (2001). **Epstein-Barr virus immediate-early protein BRLF1 induces the lytic form of viral replication through a mechanism involving phosphatidylinositol-3 kinase activation**. J Virol *75 (13)*, 6135-6142, doi: 10.1128/jvi.75.13.6135-6142.2001.

Das, S. K., Tsukamura, H., Paria, B. C., Andrews, G. K. and Dey, S. K. (1994). **Differential expression of epidermal growth factor receptor (EGF-R) gene and regulation of EGF-R bioactivity by progesterone and estrogen in the adult mouse uterus**. Endocrinology *134 (2)*, 971-981, doi: 10.1210/endo.134.2.7507841.

Davies, A. H., Grand, R. J., Evans, F. J. and Rickinson, A. B. (1991). **Induction of Epstein-Barr virus lytic cycle by tumor-promoting and non-tumor-promoting phorbol esters requires active protein kinase C**. J Virol *65 (12)*, 6838-6844, doi: 10.1128/jvi.65.12.6838-6844.1991.

De-The, G., Ho, H. C., Kwan, H. C., Desgranges, C. and Favre, M. C. (1970). **Nasopharyngeal carcinoma (NPC). I. Types of cultures derived from tumour biopsies and non-tumorous tissues of Chinese patients with special reference to lymphoblastoid transformation**. Int J Cancer *6 (2)*, 189-206, doi: 10.1002/ijc.2910060206.

de Martel, C., Ferlay, J., Franceschi, S., Vignat, J., Bray, F., Forman, D. and Plummer, M. (2012). **Global burden of cancers attributable to infections in 2008: a review and synthetic analysis**. Lancet Oncol *13 (6)*, 607-615, doi: 10.1016/S1470-2045(12)70137-7.

DeKroon, R. M., Gunawardena, H. P., Edwards, R. and Raab-Traub, N. (2018). **Global Proteomic Changes Induced by the Epstein-Barr Virus Oncoproteins Latent Membrane Protein 1 and 2A**. mBio *9 (3)*, doi: 10.1128/mBio.00959-18.

Delecluse, H. J., Hilsendegen, T., Pich, D., Zeidler, R. and Hammerschmidt, W. (1998). **Propagation and recovery of intact, infectious Epstein-Barr virus from prokaryotic to human cells**. Proc Natl Acad Sci U S A *95 (14)*, 8245-8250, doi: 10.1073/pnas.95.14.8245.

Desgranges, C., Lavoue, M. F., Patet, J. and de-The, G. (1979). **In vitro transforming activity of Epstein-Barr virus (EBV). II. Differences between M81 and B95-8 EBV strains**. Biomedicine *30 (2)*, 102-108.

Desgranges, C., Lenoir, G., de-The, G., Seigneurin, J. M., Hilgers, J. and Dubouch, P. (1976). **In vitro transforming activity of EBV. I-Establishment and properties of two EBV strains (M81 and M72) produced by immortalized Callithrix jacchus lymphocytes**. Biomedicine *25 (9)*, 349-352.

Dharnidharka, V. R. (2005). **Costimulation blockade with belatacept in renal transplantation**. N Engl J Med *353 (19)*, 2085-2086; author reply 2085-2086, doi: 10.1056/nejm200511103531919.

Dharnidharka, V. R. (2018). **Comprehensive review of post-organ transplant hematologic cancers**. Am J Transplant *18 (3)*, 537-549, doi: 10.1111/ajt.14603.

Dheekollu, J., Wiedmer, A., Ayyanathan, K., Deakyne, J. S., Messick, T. E. and Lieberman, P. M. (2021). **Cell-cycle-dependent EBNA1-DNA crosslinking promotes replication termination at oriP and viral episome maintenance**. Cell *184 (3)*, 643-654.e613, doi: 10.1016/j.cell.2020.12.022.

DiAugustine, R. P., Petrusz, P., Bell, G. I., Brown, C. F., Korach, K. S., McLachlan, J. A. and Teng, C. T. (1988).

Influence of estrogens on mouse uterine epidermal growth factor precursor protein and messenger ribonucleic acid. Endocrinology *122 (6)*, 2355-2363, doi: 10.1210/endo-122-6-2355.

Dierickx, D. and Habermann, T. M. (2018). **Post-Transplantation Lymphoproliferative Disorders in Adults**. N Engl J Med *378 (6)*, 549-562, doi: 10.1056/NEJMra1702693.

Dierickx, D., Tousseyn, T. and Gheysens, O. (2015). **How I treat posttransplant lymphoproliferative disorders**. Blood *126 (20)*, 2274-2283, doi: 10.1182/blood-2015-05-615872.

Dochi, H., Kondo, S., Murata, T., Fukuyo, M., Nanbo, A., Wakae, K., Jiang, W. P., Hamabe-Horiike, T., Tanaka, M., Nishiuchi, T., Mizokami, H., Moriyama-Kita, M., Kobayashi, E., Hirai, N., Komori, T., Ueno, T., Nakanishi, Y., Hatano, M., Endo, K., Sugimoto, H., Wakisaka, N., Juang, S. H., Muramatsu, M., Kaneda, A. and Yoshizaki, T. (2022). **Estrogen induces the expression of EBV lytic protein ZEBRA, a marker of poor prognosis in nasopharyngeal carcinoma**. Cancer Sci *113 (8)*, 2862-2877, doi: 10.1111/cas.15440.

Edwards, R. H., Marquitz, A. R. and Raab-Traub, N. (2015). **Changes in expression induced by Epstein-Barr Virus LMP1-CTAR1: potential role of bcl3**. mBio *6 (2)*, doi: 10.1128/mBio.00441-15.

Elgui de Oliveira, D., Muller-Coan, B. G. and Pagano, J. S. (2016). **Viral Carcinogenesis Beyond Malignant Transformation: EBV in the Progression of Human Cancers**. Trends Microbiol *24 (8)*, 649-664, doi: 10.1016/j.tim.2016.03.008.

Epstein, A. (2015). **Why and How Epstein-Barr Virus Was Discovered 50 Years Ago**. Curr Top Microbiol Immunol *390 (Pt 1)*, 3-15, doi: 10.1007/978-3-319-22822-8_1.

Eva, R., Dassie, E., Caswell, P. T., Dick, G., ffrench-Constant, C., Norman, J. C. and Fawcett, J. W. (2010). **Rab11 and its effector Rab coupling protein contribute to the trafficking of beta 1 integrins during axon growth in adult dorsal root ganglion neurons and PC12 cells**. J Neurosci *30 (35)*, 11654-11669, doi: 10.1523/JNEUROSCI.2425-10.2010.

Evens, A. M., Danilov, A., Jagadeesh, D., Sperling, A., Kim, S. H., Vaca, R., Wei, C., Rector, D., Sundaram, S., Reddy, N., Lin, Y., Farooq, U., D'Angelo, C., Bond, D. A., Berg, S., Churnetski, M. C., Godara, A., Khan, N., Choi, Y. K., Yazdy, M., Rabinovich, E., Varma, G., Karmali, R., Mian, A., Savani, M., Burkart, M., Martin, P., Ren, A., Chauhan, A., Diefenbach, C., Straker-Edwards, A., Klein, A. K., Blum, K. A., Boughan, K. M., Smith, S. E., Haverkos, B. M., Orellana-Noia, V. M., Kenkre, V. P., Zayac, A., Ramdial, J., Maliske, S. M., Epperla, N., Venugopal, P., Feldman, T. A., Smith, S. D., Stadnik, A., David, K. A., Naik, S., Lossos, I. S., Lunning, M. A., Caimi, P., Kamdar, M., Palmisiano, N., Bachanova, V., Portell, C. A., Phillips, T., Olszewski, A. J. and Alderuccio, J. P. (2021). **Burkitt lymphoma in the modern era: real-world outcomes and prognostication across 30 US cancer centers**. Blood *137 (3)*, 374-386, doi: 10.1182/blood.2020006926.

Everett, R. D., Parada, C., Gripon, P., Sirma, H. and Orr, A. (2008). **Replication of ICP0-null mutant herpes simplex virus type 1 is restricted by both PML and Sp100**. J Virol *82 (6)*, 2661-2672, doi: 10.1128/jvi.02308-07.

Fahmi, H., Cochet, C., Hmama, Z., Opolon, P. and Joab, I. (2000). **Transforming growth factor beta 1 stimulates expression of the Epstein-Barr virus BZLF1 immediate-early gene product ZEBRA by an indirect mechanism which requires the MAPK kinase pathway**. J Virol *74 (13)*, 5810-5818, doi: 10.1128/jvi.74.13.5810-5818.2000.

Fan, G. H., Lapierre, L. A., Goldenring, J. R. and Richmond, A. (2003). **Differential regulation of CXCR2 trafficking by Rab GTPases**. Blood *101 (6)*, 2115-2124, doi: 10.1182/blood-2002-07-1965.

Fang, C. Y., Lee, C. H., Wu, C. C., Chang, Y. T., Yu, S. L., Chou, S. P., Huang, P. T., Chen, C. L., Hou, J. W., Chang, Y., Tsai, C. H., Takada, K. and Chen, J. Y. (2009). **Recurrent chemical reactivations of EBV promotes genome instability and enhances tumor progression of nasopharyngeal carcinoma cells**. Int J Cancer *124 (9)*, 2016-2025, doi: 10.1002/ijc.24179.

Farrell, P. J. (2019). **Epstein-Barr Virus and Cancer**. Annu Rev Pathol *14*, 29-53, doi: 10.1146/annurev-pathmechdis-012418-013023.

Fernandez-de Céspedes, M. V., Hoffman, H. K., Carter, H., Simons, L. M., Naing, L., Ablan, S. D., Scheiblin, D. A., Hultquist, J. F., van Engelenburg, S. B. and Freed, E. O. (2022). **Rab11-FIP1C Is Dispensable for HIV-1 Replication in Primary CD4(+) T Cells, but Its Role Is Cell Type Dependent in Immortalized Human T-Cell Lines**. J Virol *96 (23)*, e0087622, doi: 10.1128/jvi.00876-22.

Fingeroth, J. D., Diamond, M. E., Sage, D. R., Hayman, J. and Yates, J. L. (1999). **CD21-Dependent infection of an epithelial cell line, 293, by Epstein-Barr virus**. J Virol *73 (3)*, 2115-2125, doi: 10.1128/JVI.73.3.2115-2125.1999.

Flemington, E. and Speck, S. H. (1990). **Autoregulation of Epstein-Barr virus putative lytic switch gene BZLF1**. J Virol *64 (3)*, 1227-1232, doi: 10.1128/JVI.64.3.1227-1232.1990.

Funch, D. P., Ko, H. H., Travasso, J., Brady, J., Kew, C. E., 2nd, Nalesnik, M. A. and Walker, A. M. (2005). **Posttransplant lymphoproliferative disorder among renal transplant patients in relation to the use of mycophenolate mofetil**. Transplantation *80 (9)*, 1174-1180, doi: 10.1097/01.tp.0000169035.10572.c6.

Furukawa, S., Wei, L., Krams, S. M., Esquivel, C. O. and Martinez, O. M. (2013). **PI3Kδ inhibition augments the efficacy of rapamycin in suppressing proliferation of Epstein-Barr virus (EBV)+ B cell lymphomas**. Am J Transplant *13 (8)*, 2035-2043, doi: 10.1111/ajt.12328.

Gewurz, B. E., Mar, J. C., Padi, M., Zhao, B., Shinners, N. P., Takasaki, K., Bedoya, E., Zou, J. Y., Cahir-McFarland, E., Quackenbush, J. and Kieff, E. (2011). **Canonical NF-kappaB activation is essential for Epstein-Barr virus latent membrane protein 1 TES2/CTAR2 gene regulation**. J Virol *85 (13)*, 6764-6773, doi: 10.1128/JVI.00422-11.

Glotz, D., Chapman, J. R., Dharnidharka, V. R., Hanto, D. W., Castro, M. C., Hirsch, H. H., Leblond, V., Mehta, A. K., Moulin, B., Pagliuca, A., Pascual, J., Rickinson, A. B., Russo, F. P., Trappe, R. U., Webster, A. C., Zuckermann, A. O. and Gross, T. G. (2012). **The Seville expert workshop for progress in posttransplant lymphoproliferative disorders**. Transplantation *94 (8)*, 784-793, doi: 10.1097/TP.0b013e318269e64f.

Go, C. D., Knight, J. D. R., Rajasekharan, A., Rathod, B., Hesketh, G. G., Abe, K. T., Youn, J. Y., Samavarchi-Tehrani, P., Zhang, H., Zhu, L. Y., Popiel, E., Lambert, J. P., Coyaud, É., Cheung, S. W. T., Rajendran, D., Wong, C. J., Antonicka, H., Pelletier, L., Palazzo, A. F., Shoubridge, E. A., Raught, B. and Gingras, A. C. (2021). **A proximity-dependent biotinylation map of a human cell**. Nature *595 (7865)*, 120-124, doi: 10.1038/s41586-021-03592-2.

Gopal, S. and Gross, T. G. (2018). **How I treat Burkitt lymphoma in children, adolescents, and young adults in sub-Saharan Africa**. Blood *132 (3)*, 254-263, doi: 10.1182/blood-2018-04-844472.

Gorres, K. L., Daigle, D., Mohanram, S. and Miller, G. (2014). **Activation and repression of Epstein-Barr Virus and Kaposi's sarcoma-associated herpesvirus lytic cycles by short- and medium-chain fatty acids**. J Virol *88 (14)*, 8028-8044, doi: 10.1128/JVI.00722-14.

Grande, B. M., Gerhard, D. S., Jiang, A., Griner, N. B., Abramson, J. S., Alexander, T. B., Allen, H., Ayers, L. W., Bethony, J. M., Bhatia, K., Bowen, J., Casper, C., Choi, J. K., Culibrk, L., Davidsen, T. M., Dyer, M. A., Gastier-Foster, J. M., Gesuwan, P., Greiner, T. C., Gross, T. G., Hanf, B., Harris, N. L., He, Y., Irvin, J. D., Jaffe, E. S., Jones, S. J. M., Kerchan, P., Knoetze, N., Leal, F. E., Lichtenberg, T. M., Ma, Y., Martin, J. P., Martin, M. R., Mbulaiteye, S. M., Mullighan, C. G., Mungall, A. J., Namirembe, C., Novik, K., Noy, A., Ogwang, M. D., Omoding, A., Orem, J., Reynolds, S. J., Rushton, C. K., Sandlund, J. T., Schmitz, R., Taylor, C., Wilson, W. H., Wright, G. W., Zhao, E. Y., Marra, M. A., Morin, R. D. and Staudt, L. M. (2019). **Genome-wide discovery of somatic coding and noncoding mutations in pediatric endemic and sporadic Burkitt lymphoma**. Blood *133 (12)*, 1313-1324, doi: 10.1182/blood-2018-09-871418.

Green, M. (2001). **Management of Epstein-Barr virus-induced post-transplant lymphoproliferative disease in recipients of solid organ transplantation**. Am J Transplant *1 (2)*, 103-108.

Gruffat, H. and Sergeant, A. (1994). **Characterization of the DNA-binding site repertoire for the Epstein-Barr virus transcription factor R**. Nucleic Acids Res *22 (7)*, 1172-1178, doi: 10.1093/nar/22.7.1172.

Grulich, A. E., van Leeuwen, M. T., Falster, M. O. and Vajdic, C. M. (2007). **Incidence of cancers in people with HIV/AIDS compared with immunosuppressed transplant recipients: a meta-analysis**. Lancet *370 (9581)*, 59-67, doi: 10.1016/s0140-6736(07)61050-2.

Gulley, M. L. (2015). **Genomic assays for Epstein-Barr virus-positive gastric adenocarcinoma**. Exp Mol Med *47 (1)*, e134, doi: 10.1038/emm.2014.93.

Gunven, P., Klein, G., Henle, G., Henle, W. and Clifford, P. (1970). **Epstein-Barr virus in Burkitt's lymphoma and nasopharyngeal carcinoma. Antibodies to EBV associated membrane and viral capsid antigens in Burkitt lymphoma patients**. Nature *228 (5276)*, 1053-1056, doi: 10.1038/2281053a0.

Hales, C. M., Griner, R., Hobdy-Henderson, K. C., Dorn, M. C., Hardy, D., Kumar, R., Navarre, J., Chan, E. K., Lapierre, L. A. and Goldenring, J. R. (2001). **Identification and characterization of a family of Rab11-interacting proteins**. J Biol Chem *276 (42)*, 39067-39075, doi: 10.1074/jbc.M104831200.

Hatton, O. L., Harris-Arnold, A., Schaffert, S., Krams, S. M. and Martinez, O. M. (2014). **The interplay between Epstein-Barr virus and B lymphocytes: implications for infection, immunity, and disease**. Immunol Res *58 (2-3)*, 268-276, doi: 10.1007/s12026-014-8496-1.

Heldwein, E. E. (2016). **gH/gL supercomplexes at early stages of herpesvirus entry**. Curr Opin Virol *18*, 1-8, doi: 10.1016/j.coviro.2016.01.010.

Henle, W., Diehl, V., Kohn, G., Zur Hausen, H. and Henle, G. (1967). **Herpes-type virus and chromosome marker in normal leukocytes after growth with irradiated Burkitt cells**. Science *157 (3792)*, 1064-1065, doi: 10.1126/science.157.3792.1064.

Hochberg, D., Souza, T., Catalina, M., Sullivan, J. L., Luzuriaga, K. and Thorley-Lawson, D. A. (2004). **Acute infection with Epstein-Barr virus targets and overwhelms the peripheral memory B-cell compartment with resting, latently infected cells**. J Virol *78 (10)*, 5194-5204, doi: 10.1128/jvi.78.10.5194-5204.2004.

Horgan, C. P. and McCaffrey, M. W. (2009). **The dynamic Rab11-FIPs**. Biochem Soc Trans *37 (Pt 5)*, 1032-1036, doi: 10.1042/BST0371032.

Huang, S. Y., Fang, C. Y., Tsai, C. H., Chang, Y., Takada, K., Hsu, T. Y. and Chen, J. Y. (2010). **N-methyl-N'-nitro-N-nitrosoguanidine induces and cooperates with 12-O-tetradecanoylphorbol-1,3-acetate/sodium butyrate to enhance Epstein-Barr virus reactivation and genome instability in nasopharyngeal carcinoma cells**. Chem Biol Interact *188 (3)*, 623-634, doi: 10.1016/j.cbi.2010.09.020.

Hutt-Fletcher, L. M. (2007). **Epstein-Barr virus entry**. J Virol *81 (15)*, 7825-7832, doi: 10.1128/JVI.00445-07.

Hutt-Fletcher, L. M. (2015). **EBV glycoproteins: where are we now?** Future Virol *10 (10)*, 1155-1162, doi: 10.2217/fvl.15.80.

Iannantuono, N. V. G. and Emery, G. (2021). **Rab11FIP1 maintains Rab35 at the intercellular bridge to promote actin removal and abscission**. J Cell Sci *134 (12)*, doi: 10.1242/jcs.244384.

Iempridee, T., Das, S., Xu, I. and Mertz, J. E. (2011). **Transforming growth factor beta-induced reactivation of Epstein-Barr virus involves multiple Smad-binding elements cooperatively activating expression of the latent-lytic switch BZLF1 gene**. J Virol *85 (15)*, 7836-7848, doi: 10.1128/JVI.01197-10.

Imai, K., Inoue, H., Tamura, M., Cueno, M. E., Inoue, H., Takeichi, O., Kusama, K., Saito, I. and Ochiai, K. (2012). **The periodontal pathogen Porphyromonas gingivalis induces the Epstein-Barr virus lytic switch transactivator ZEBRA by histone modification**. Biochimie *94 (3)*, 839-846, doi: 10.1016/j.biochi.2011.12.001.

Imai, S., Koizumi, S., Sugiura, M., Tokunaga, M., Uemura, Y., Yamamoto, N., Tanaka, S., Sato, E. and Osato, T. (1994). **Gastric carcinoma: monoclonal epithelial malignant cells expressing Epstein-Barr virus latent infection protein**. Proc Natl Acad Sci U S A *91 (19)*, 9131-9135, doi: 10.1073/pnas.91.19.9131.

Iwakiri, D., Zhou, L., Samanta, M., Matsumoto, M., Ebihara, T., Seya, T., Imai, S., Fujieda, M., Kawa, K. and Takada, K. (2009). **Epstein-Barr virus (EBV)-encoded small RNA is released from EBV-infected cells and activates signaling from Toll-like receptor 3**. J Exp Med *206 (10)*, 2091-2099, doi: 10.1084/jem.20081761.

Janz, A., Oezel, M., Kurzeder, C., Mautner, J., Pich, D., Kost, M., Hammerschmidt, W. and Delecluse, H. J. (2000). **Infectious Epstein-Barr virus lacking major glycoprotein BLLF1 (gp350/220) demonstrates the existence of additional viral ligands**. J Virol *74 (21)*, 10142-10152, doi: 10.1128/jvi.74.21.10142-10152.2000.

Java, A., Liszewski, M. K., Hourcade, D. E., Zhang, F. and Atkinson, J. P. (2015). **Role of complement receptor 1 (CR1; CD35) on epithelial cells: A model for understanding complement-mediated damage in the kidney**. Mol Immunol *67 (2 Pt B)*, 584-595, doi: 10.1016/j.molimm.2015.07.016.

Jia, W. H. and Qin, H. D. (2012). **Non-viral environmental risk factors for nasopharyngeal carcinoma: a systematic review**. Semin Cancer Biol *22 (2)*, 117-126, doi: 10.1016/j.semcancer.2012.01.009.

Jiang, R., Gu, X., Moore-Medlin, T. N., Nathan, C. A. and Hutt-Fletcher, L. M. (2012). **Oral dysplasia and squamous cell carcinoma: correlation between increased expression of CD21, Epstein-Barr virus and CK19**. Oral Oncol *48 (9)*, 836-841, doi: 10.1016/j.oraloncology.2012.03.017.

Jin, M. and Goldenring, J. R. (2006). **The Rab11-FIP1/RCP gene codes for multiple protein transcripts related to the plasma membrane recycling system**. Biochim Biophys Acta *1759 (6)*, 281-295, doi: 10.1016/j.bbaexp.2006.06.001.

Jing, J., Junutula, J. R., Wu, C., Burden, J., Matern, H., Peden, A. A. and Prekeris, R. (2010). **FIP1/RCP binding to Golgin-97 regulates retrograde transport from recycling endosomes to the trans-Golgi network**. Mol Biol Cell *21 (17)*, 3041-3053, doi: 10.1091/mbc.E10-04-0313.

Jochum, S., Moosmann, A., Lang, S., Hammerschmidt, W. and Zeidler, R. (2012). **The EBV immunoevasins vIL-10 and BNLF2a protect newly infected B cells from immune recognition and elimination**. PLoS Pathog *8 (5)*, e1002704, doi: 10.1371/journal.ppat.1002704.

Kafuko, G. W. and Burkitt, D. P. (1970). **Burkitt's lymphoma and malaria**. Int J Cancer *6 (1)*, 1-9, doi: 10.1002/ijc.2910060102.

Kaiser-McCaw, B., Epstein, A. L., Kaplan, H. S. and Hecht, F. (1977). **Chromosome 14 translocation in African and North American Burkitt's lymphoma**. Int J Cancer *19 (4)*, 482-486, doi: 10.1002/ijc.2910190408.

Kalla, M., Schmeinck, A., Bergbauer, M., Pich, D. and Hammerschmidt, W. (2010). **AP-1 homolog BZLF1 of Epstein-Barr virus has two essential functions dependent on the epigenetic state of the viral genome**. Proc Natl Acad Sci U S A *107 (2)*, 850-855, doi: 10.1073/pnas.0911948107.

Kanda, T., Furuse, Y., Oshitani, H. and Kiyono, T. (2016). **Highly Efficient CRISPR/Cas9-Mediated Cloning and Functional Characterization of Gastric Cancer-Derived Epstein-Barr Virus Strains**. J Virol *90 (9)*, 4383-4393, doi: 10.1128/JVI.00060-16.

Kaneda, A., Matsusaka, K., Aburatani, H. and Fukayama, M. (2012). **Epstein-Barr virus infection as an**

epigenetic driver of tumorigenesis. Cancer Res *72 (14)*, 3445-3450, doi: 10.1158/0008-5472.can-11-3919.

Kang, D., Skalsky, R. L. and Cullen, B. R. (2015). **EBV BART MicroRNAs Target Multiple Pro-apoptotic Cellular Genes to Promote Epithelial Cell Survival**. PLoS Pathog *11 (6)*, e1004979, doi: 10.1371/journal.ppat.1004979.

Kapatai, G. and Murray, P. (2007). **Contribution of the Epstein Barr virus to the molecular pathogenesis of Hodgkin lymphoma**. J Clin Pathol *60 (12)*, 1342-1349, doi: 10.1136/jcp.2007.050146.

Kapoor, P., Lavoie, B. D. and Frappier, L. (2005). **EBP2 plays a key role in Epstein-Barr virus mitotic segregation and is regulated by aurora family kinases**. Mol Cell Biol *25 (12)*, 4934-4945, doi: 10.1128/MCB.25.12.4934-4945.2005.

Kaymaz, Y., Oduor, C. I., Yu, H., Otieno, J. A., Ong'echa, J. M., Moormann, A. M. and Bailey, J. A. (2017). **Comprehensive Transcriptome and Mutational Profiling of Endemic Burkitt Lymphoma Reveals EBV Type-Specific Differences**. Mol Cancer Res *15 (5)*, 563-576, doi: 10.1158/1541-7786.mcr-16-0305.

Kempkes, B. and Robertson, E. S. (2015). **Epstein-Barr virus latency: current and future perspectives**. Curr Opin Virol *14*, 138-144, doi: 10.1016/j.coviro.2015.09.007.

Kenney, S. C. and Mertz, J. E. (2014). **Regulation of the latent-lytic switch in Epstein-Barr virus**. Semin Cancer Biol *26*, 60-68, doi: 10.1016/j.semcancer.2014.01.002.

Kerr, J. R. (2019). **Epstein-Barr virus (EBV) reactivation and therapeutic inhibitors**. J Clin Pathol *72 (10)*, 651-658, doi: 10.1136/jclinpath-2019-205822.

Khalil, M. A. M., Khalil, M. A. U., Khan, T. F. T. and Tan, J. (2018). **Drug-Induced Hematological Cytopenia in Kidney Transplantation and the Challenges It Poses for Kidney Transplant Physicians**. J Transplant *2018*, 9429265, doi: 10.1155/2018/9429265.

Khan, G. and Hashim, M. J. (2014). **Global burden of deaths from Epstein-Barr virus attributable malignancies 1990-2010**. Infect Agent Cancer *9 (1)*, 38, doi: 10.1186/1750-9378-9-38.

Kirk, A. D., Cherikh, W. S., Ring, M., Burke, G., Kaufman, D., Knechtle, S. J., Potdar, S., Shapiro, R., Dharnidharka, V. R. and Kauffman, H. M. (2007). **Dissociation of depletional induction and posttransplant lymphoproliferative disease in kidney recipients treated with alemtuzumab**. Am J Transplant *7 (11)*, 2619-2625, doi: 10.1111/j.1600-6143.2007.01972.x.

Kraus, R. J., Yu, X., Cordes, B. A., Sathiamoorthi, S., Iempridee, T., Nawandar, D. M., Ma, S., Romero-Masters, J. C., McChesney, K. G., Lin, Z., Makielski, K. R., Lee, D. L., Lambert, P. F., Johannsen, E. C., Kenney, S. C. and Mertz, J. E. (2017). **Hypoxia-inducible factor-1alpha plays roles in Epstein-Barr virus's natural life cycle and tumorigenesis by inducing lytic infection through direct binding to the immediate-early BZLF1 gene promoter**. PLoS Pathog *13 (6)*, e1006404, doi: 10.1371/journal.ppat.1006404.

Kripalani-Joshi, S. and Law, H. Y. (1994). **Identification of integrated Epstein-Barr virus in nasopharyngeal carcinoma using pulse field gel electrophoresis**. Int J Cancer *56 (2)*, 187-192, doi: 10.1002/ijc.2910560207.

Kutok, J. L. and Wang, F. (2006). **Spectrum of Epstein-Barr virus-associated diseases**. Annu Rev Pathol *1*, 375-404, doi: 10.1146/annurev.pathol.1.110304.100209.

Landgren, O., Gilbert, E. S., Rizzo, J. D., Socié, G., Banks, P. M., Sobocinski, K. A., Horowitz, M. M., Jaffe, E. S., Kingma, D. W., Travis, L. B., Flowers, M. E., Martin, P. J., Deeg, H. J. and Curtis, R. E. (2009). **Risk factors for lymphoproliferative disorders after allogeneic hematopoietic cell transplantation**. Blood *113 (20)*, 4992-5001, doi: 10.1182/blood-2008-09-178046.

Lei, T., Yuen, K. S., Xu, R., Tsao, S. W., Chen, H., Li, M., Kok, K. H. and Jin, D. Y. (2013). **Targeting of DICE1 tumor suppressor by Epstein–Barr virus-encoded miR-BART3* microRNA in nasopharyngeal carcinoma**. International journal of cancer *133 (1)*, 79-87.

Li, L., Zhang, Y., Guo, B. B., Chan, F. K. and Tao, Q. (2014). **Oncogenic induction of cellular high CpG methylation by Epstein-Barr virus in malignant epithelial cells**. Chin J Cancer *33 (12)*, 604-608, doi: 10.5732/cjc.014.10191.

Li, Y. Y., Chung, G. T., Lui, V. W., To, K. F., Ma, B. B., Chow, C., Woo, J. K., Yip, K. Y., Seo, J., Hui, E. P., Mak, M. K., Rusan, M., Chau, N. G., Or, Y. Y., Law, M. H., Law, P. P., Liu, Z. W., Ngan, H. L., Hau, P. M., Verhoeft, K. R., Poon, P. H., Yoo, S. K., Shin, J. Y., Lee, S. D., Lun, S. W., Jia, L., Chan, A. W., Chan, J. Y., Lai, P. B., Fung, C. Y., Hung, S. T., Wang, L., Chang, A. M., Chiosea, S. I., Hedberg, M. L., Tsao, S. W., van Hasselt, A. C., Chan, A. T., Grandis, J. R., Hammerman, P. S. and Lo, K. W. (2017). **Exome and genome sequencing of nasopharynx cancer identifies NF-κB pathway activating mutations**. Nat Commun *8*, 14121, doi: 10.1038/ncomms14121.

Lindsay, A. J., Hendrick, A. G., Cantalupo, G., Senic-Matuglia, F., Goud, B., Bucci, C. and McCaffrey, M. W. (2002). **Rab coupling protein (RCP), a novel Rab4 and Rab11 effector protein**. J Biol Chem *277 (14)*, 12190-12199, doi: 10.1074/jbc.M108665200.

Lindsay, A. J. and McCaffrey, M. W. (2002). **Rab11-FIP2 functions in transferrin recycling and associates with endosomal membranes via its COOH-terminal domain**. J Biol Chem *277 (30)*, 27193-27199, doi: 10.1074/jbc.M200757200.

Lindsay, A. J. and McCaffrey, M. W. (2004). **The C2 domains of the class I Rab11 family of interacting proteins target recycling vesicles to the plasma membrane**. J Cell Sci *117 (Pt 19)*, 4365-4375, doi: 10.1242/jcs.01280.

Liu, P., Cheng, H., Roberts, T. M. and Zhao, J. J. (2009). **Targeting the phosphoinositide 3-kinase pathway in cancer**. Nat Rev Drug Discov *8 (8)*, 627-644, doi: 10.1038/nrd2926.

Liu, S., Liu, P., Borras, A., Chatila, T. and Speck, S. H. (1997). **Cyclosporin A-sensitive induction of the Epstein-Barr virus lytic switch is mediated via a novel pathway involving a MEF2 family member**. Embo j *16 (1)*, 143-153, doi: 10.1093/emboj/16.1.143.

Liu, Y. and Barta, S. K. (2019). **Diffuse large B-cell lymphoma: 2019 update on diagnosis, risk stratification, and treatment**. Am J Hematol *94 (5)*, 604-616, doi: 10.1002/ajh.25460.

Lo, K. W., Chung, G. T. and To, K. F. (2012). **Deciphering the molecular genetic basis of NPC through molecular, cytogenetic, and epigenetic approaches**. Semin Cancer Biol *22 (2)*, 79-86, doi: 10.1016/j.semcancer.2011.12.011.

Lopez, C., Kleinheinz, K., Aukema, S. M., Rohde, M., Bernhart, S. H., Hubschmann, D., Wagener, R., Toprak, U. H., Raimondi, F., Kreuz, M., Waszak, S. M., Huang, Z., Sieverling, L., Paramasivam, N., Seufert, J., Sungalee, S., Russell, R. B., Bausinger, J., Kretzmer, H., Ammerpohl, O., Bergmann, A. K., Binder, H., Borkhardt, A., Brors, B., Claviez, A., Doose, G., Feuerbach, L., Haake, A., Hansmann, M. L., Hoell, J., Hummel, M., Korbel, J. O., Lawerenz, C., Lenze, D., Radlwimmer, B., Richter, J., Rosenstiel, P., Rosenwald, A., Schilhabel, M. B., Stein, H., Stilgenbauer, S., Stadler, P. F., Szczepanowski, M., Weniger, M. A., Zapatka, M., Eils, R., Lichter, P., Loeffler, M., Moller, P., Trumper, L., Klapper, W., Consortium, I. M.-S., Hoffmann, S., Kuppers, R., Burkhardt, B., Schlesner, M. and Siebert, R. (2019). **Genomic and transcriptomic changes complement each other in the pathogenesis of sporadic Burkitt lymphoma**. Nat Commun *10 (1)*, 1459, doi: 10.1038/s41467-019-08578-3.

Lu, T. X., Liang, J. H., Miao, Y., Fan, L., Wang, L., Qu, X. Y., Cao, L., Gong, Q. X., Wang, Z., Zhang, Z. H., Xu, W. and Li, J. Y. (2015). **Epstein-Barr virus positive diffuse large B-cell lymphoma predict poor outcome, regardless of the age**. Sci Rep *5*, 12168, doi: 10.1038/srep12168.

Luftig, M., Yasui, T., Soni, V., Kang, M. S., Jacobson, N., Cahir-McFarland, E., Seed, B. and Kieff, E. (2004). **Epstein-Barr virus latent infection membrane protein 1 TRAF-binding site induces NIK/IKK alpha-dependent noncanonical NF-kappaB activation**. Proc Natl Acad Sci U S A *101 (1)*, 141-146, doi: 10.1073/pnas.2237183100.

Lung, H. L., Cheung, A. K., Ko, J. M., Cheng, Y., Stanbridge, E. J. and Lung, M. L. (2012). **Deciphering the molecular genetic basis of NPC through functional approaches**. Semin Cancer Biol *22 (2)*, 87-95, doi: 10.1016/j.semcancer.2011.11.002.

Luskin, M. R., Heil, D. S., Tan, K. S., Choi, S., Stadtmauer, E. A., Schuster, S. J., Porter, D. L., Vonderheide, R. H., Bagg, A., Heitjan, D. F., Tsai, D. E. and Reshef, R. (2015). **The Impact of EBV Status on Characteristics and Outcomes of Posttransplantation Lymphoproliferative Disorder**. Am J Transplant *15 (10)*, 2665-2673, doi: 10.1111/ajt.13324.

Machesky, L. M. (2019). **Rab11FIP proteins link endocytic recycling vesicles for cytoskeletal transport and tethering**. Biosci Rep *39 (1)*, doi: 10.1042/BSR20182219.

Mainou, B. A., Everly, D. N., Jr. and Raab-Traub, N. (2005). **Epstein-Barr virus latent membrane protein 1 CTAR1 mediates rodent and human fibroblast transformation through activation of PI3K**. Oncogene *24 (46)*, 6917-6924, doi: 10.1038/sj.onc.1208846.

Martel-Renoir, D., Grunewald, V., Touitou, R., Schwaab, G. and Joab, I. (1995). **Qualitative analysis of the expression of Epstein-Barr virus lytic genes in nasopharyngeal carcinoma biopsies**. J Gen Virol *76 (Pt 6)*, 1401-1408, doi: 10.1099/0022-1317-76-6-1401.

McKenzie, J. and El-Guindy, A. (2015). **Epstein-Barr Virus Lytic Cycle Reactivation**. Curr Top Microbiol Immunol *391*, 237-261, doi: 10.1007/978-3-319-22834-1_8.

McMahon, S. B. (2014). **MYC and the control of apoptosis**. Cold Spring Harb Perspect Med *4 (7)*, a014407, doi: 10.1101/cshperspect.a014407.

Mellman, I. (1996). **Endocytosis and molecular sorting**. Annual review of cell and developmental biology *12 (1)*, 575-625.

Miller, G., El-Guindy, A., Countryman, J., Ye, J. and Gradoville, L. (2007). **Lytic cycle switches of oncogenic human gammaherpesviruses**. Adv Cancer Res *97*, 81-109, doi: 10.1016/S0065-230X(06)97004-3.

Miller, N. and Hutt-Fletcher, L. M. (1992). **Epstein-Barr virus enters B cells and epithelial cells by different routes**. J Virol *66 (6)*, 3409-3414, doi: 10.1128/JVI.66.6.3409-3414.1992.

Miller, W. E., Earp, H. S. and Raab-Traub, N. (1995). **The Epstein-Barr virus latent membrane protein 1 induces expression of the epidermal growth factor receptor**. Journal of virology *69 (7)*, 4390-4398.

Minami, K., Tambe, Y., Watanabe, R., Isono, T., Haneda, M., Isobe, K., Kobayashi, T., Hino, O., Okabe, H., Chano, T. and Inoue, H. (2007). **Suppression of viral replication by stress-inducible GADD34 protein via the mammalian serine/threonine protein kinase mTOR pathway**. J Virol *81 (20)*, 11106-11115, doi: 10.1128/jvi.01063-07.

Mitra, S., Federico, L., Zhao, W., Dennison, J., Sarkar, T. R., Zhang, F., Takiar, V., Cheng, K. W., Mani, S., Lee, J. S. and Mills, G. B. (2016). **Rab25 acts as an oncogene in luminal B breast cancer and is causally associated with Snail driven EMT**. Oncotarget *7 (26)*, 40252-40265, doi: 10.18632/oncotarget.9730.

Miyashita, E. M., Yang, B., Babcock, G. J. and Thorley-Lawson, D. A. (1997). **Identification of the site of Epstein-Barr virus persistence in vivo as a resting B cell**. J Virol *71 (7)*, 4882-4891, doi: 10.1128/jvi.71.7.4882-4891.1997.

Mohl, B. S., Chen, J. and Longnecker, R. (2019). **Gammaherpesvirus entry and fusion: A tale how two human**

pathogenic viruses enter their host cells. Adv Virus Res *104*, 313-343, doi: 10.1016/bs.aivir.2019.05.006.

Molesworth, S. J., Lake, C. M., Borza, C. M., Turk, S. M. and Hutt-Fletcher, L. M. (2000). **Epstein-Barr virus gH is essential for penetration of B cells but also plays a role in attachment of virus to epithelial cells**. J Virol *74 (14)*, 6324-6332, doi: 10.1128/jvi.74.14.6324-6332.2000.

Montes-Moreno, S., Odqvist, L., Diaz-Perez, J. A., Lopez, A. B., de Villambrosía, S. G., Mazorra, F., Castillo, M. E., Lopez, M., Pajares, R., García, J. F., Mollejo, M., Camacho, F. I., Ruiz-Marcellán, C., Adrados, M., Ortiz, N., Franco, R., Ortiz-Hidalgo, C., Suarez-Gauthier, A., Young, K. H. and Piris, M. A. (2012). **EBV-positive diffuse large B-cell lymphoma of the elderly is an aggressive post-germinal center B-cell neoplasm characterized by prominent nuclear factor-kB activation**. Mod Pathol *25 (7)*, 968-982, doi: 10.1038/modpathol.2012.52.

Moore, M. D., Cannon, M. J., Sewall, A., Finlayson, M., Okimoto, M. and Nemerow, G. R. (1991). **Inhibition of Epstein-Barr virus infection in vitro and in vivo by soluble CR2 (CD21) containing two short consensus repeats**. J Virol *65 (7)*, 3559-3565, doi: 10.1128/JVI.65.7.3559-3565.1991.

Moore, M. D., DiScipio, R. G., Cooper, N. R. and Nemerow, G. R. (1989). **Hydrodynamic, electron microscopic, and ligand-binding analysis of the Epstein-Barr virus/C3dg receptor (CR2)**. J Biol Chem *264 (34)*, 20576-20582.

Morscio, J. and Tousseyn, T. (2016). **Recent insights in the pathogenesis of post-transplantation lymphoproliferative disorders**. World J Transplant *6 (3)*, 505-516, doi: 10.5500/wjt.v6.i3.505.

Morton, L. M., Wang, S. S., Devesa, S. S., Hartge, P., Weisenburger, D. D. and Linet, M. S. (2006). **Lymphoma incidence patterns by WHO subtype in the United States, 1992-2001**. Blood *107 (1)*, 265-276, doi: 10.1182/blood-2005-06-2508.

Mukku, V. R. and Stancel, G. M. (1985). **Regulation of epidermal growth factor receptor by estrogen**. J Biol Chem *260 (17)*, 9820-9824.

Murata, T., Sato, Y. and Kimura, H. (2014). **Modes of infection and oncogenesis by the Epstein-Barr virus**. Rev Med Virol *24 (4)*, 242-253, doi: 10.1002/rmv.1786.

Murphy, G., Pfeiffer, R., Camargo, M. C. and Rabkin, C. S. (2009). **Meta-analysis shows that prevalence of Epstein-Barr virus-positive gastric cancer differs based on sex and anatomic location**. Gastroenterology *137 (3)*, 824-833, doi: 10.1053/j.gastro.2009.05.001.

Nanbo, A., Terada, H., Kachi, K., Takada, K. and Matsuda, T. (2012). **Roles of cell signaling pathways in cell-to-cell contact-mediated Epstein-Barr virus transmission**. J Virol *86 (17)*, 9285-9296, doi: 10.1128/jvi.00712-12.

Naseem, M., Barzi, A., Brezden-Masley, C., Puccini, A., Berger, M. D., Tokunaga, R., Battaglin, F., Soni, S., McSkane, M., Zhang, W. and Lenz, H. J. (2018). **Outlooks on Epstein-Barr virus associated gastric cancer**. Cancer Treat Rev *66*, 15-22, doi: 10.1016/j.ctrv.2018.03.006.

Nedvetsky, P. I., Stefan, E., Frische, S., Santamaria, K., Wiesner, B., Valenti, G., Hammer, J. A., 3rd, Nielsen, S., Goldenring, J. R., Rosenthal, W. and Klussmann, E. (2007). **A Role of myosin Vb and Rab11-FIP2 in the aquaporin-2 shuttle**. Traffic *8 (2)*, 110-123, doi: 10.1111/j.1600-0854.2006.00508.x.

Ngoma, T., Adde, M., Durosinmi, M., Githang'a, J., Aken'Ova, Y., Kaijage, J., Adeodou, O., Rajab, J., Brown, B. J., Leoncini, L., Naresh, K., Raphael, M., Hurwitz, N., Scanlan, P., Rohatiner, A., Venzon, D. and Magrath, I. (2012). **Treatment of Burkitt lymphoma in equatorial Africa using a simple three-drug combination followed by a salvage regimen for patients with persistent or recurrent disease**. Br J Haematol *158 (6)*, 749-762, doi: 10.1111/j.1365-2141.2012.09236.x.

Niller, H. H., Wolf, H. and Minarovits, J. (2009). **Epigenetic dysregulation of the host cell genome in Epstein-Barr virus-associated neoplasia**. Semin Cancer Biol *19 (3)*, 158-164, doi: 10.1016/j.semcancer.2009.02.012.

Norseen, J., Johnson, F. B. and Lieberman, P. M. (2009). **Role for G-quadruplex RNA binding by Epstein-Barr virus nuclear antigen 1 in DNA replication and metaphase chromosome attachment**. J Virol *83 (20)*, 10336-10346, doi: 10.1128/JVI.00747-09.

Notarte, K. I., Senanayake, S., Macaranas, I., Albano, P. M., Mundo, L., Fennell, E., Leoncini, L. and Murray, P. (2021). **MicroRNA and Other Non-Coding RNAs in Epstein-Barr Virus-Associated Cancers**. Cancers (Basel) *13 (15)*, doi: 10.3390/cancers13153909.

O'Malley, B. W., Tsai, S. Y., Bagchi, M., Weigel, N. L., Schrader, W. T. and Tsai, M. J. (1991). **Molecular mechanism of action of a steroid hormone receptor**. Recent Prog Horm Res *47*, 1-24; discussion 24-26, doi: 10.1016/b978-0-12-571147-0.50005-6.

Oda, T., Imai, S., Chiba, S. and Takada, K. (2000). **Epstein-Barr virus lacking glycoprotein gp85 cannot infect B cells and epithelial cells**. Virology *276 (1)*, 52-58, doi: 10.1006/viro.2000.0531.

Oduor, C. I., Kaymaz, Y., Chelimo, K., Otieno, J. A., Ong'echa, J. M., Moormann, A. M. and Bailey, J. A. (2017). **Integrative microRNA and mRNA deep-sequencing expression profiling in endemic Burkitt lymphoma**. BMC Cancer *17 (1)*, 761, doi: 10.1186/s12885-017-3711-9.

Panda, A., Mehnert, J. M., Hirshfield, K. M., Riedlinger, G., Damare, S., Saunders, T., Kane, M., Sokol, L., Stein, M. N., Poplin, E., Rodriguez-Rodriguez, L., Silk, A. W., Aisner, J., Chan, N., Malhotra, J., Frankel, M., Kaufman, H. L., Ali, S., Ross, J. S., White, E. P., Bhanot, G. and Ganesan, S. (2018). **Immune Activation and Benefit From Avelumab in EBV-Positive Gastric Cancer**. J Natl Cancer Inst *110 (3)*, 316-320, doi: 10.1093/jnci/djx213.

Panea, R. I., Love, C. L., Shingleton, J. R., Reddy, A., Bailey, J. A., Moormann, A. M., Otieno, J. A., Ong'echa, J. M., Oduor, C. I., Schroeder, K. M. S., Masalu, N., Chao, N. J., Agajanian, M., Major, M. B., Fedoriw, Y., Richards, K. L., Rymkiewicz, G., Miles, R. R., Alobeid, B., Bhagat, G., Flowers, C. R., Ondrejka, S. L., Hsi, E. D., Choi, W. W. L., Au-Yeung, R. K. H., Hartmann, W., Lenz, G., Meyerson, H., Lin, Y. Y., Zhuang, Y., Luftig, M. A., Waldrop, A., Dave, T., Thakkar, D., Sahay, H., Li, G., Palus, B. C., Seshadri, V., Kim, S. Y., Gascoyne, R. D., Levy, S., Mukhopadyay, M., Dunson, D. B. and Dave, S. S. (2019). **The whole-genome landscape of Burkitt lymphoma subtypes**. Blood *134 (19)*, 1598-1607, doi: 10.1182/blood.2019001880.

Peden, A. A., Schonteich, E., Chun, J., Junutula, J. R., Scheller, R. H. and Prekeris, R. (2004). **The RCP-Rab11 complex regulates endocytic protein sorting**. Mol Biol Cell *15 (8)*, 3530-3541, doi: 10.1091/mbc.e03-12-0918.

Prekeris, R., Klumperman, J. and Scheller, R. H. (2000). **A Rab11/Rip11 protein complex regulates apical membrane trafficking via recycling endosomes**. Mol Cell *6 (6)*, 1437-1448, doi: 10.1016/s1097-2765(00)00140-4.

Price, A. M. and Luftig, M. A. (2014). **Dynamic Epstein-Barr virus gene expression on the path to B-cell transformation**. Adv Virus Res *88*, 279-313, doi: 10.1016/B978-0-12-800098-4.00006-4.

Qi, M., Williams, J. A., Chu, H., Chen, X., Wang, J. J., Ding, L., Akhirome, E., Wen, X., Lapierre, L. A., Goldenring, J. R. and Spearman, P. (2013). **Rab11-FIP1C and Rab14 direct plasma membrane sorting and particle incorporation of the HIV-1 envelope glycoprotein complex**. PLoS Pathog *9 (4)*, e1003278, doi: 10.1371/journal.ppat.1003278.

Qiu, M. Z., He, C. Y., Lu, S. X., Guan, W. L., Wang, F., Wang, X. J., Jin, Y., Wang, F. H., Li, Y. H. and Shao, J. Y. (2020). **Prospective observation: Clinical utility of plasma Epstein–Barr virus DNA load in EBV-associated gastric carcinoma patients**. International journal of cancer *146 (1)*, 272-280.

Raab-Traub, N. (2012). **Novel mechanisms of EBV-induced oncogenesis**. Curr Opin Virol *2 (4)*, 453-458, doi: 10.1016/j.coviro.2012.07.001.

Raab-Traub, N. and Flynn, K. (1986). **The structure of the termini of the Epstein-Barr virus as a marker of clonal cellular proliferation**. Cell *47 (6)*, 883-889, doi: 10.1016/0092-8674(86)90803-2.

Ragoczy, T., Heston, L. and Miller, G. (1998). **The Epstein-Barr virus Rta protein activates lytic cycle genes and can disrupt latency in B lymphocytes**. J Virol *72 (10)*, 7978-7984, doi: 10.1128/JVI.72.10.7978-7984.1998.

Rainero, E., Caswell, P. T., Muller, P. A., Grindlay, J., McCaffrey, M. W., Zhang, Q., Wakelam, M. J., Vousden, K. H., Graziani, A. and Norman, J. C. (2012). **Diacylglycerol kinase alpha controls RCP-dependent integrin trafficking to promote invasive migration**. J Cell Biol *196 (2)*, 277-295, doi: 10.1083/jcb.201109112.

Reshef, R., Vardhanabhuti, S., Luskin, M. R., Heitjan, D. F., Hadjiliadis, D., Goral, S., Krok, K. L., Goldberg, L. R., Porter, D. L., Stadtmauer, E. A. and Tsai, D. E. (2011). **Reduction of immunosuppression as initial therapy for posttransplantation lymphoproliferative disorder(★)**. Am J Transplant *11 (2)*, 336-347, doi: 10.1111/j.1600-6143.2010.03387.x.

Ribeiro, J., Malta, M., Galaghar, A., Silva, F., Afonso, L. P., Medeiros, R. and Sousa, H. (2017). **P53 deregulation in Epstein-Barr virus-associated gastric cancer**. Cancer Lett *404*, 37-43, doi: 10.1016/j.canlet.2017.07.010.

Rickinson, A. B. (2014). **Co-infections, inflammation and oncogenesis: future directions for EBV research**. Semin Cancer Biol *26*, 99-115, doi: 10.1016/j.semcancer.2014.04.004.

Robinson, M. S., Watts, C. and Zerial, M. (1996). **Membrane dynamics in endocytosis**. Cell *84 (1)*, 13-21.

Sabattini, E., Bacci, F., Sagramoso, C. and Pileri, S. A. (2010). **WHO classification of tumours of haematopoietic and lymphoid tissues in 2008: an overview**. Pathologica *102 (3)*, 83-87.

Sang, A. X., McPherson, M. C., Ivison, G. T., Qu, X., Rigdon, J., Esquivel, C. O., Krams, S. M. and Martinez, O. M. (2019). **Dual blockade of the PI3K/Akt/mTOR pathway inhibits posttransplant Epstein-Barr virus B cell lymphomas and promotes allograft survival**. Am J Transplant *19 (5)*, 1305-1314, doi: 10.1111/ajt.15216.

Satou, A., Asano, N., Nakazawa, A., Osumi, T., Tsurusawa, M., Ishiguro, A., Elsayed, A. A., Nakamura, N., Ohshima, K., Kinoshita, T. and Nakamura, S. (2015). **Epstein-Barr virus (EBV)-positive sporadic burkitt lymphoma: an age-related lymphoproliferative disorder?** Am J Surg Pathol *39 (2)*, 227-235, doi: 10.1097/PAS.0000000000000332.

Savani, B. N., Pohlmann, P. R., Jagasia, M., Chinratanalab, W., Kassim, A., Engelhardt, B., Greer, J., Schuening, F. and Goodman, S. (2009). **Does peritransplantation use of rituximab reduce the risk of EBV reactivation and PTLPD?** Blood *113 (24)*, 6263-6264, doi: 10.1182/blood-2009-04-213892.

Schafer, J. C., McRae, R. E., Manning, E. H., Lapierre, L. A. and Goldenring, J. R. (2016). **Rab11-FIP1A regulates early trafficking into the recycling endosomes**. Exp Cell Res *340 (2)*, 259-273, doi: 10.1016/j.yexcr.2016.01.003.

Schlager, S., Speck, S. H. and Woisetschläger, M. (1996). **Transcription of the Epstein-Barr virus nuclear antigen 1 (EBNA1) gene occurs before induction of the BCR2 (Cp) EBNA gene promoter during the initial stages of infection in B cells**. J Virol *70 (6)*, 3561-3570, doi: 10.1128/jvi.70.6.3561-3570.1996.

Schmitz, R., Ceribelli, M., Pittaluga, S., Wright, G. and Staudt, L. M. (2014). **Oncogenic mechanisms in Burkitt lymphoma**. Cold Spring Harb Perspect Med *4 (2)*, doi: 10.1101/cshperspect.a014282.

Schmitz, R., Young, R. M., Ceribelli, M., Jhavar, S., Xiao, W., Zhang, M., Wright, G., Shaffer, A. L., Hodson, D. J.,

Buras, E., Liu, X., Powell, J., Yang, Y., Xu, W., Zhao, H., Kohlhammer, H., Rosenwald, A., Kluin, P., Muller-Hermelink, H. K., Ott, G., Gascoyne, R. D., Connors, J. M., Rimsza, L. M., Campo, E., Jaffe, E. S., Delabie, J., Smeland, E. B., Ogwang, M. D., Reynolds, S. J., Fisher, R. I., Braziel, R. M., Tubbs, R. R., Cook, J. R., Weisenburger, D. D., Chan, W. C., Pittaluga, S., Wilson, W., Waldmann, T. A., Rowe, M., Mbulaiteye, S. M., Rickinson, A. B. and Staudt, L. M. (2012). **Burkitt lymphoma pathogenesis and therapeutic targets from structural and functional genomics**. Nature *490 (7418)*, 116-120, doi: 10.1038/nature11378.

Sears, J., Ujihara, M., Wong, S., Ott, C., Middeldorp, J. and Aiyar, A. (2004). **The amino terminus of Epstein-Barr Virus (EBV) nuclear antigen 1 contains AT hooks that facilitate the replication and partitioning of latent EBV genomes by tethering them to cellular chromosomes**. J Virol *78 (21)*, 11487-11505, doi: 10.1128/JVI.78.21.11487-11505.2004.

Sehn, L. H., Donaldson, J., Chhanabhai, M., Fitzgerald, C., Gill, K., Klasa, R., MacPherson, N., O'Reilly, S., Spinelli, J. J., Sutherland, J., Wilson, K. S., Gascoyne, R. D. and Connors, J. M. (2005). **Introduction of combined CHOP plus rituximab therapy dramatically improved outcome of diffuse large B-cell lymphoma in British Columbia**. J Clin Oncol *23 (22)*, 5027-5033, doi: 10.1200/jco.2005.09.137.

Sengupta, S., den Boon, J. A., Chen, I. H., Newton, M. A., Dahl, D. B., Chen, M., Cheng, Y. J., Westra, W. H., Chen, C. J., Hildesheim, A., Sugden, B. and Ahlquist, P. (2006). **Genome-wide expression profiling reveals EBV-associated inhibition of MHC class I expression in nasopharyngeal carcinoma**. Cancer Res *66 (16)*, 7999-8006, doi: 10.1158/0008-5472.can-05-4399.

Shao, Y. M., Poirier, S., Ohshima, H., Malaveille, C., Zeng, Y., de The, G. and Bartsch, H. (1988). **Epstein-Barr virus activation in Raji cells by extracts of preserved food from high risk areas for nasopharyngeal carcinoma**. Carcinogenesis *9 (8)*, 1455-1457, doi: 10.1093/carcin/9.8.1455.

Shumilov, A., Tsai, M. H., Schlosser, Y. T., Kratz, A. S., Bernhardt, K., Fink, S., Mizani, T., Lin, X., Jauch, A., Mautner, J., Kopp-Schneider, A., Feederle, R., Hoffmann, I. and Delecluse, H. J. (2017). **Epstein-Barr virus particles induce centrosome amplification and chromosomal instability**. Nat Commun *8*, 14257, doi: 10.1038/ncomms14257.

Shuto, T., Nishikawa, J., Shimokuri, K., Yanagi, A., Takagi, T., Takagi, F., Miura, O., Iida, M., Nagano, H., Takemoto, Y., Harada, E., Suehiro, Y., Yamasaki, T., Okamoto, T. and Sakaida, I. (2019). **Establishment of a Screening Method for Epstein-Barr Virus-Associated Gastric Carcinoma by Droplet Digital PCR**. Microorganisms *7 (12)*, doi: 10.3390/microorganisms7120628.

Sinclair, A. J. (2013). **Epigenetic control of Epstein-Barr virus transcription - relevance to viral life cycle?** Front Genet *4*, 161, doi: 10.3389/fgene.2013.00161.

Sinha, S. and Gajra, A. (2022). **Nasopharyngeal Cancer**. In: StatPearls, Treasure Island (FL).

Soltani, S., Zakeri, A., Tabibzadeh, A., Zakeri, A. M., Zandi, M., Siavoshi, S., Seifpour, S. and Farahani, A. (2021). **A review on EBV encoded and EBV-induced host microRNAs expression profile in different lymphoma types**. Mol Biol Rep *48 (2)*, 1801-1817, doi: 10.1007/s11033-021-06152-z.

Spear, P. G. and Longnecker, R. (2003). **Herpesvirus entry: an update**. J Virol *77 (19)*, 10179-10185, doi: 10.1128/jvi.77.19.10179-10185.2003.

Spender, L. C., Lucchesi, W., Bodelon, G., Bilancio, A., Karstegl, C. E., Asano, T., Dittrich-Breiholz, O., Kracht, M., Vanhaesebroeck, B. and Farrell, P. J. (2006). **Cell target genes of Epstein–Barr virus transcription factor EBNA-2: induction of the p55 α regulatory subunit of PI3-kinase and its role in survival of EREB2. 5 cells**. Journal of general virology *87 (10)*, 2859-2867.

Sugiura, M., Imai, S., Tokunaga, M., Koizumi, S., Uchizawa, M., Okamoto, K. and Osato, T. (1996). **Transcriptional analysis of Epstein-Barr virus gene expression in EBV-positive gastric carcinoma: unique viral latency in the tumour cells**. Br J Cancer *74 (4)*, 625-631, doi: 10.1038/bjc.1996.412.

Swerdlow, S. H., Campo, E., Pileri, S. A., Harris, N. L., Stein, H., Siebert, R., Advani, R., Ghielmini, M., Salles, G. A., Zelenetz, A. D. and Jaffe, E. S. (2016). **The 2016 revision of the World Health Organization classification of lymphoid neoplasms**. Blood *127 (20)*, 2375-2390, doi: 10.1182/blood-2016-01-643569.

Szymula, A., Palermo, R. D., Bayoumy, A., Groves, I. J., Ba Abdullah, M., Holder, B. and White, R. E. (2018). **Epstein-Barr virus nuclear antigen EBNA-LP is essential for transforming naive B cells, and facilitates recruitment of transcription factors to the viral genome**. PLoS pathogens *14 (2)*, e1006890.

Tanner, J., Weis, J., Fearon, D., Whang, Y. and Kieff, E. (1987). **Epstein-Barr virus gp350/220 binding to the B lymphocyte C3d receptor mediates adsorption, capping, and endocytosis**. Cell *50 (2)*, 203-213, doi: 10.1016/0092-8674(87)90216-9.

Tanner, J., Whang, Y., Sample, J., Sears, A. and Kieff, E. (1988). **Soluble gp350/220 and deletion mutant glycoproteins block Epstein-Barr virus adsorption to lymphocytes**. J Virol *62 (12)*, 4452-4464, doi: 10.1128/JVI.62.12.4452-4464.1988.

Taylor, G. M., Raghuwanshi, S. K., Rowe, D. T., Wadowsky, R. M. and Rosendorff, A. (2011). **Endoplasmic reticulum stress causes EBV lytic replication**. Blood *118 (20)*, 5528-5539, doi: 10.1182/blood-2011-04-347112.

Thorley-Lawson, D. A. (2015). **EBV Persistence--Introducing the Virus**. Curr Top Microbiol Immunol *390 (Pt 1)*, 151-209, doi: 10.1007/978-3-319-22822-8_8.

Tsai, M. H., Raykova, A., Klinke, O., Bernhardt, K., Gartner, K., Leung, C. S., Geletneky, K., Sertel, S., Munz, C., Feederle, R. and Delecluse, H. J. (2013). **Spontaneous lytic replication and epitheliotropism define an Epstein-Barr virus strain found in carcinomas**. Cell Rep *5 (2)*, 458-470, doi: 10.1016/j.celrep.2013.09.012.

Tsao, S. W., Tsang, C. M. and Lo, K. W. (2017). **Epstein-Barr virus infection and nasopharyngeal carcinoma**. Philos Trans R Soc Lond B Biol Sci *372 (1732)*, doi: 10.1098/rstb.2016.0270.

Ushiku, T., Chong, J. M., Uozaki, H., Hino, R., Chang, M. S., Sudo, M., Rani, B. R., Sakuma, K., Nagai, H. and Fukayama, M. (2007). **p73 gene promoter methylation in Epstein-Barr virus-associated gastric carcinoma**. Int J Cancer *120 (1)*, 60-66, doi: 10.1002/ijc.22275.

van Beek, J., zur Hausen, A., Klein Kranenbarg, E., van de Velde, C. J., Middeldorp, J. M., van den Brule, A. J., Meijer, C. J. and Bloemena, E. (2004). **EBV-positive gastric adenocarcinomas: a distinct clinicopathologic entity with a low frequency of lymph node involvement**. J Clin Oncol *22 (4)*, 664-670, doi: 10.1200/jco.2004.08.061.

van Leeuwen, M. T., Turner, J. J., Joske, D. J., Falster, M. O., Srasuebkul, P., Meagher, N. S., Grulich, A. E., Giles, G. G. and Vajdic, C. M. (2014). **Lymphoid neoplasm incidence by WHO subtype in Australia 1982-2006**. Int J Cancer *135 (9)*, 2146-2156, doi: 10.1002/ijc.28849.

Vincenti, F., Mendez, R., Pescovitz, M., Rajagopalan, P. R., Wilkinson, A. H., Butt, K., Laskow, D., Slakey, D. P., Lorber, M. I., Garg, J. P. and Garovoy, M. (2007). **A phase I/II randomized open-label multicenter trial of efalizumab, a humanized anti-CD11a, anti-LFA-1 in renal transplantation**. Am J Transplant *7 (7)*, 1770-1777, doi: 10.1111/j.1600-6143.2007.01845.x.

von Grabowiecki, Y., Phatak, V., Aschauer, L. and Muller, P. A. J. (2021). **Rab11-FIP1/RCP Functions as a Major Signalling Hub in the Oncogenic Roles of Mutant p53 in Cancer**. Front Oncol *11*, 804107, doi: 10.3389/fonc.2021.804107.

Vrzalikova, K., Vockerodt, M., Leonard, S., Bell, A., Wei, W., Schrader, A., Wright, K. L., Kube, D., Rowe, M., Woodman, C. B. and Murray, P. G. (2011). **Down-regulation of BLIMP1alpha by the EBV oncogene, LMP-1, disrupts the plasma cell differentiation program and prevents viral replication in B cells:**

implications for the pathogenesis of EBV-associated B-cell lymphomas. Blood *117 (22)*, 5907-5917, doi: 10.1182/blood-2010-09-307710.

Wang, H. B., Zhang, H., Zhang, J. P., Li, Y., Zhao, B., Feng, G. K., Du, Y., Xiong, D., Zhong, Q., Liu, W. L., Du, H., Li, M. Z., Huang, W. L., Tsao, S. W., Hutt-Fletcher, L., Zeng, Y. X., Kieff, E. and Zeng, M. S. (2015). **Neuropilin 1 is an entry factor that promotes EBV infection of nasopharyngeal epithelial cells**. Nat Commun *6*, 6240, doi: 10.1038/ncomms7240.

Wang, J., Yu, F., Wei, W., Huang, J., Shao, Y., Yan, J., Mao, L., Yu, W., Xie, W. and Jin, J. (2023). **Simplifying genetic classifiers by six mutated genes in diffuse large B-cell lymphoma**. Genes Dis *10 (1)*, 37-40, doi: 10.1016/j.gendis.2022.03.014.

Wang, Q., Zhu, N., Hu, J., Wang, Y., Xu, J., Gu, Q., Lieberman, P. M. and Yuan, Y. (2020). **The mTOR inhibitor manassantin B reveals a crucial role of mTORC2 signaling in Epstein-Barr virus reactivation**. J Biol Chem *295 (21)*, 7431-7441, doi: 10.1074/jbc.RA120.012645.

Wille, C. K., Nawandar, D. M., Panfil, A. R., Ko, M. M., Hagemeier, S. R. and Kenney, S. C. (2013). **Viral genome methylation differentially affects the ability of BZLF1 versus BRLF1 to activate Epstein-Barr virus lytic gene expression and viral replication**. J Virol *87 (2)*, 935-950, doi: 10.1128/JVI.01790-12.

Woellmer, A., Arteaga-Salas, J. M. and Hammerschmidt, W. (2012). **BZLF1 governs CpG-methylated chromatin of Epstein-Barr Virus reversing epigenetic repression**. PLoS Pathog *8 (9)*, e1002902, doi: 10.1371/journal.ppat.1002902.

Woisetschlaeger, M., Yandava, C. N., Furmanski, L. A., Strominger, J. L. and Speck, S. H. (1990). **Promoter switching in Epstein-Barr virus during the initial stages of infection of B lymphocytes**. Proc Natl Acad Sci U S A *87 (5)*, 1725-1729, doi: 10.1073/pnas.87.5.1725.

Wu, C. C., Liu, M. T., Chang, Y. T., Fang, C. Y., Chou, S. P., Liao, H. W., Kuo, K. L., Hsu, S. L., Chen, Y. R., Wang, P. W., Chen, Y. L., Chuang, H. Y., Lee, C. H., Chen, M., Wayne Chang, W. S. and Chen, J. Y. (2010). **Epstein-Barr virus DNase (BGLF5) induces genomic instability in human epithelial cells**. Nucleic Acids Res *38 (6)*, 1932-1949, doi: 10.1093/nar/gkp1169.

Xiao, J., Palefsky, J. M., Herrera, R., Berline, J. and Tugizov, S. M. (2008). **The Epstein-Barr virus BMRF-2 protein facilitates virus attachment to oral epithelial cells**. Virology *370 (2)*, 430-442, doi: 10.1016/j.virol.2007.09.012.

Xiong, D., Du, Y., Wang, H. B., Zhao, B., Zhang, H., Li, Y., Hu, L. J., Cao, J. Y., Zhong, Q., Liu, W. L., Li, M. Z., Zhu, X. F., Tsao, S. W., Hutt-Fletcher, L. M., Song, E., Zeng, Y. X., Kieff, E. and Zeng, M. S. (2015). **Nonmuscle myosin heavy chain IIA mediates Epstein-Barr virus infection of nasopharyngeal epithelial cells**. Proc Natl Acad Sci U S A *112 (35)*, 11036-11041, doi: 10.1073/pnas.1513359112.

Yanagi, A., Nishikawa, J., Shimokuri, K., Shuto, T., Takagi, T., Takagi, F., Kobayashi, Y., Yamamoto, M., Miura, O., Yanai, H., Suehiro, Y., Yamasaki, T., Yoshiyama, H. and Sakaida, I. (2019). **Clinicopathologic Characteristics of Epstein-Barr Virus-Associated Gastric Cancer Over the Past Decade in Japan**. Microorganisms *7 (9)*, doi: 10.3390/microorganisms7090305.

Yang, J., Liu, Z., Zeng, B., Hu, G. and Gan, R. (2020). **Epstein-Barr virus-associated gastric cancer: A distinct subtype**. Cancer Lett *495*, 191-199, doi: 10.1016/j.canlet.2020.09.019.

Younes, A. and Ansell, S. M. (2016). **Novel agents in the treatment of Hodgkin lymphoma: Biological basis and clinical results**. Semin Hematol *53 (3)*, 186-189, doi: 10.1053/j.seminhematol.2016.05.011.

Young, J. L., Jr. and Miller, R. W. (1975). **Incidence of malignant tumors in U. S. children**. J Pediatr *86 (2)*, 254-258, doi: 10.1016/s0022-3476(75)80484-7.

Young, K. A., Chen, X. S., Holers, V. M. and Hannan, J. P. (2007). **Isolating the Epstein-Barr virus gp350/220**

binding site on complement receptor type 2 (CR2/CD21). J Biol Chem *282 (50)*, 36614-36625, doi: 10.1074/jbc.M706324200.

Young, L. S. and Dawson, C. W. (2014). **Epstein-Barr virus and nasopharyngeal carcinoma**. Chin J Cancer *33 (12)*, 581-590, doi: 10.5732/cjc.014.10197.

Young, L. S. and Murray, P. G. (2003). **Epstein-Barr virus and oncogenesis: from latent genes to tumours**. Oncogene *22 (33)*, 5108-5121, doi: 10.1038/sj.onc.1206556.

Young, L. S. and Rickinson, A. B. (2004). **Epstein-Barr virus: 40 years on**. Nat Rev Cancer *4 (10)*, 757-768, doi: 10.1038/nrc1452.

Zalani, S., Holley-Guthrie, E. and Kenney, S. (1996). **Epstein-Barr viral latency is disrupted by the immediate-early BRLF1 protein through a cell-specific mechanism**. Proc Natl Acad Sci U S A *93 (17)*, 9194-9199, doi: 10.1073/pnas.93.17.9194.

Zhang, H., Li, Y., Wang, H. B., Zhang, A., Chen, M. L., Fang, Z. X., Dong, X. D., Li, S. B., Du, Y., Xiong, D., He, J. Y., Li, M. Z., Liu, Y. M., Zhou, A. J., Zhong, Q., Zeng, Y. X., Kieff, E., Zhang, Z., Gewurz, B. E., Zhao, B. and Zeng, M. S. (2018). **Ephrin receptor A2 is an epithelial cell receptor for Epstein-Barr virus entry**. Nat Microbiol *3 (2)*, 1-8, doi: 10.1038/s41564-017-0080-8.

Zhang, J., Jia, L., Tsang, C. M. and Tsao, S. W. (2017). **EBV Infection and Glucose Metabolism in Nasopharyngeal Carcinoma**. Adv Exp Med Biol *1018*, 75-90, doi: 10.1007/978-981-10-5765-6_6.

Zhang, J., Liu, X., Datta, A., Govindarajan, K., Tam, W. L., Han, J., George, J., Wong, C., Ramnarayanan, K., Phua, T. Y., Leong, W. Y., Chan, Y. S., Palanisamy, N., Liu, E. T., Karuturi, K. M., Lim, B. and Miller, L. D. (2009). **RCP is a human breast cancer-promoting gene with Ras-activating function**. J Clin Invest *119 (8)*, 2171-2183, doi: 10.1172/jci37622.

Zhang, J., Wang, F., Xu, J., Wang, X., Ye, F. and Xie, X. (2016). **Micro ribonucleic acid-93 promotes oncogenesis of cervical cancer by targeting RAB11 family interacting protein 1**. J Obstet Gynaecol Res *42 (9)*, 1168-1179, doi: 10.1111/jog.13027.

Zhao, B., Maruo, S., Cooper, A., R. Chase, M., Johannsen, E., Kieff, E. and Cahir-McFarland, E. (2006). **RNAs induced by Epstein–Barr virus nuclear antigen 2 in lymphoblastoid cell lines**. Proceedings of the National Academy of Sciences *103 (6)*, 1900-1905.

Zhu, D. D., Zhang, J., Deng, W., Yip, Y. L., Lung, H. L., Tsang, C. M., Law, W. T., Yang, J., Lau, V. M., Shuen, W. H., Lung, M. L., Cheung, A. L. and Tsao, S. W. (2016). **Significance of NF-kappaB activation in immortalization of nasopharyngeal epithelial cells**. Int J Cancer *138 (5)*, 1175-1185, doi: 10.1002/ijc.29850.

Zhu, N., Wang, Q., Wu, Z., Wang, Y., Zeng, M. S. and Yuan, Y. (2022). **Epstein-Barr Virus LMP1-Activated mTORC1 and mTORC2 Coordinately Promote Nasopharyngeal Cancer Stem Cell Properties**. J Virol *96 (5)*, e0194121, doi: 10.1128/jvi.01941-21.

Zimmermann, J. and Hammerschmidt, W. (1995). **Structure and role of the terminal repeats of Epstein-Barr virus in processing and packaging of virion DNA**. J Virol *69 (5)*, 3147-3155, doi: 10.1128/JVI.69.5.3147-3155.1995.

Acknowledgements

First and foremost, I would like to express my heartfelt gratitude to my supervisor, Prof. H.-J. Delecluse, for his unwavering guidance, mentorship, and support throughout these years of my work. His belief in my abilities and the freedom he granted me to grow as a researcher have been invaluable. I am forever grateful for his constant availability and guidance, which I will always cherish. I would also like to extend my thanks to Prof. Dr. Martin Müller and Dr. Florence Baudin, who served as members of my Thesis Advisory Committee. Their supervision and expertise have helped me stay focused on the core questions of my Ph.D. project, ensuring its relevance and significance.

As a Ph.D. student, reaching this milestone was not a solitary achievement. There are countless individuals to whom I owe my gratitude. To my dear fellow lab members, your presence and contributions have enriched my journey. I deeply appreciate the moments we shared and the valuable advice you provided. Your support and encouragement have carried me through challenging times, and your unwavering support has made me stronger and more determined. I would like to express my special appreciation to Zhe for setting a good example of discipline in both life and the lab. Your guidance and assistance with experiments have saved me invaluable time. To Francesco, I am immensely grateful for your guidance and teachings in the field of bioscience. You have taught me that pursuing a Ph.D. is not merely following instructions but entails gaining independence, thinking outside the box, and broadening scientific horizons through reading and engaging in discussions. To Dwain, from the very beginning when I felt like an outsider in the lab, being far from my home in China and navigating a completely new field, your unwavering emotional support and project guidance have been invaluable. To Remy, thank you for always being there to provide advice and help whenever I encountered problems. Our discussions and collaborative problem-solving have been instrumental in the path of my Ph.D. Your expertise and assistance with cloning and experimental design have made my journey fulfilling. To Hao, thank you for your invaluable contributions to my project. I greatly enjoyed our discussions, and the moments of excitement when our ideas seemed to align and propel my project forward. I hope to see you back in China soon, and I wish you all the best with your own project. To Qipeng, we have shared the same lab room for nearly two years. I appreciate your efforts in maintaining a tidy and conducive working environment, taking care of the small details that often go unnoticed. To Lu Lu, thank you for always being there for me. Your unwavering support has been a source of strength during challenging times. With your encouragement, I have been able to focus solely on my research without worrying about

anything else. To my American Mom, Pam, I am grateful for your unwavering trust in me and your continuous encouragement to persevere until the end. Your love and support have helped me endure the harsh winters here in Germany, and now, I am approaching the final stages of this journey. To the doorman, Kai, thank you for always believing in me, even during the darkest nights that seemed never-ending and tedious. Your encouragement has been a beacon of hope, guiding me towards the light and the beauty that lie ahead. To all those whose names I may not have mentioned, please know that your belief in me and your support will forever be cherished in my heart. The closeness and friendship we shared have been a blessing in my life. Lastly, to my beloved family, your unconditional love and unwavering support have illuminated the darkest moments of my Ph.D. life. Being far away from you has made me realize the true importance of family in my life. Your love has been my guiding light throughout this journey.

Curriculum Vitae

PERSONAL INFORMATION
Name: Cheng, Xianliang
Date of Birth: 01/01/1993
Place of Birth: Heilongjiang
Nationality: Chinese
Marital Status: Single

PRIMARY AND SECONDARY SCHOOLS

2000-2006 Harbin Shuangcheng District Third Primary School, Harbin, Heilongjiang, P.R. China
2006-2009 Harbin Shuangcheng District Eighth Middle School, Harbin, Heilongjiang, P.R. China
2009-2012 Harbin Shuangcheng District Zhongzhi Senior High School, Harbin, Heilongjiang, P.R. China

(07/06/2012-08/06/2012) Secondary School final exam/A-levels/High school graduation

UNIVERSTIY

September 2016 – July 2019 Kunming Medical University, Kunming, Yunnan, P.R. China
Received for Master of Medicine in Pharmacology in July 2019
September 2012 – July 2016 Kunming Medical University, Kunming, Yunnan, P.R. China
Received Bachelor of Medical Science in July 2016

EIDESSTATTLICHE VERSICHERUNG

1. Bei der eingereichten Dissertation zu dem Thema

Cellular control of spontaneous replication in B cells infected by the Epstein-Barr virus

handelt es sich um meine eigenständig erbrachte Leistung.

2. Ich habe nur die angegebenen Quellen und Hilfsmittel benutzt und mich keiner unzulässigen Hilfe Dritter bedient. Insbesondere habe ich wörtlich oder sinngemäß aus anderen Werken übernommene Inhalte als solche kenntlich gemacht.

3. Die Arbeit oder Teile davon habe ich bislang nicht an einer Hochschule des In- oder Auslands als Bestandteil einer Prüfungs- oder Qualifikationsleistung vorgelegt.*

4. Die Richtigkeit der vorstehenden Erklärungen bestätige ich.

5. Die Bedeutung der eidesstattlichen Versicherung und die strafrechtlichen Folgen einer unrichtigen oder unvollständigen eidesstattlichen Versicherung sind mir bekannt. Ich versichere an Eides statt, dass ich nach bestem Wissen die reine Wahrheit erklärt und nichts verschwiegen habe.

Place, Date *doctoral candidate's signature*

3. Die Arbeit oder Teile davon habe ich wie folgt an einer Hochschule des In- oder Auslands als Bestandteil einer Prüfungs- oder Qualifikationsleistung vorgelegt:

Titel der Arbeit:

Hochschule und Jahr:

Art der Prüfungs- oder Qualifikationsleistung: